Periodic-orbit theory of universality in quantum chaos

Sebastian Müller,[1] Stefan Heusler,[1] Petr Braun,[1,2] Fritz Haake,[1] and Alexander Altland[3]
[1]*Fachbereich Physik, Universität Duisburg-Essen, 45117 Essen, Germany*
[2]*Institute of Physics, Saint Petersburg University, 198504 Saint Petersburg, Russia*
[3]*Institut für Theoretische Physik, Zülpicher Strasse 77, 50937 Köln, Germany*
(Received 23 March 2005; published 13 October 2005)

We argue semiclassically, on the basis of Gutzwiller's periodic-orbit theory, that full classical chaos is paralleled by quantum energy spectra with universal spectral statistics, in agreement with random-matrix theory. For dynamics from all three Wigner-Dyson symmetry classes, we calculate the small-time spectral form factor $K(\tau)$ as power series in the time τ. Each term τ^n of that series is provided by specific families of pairs of periodic orbits. The contributing pairs are classified in terms of close self-encounters in phase space. The frequency of occurrence of self-encounters is calculated by invoking ergodicity. Combinatorial rules for building pairs involve nontrivial properties of permutations. We show our series to be equivalent to perturbative implementations of the nonlinear σ models for the Wigner-Dyson ensembles of random matrices and for disordered systems; our families of orbit pairs have a one-to-one relationship with Feynman diagrams known from the σ model.

DOI: 10.1103/PhysRevE.72.046207 PACS number(s): 05.45.Mt, 03.65.Sq

I. INTRODUCTION

A. Background

In the semiclassical limit, fully chaotic quantum systems display universal properties. Universal behavior has been observed for many quantities of interest in such different areas as mesoscopic transport or nuclear physics. One paradigmatic example stands out and will be the object of our investigation: According to the Bohigas-Giannoni-Schmit conjecture put forward about two decades ago [1], highly excited energy levels of generic fully chaotic systems have universal spectral statistics. This conjecture is supported by broad experimental and numerical evidence [2,3].

Level statistics can be characterized by the so-called spectral form factor. The level density $\rho(E)=\Sigma_i\delta(E-E_i)$ of a bounded quantum system (E_i denoting the energy levels) is split into a local average $\bar{\rho}(E)$ and an oscillatory part $\rho_{\mathrm{osc}}(E)$ describing fluctuations around that average. The form factor is defined as the Fourier transform of the two-point correlator $\langle\rho_{\mathrm{osc}}(E+\epsilon/2)\rho_{\mathrm{osc}}(E-\epsilon/2)\rangle$ with respect to the energy difference ϵ,

$$K(\tau)=\left\langle\int\frac{d\epsilon}{\bar{\rho}(E)}e^{(i/\hbar)\epsilon\tau T_H}\rho_{\mathrm{osc}}\left(E+\frac{\epsilon}{2}\right)\rho_{\mathrm{osc}}\left(E-\frac{\epsilon}{2}\right)\right\rangle; \quad (1)$$

here the time τ, conjugate to the energy difference, is measured in units of the so-called Heisenberg time

$$T_H=2\pi\hbar\bar{\rho}(E)=\frac{\Omega(E)}{(2\pi\hbar)^{f-1}}, \quad (2)$$

with $\Omega(E)$ denoting the volume of the energy shell and f the number of degrees of freedom. Since the study of high-lying states justifies the semiclassical limit, we may take $\hbar\to 0$, $T_H\to\infty$, for fixed τ. To make $K(\tau)$ a plottable function, two averages, $\langle\cdots\rangle$ in Eq. (1), are necessary, such as over windows of the center energy E and a small time interval $\Delta\tau\ll 1$.

Given full chaos, $K(\tau)$ is found to have a universal form, as obtained by averaging over certain *ensembles* of random matrices [2–4]. In the absence of geometric symmetries, the prediction of random-matrix theory (RMT) only depends on whether the system in question has no time-reversal ($\mathcal{T}$) invariance (unitary case), or is $\mathcal{T}$ invariant with either $\mathcal{T}^2=1$ (orthogonal case) or $\mathcal{T}^2=-1$ (symplectic case). RMT yields for $0<\tau<1$

$$K(\tau)=\begin{cases}\tau, & \text{unitary},\\ 2\tau-\tau\ln(1+2\tau) & \\ =2\tau-2\tau^2+2\tau^3-\cdots, & \text{orthogonal},\\ \dfrac{\tau}{2}-\dfrac{\tau}{4}\ln(1-\tau) & \\ =\dfrac{\tau}{2}+\dfrac{\tau^2}{4}+\dfrac{\tau^3}{8}+\cdots, & \text{symplectic}.\end{cases} \quad (3)$$

However, a proof of the faithfulness of individual chaotic dynamics to random-matrix theory, and even the assumptions required for a proof, have thus far remained a challenge. In the present paper, we take up the challenge and derive the small-τ expansion of $K(\tau)$ for *individual* systems; we employ ergodicity and hyperbolicity of the classical dynamics. Moreover, we require all classical relaxation times (related to Ruelle-Pollicott resonances and Lyapunov exponents) to be finite; we need this property to make sure that even the shortest quantum time scale of relevance, the so-called Ehrenfest time $T_E\sim\ln(\mathrm{const}/\hbar)$, is much larger than any classical time scale.

Following [5–7], we start from Gutzwiller's trace formula [8] which expresses the level density as a sum over classical periodic orbits γ,

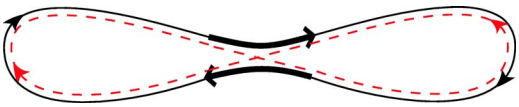

FIG. 1. (Color online) Sketch of a Sieber-Richter pair in configuration space. The partner orbits, depicted by solid and dashed lines, differ noticeably only inside an encounter of two orbit stretches (marked by antiparallel arrows, indicating the direction of motion). The sketch greatly exaggerates the difference between the two partner orbits in the loops outside the encounter and depicts the loops disproportionally short; similar remarks apply to all subsequent sketches of orbit pairs.

$$\rho_{\mathrm{osc}}(E) \sim \frac{1}{\pi\hbar}\mathrm{Re}\sum_{\gamma} A_\gamma e^{iS_\gamma/\hbar}, \tag{4}$$

wherein A_γ is the stability amplitude (including the Maslov phase) and S_γ the action of the γth orbit. By Eq. (4), the form factor becomes a double sum over orbits,

$$K(\tau) = \frac{1}{T_H}\left\langle \sum_{\gamma,\gamma'} A_\gamma A^*_{\gamma'} e^{(i/\hbar)(S_\gamma - S_{\gamma'})}\delta\left(\tau T_H - \frac{T_\gamma + T_{\gamma'}}{2}\right)\right\rangle; \tag{5}$$

T_γ is the period of γ. For $\hbar \to 0$, only families of orbit pairs with small action difference $|S_\gamma - S_{\gamma'}| \sim \hbar$ can give a systematic contribution to the form factor. For all others, the phase in Eq. (5) oscillates rapidly, and the contribution is killed by the averages indicated. Fluctuations in *quantum* spectra are thus related to *classical* correlations among orbit actions [6]. The first periodic-orbit approach to $K(\tau)$ was taken by Berry [5], who derived the leading term in Eq. (3) using "diagonal" pairs of coinciding ($\gamma' = \gamma$) and, for time $\mathcal{T}$-invariant dynamics, mutually time-reversed ($\gamma' = \mathcal{T}\gamma$) orbits, which obviously are identical in action. Starting with Argaman *et al.* [6], off-diagonal orbit pairs were studied in [9–11]. The potential importance of close self-encounters in orbit pairs was first spelled out in work on electronic transport [12] and qualitatively discussed for spectral fluctuations in [13].

The family of orbit pairs responsible for the next-to-leading order was definitely identified in Sieber's and Richter's seminal papers [7] for a homogeneously hyperbolic system, the Hadamard-Gutzwiller model (geodesic motion on a tesselated surface of negative curvature with genus 2). Their original formulation was based on small-angle self-crossings of periodic orbits in configuration space. In each pair, the partner γ' differs from γ only by narrowly avoiding one of its many self-crossings. The two orbits almost coincide in one of the two parts separated by the crossing, while they are nearly time reversed in the other part. In phase space, both orbits contain an "encounter" of two almost time-reversed orbit stretches. They differ only by their connections inside that encounter; see Fig. 1.

As shown in [14], Sieber's and Richter's reasoning can be extended to general fully chaotic two-freedom systems. One partner orbit γ' arises for each encounter. The action difference within each orbit pair [14–16] can be derived using the geometry of the invariant manifolds [17]. It thus turned out helpful to reformulate the treatment in terms of phase-space coordinates [15,16], which may also be applied to systems with more than 2 degrees of freedom [18].

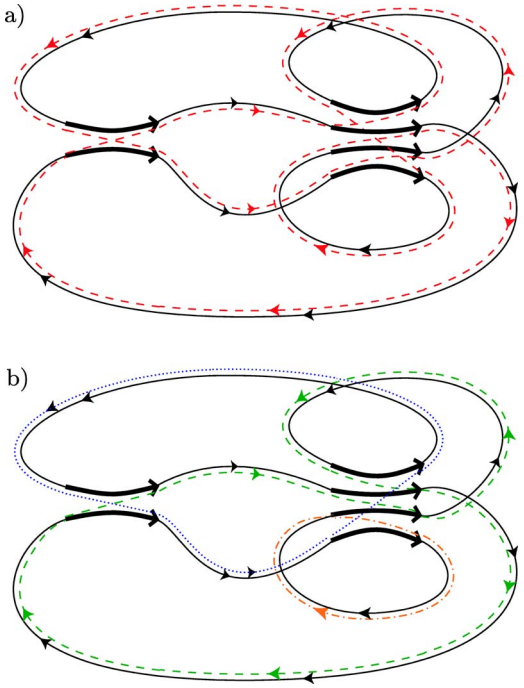

FIG. 2. (Color online) (a) Solid line: Periodic orbit γ with one 4-encounter and one 2-encounter highlighted by bold arrows. Dashed line: Partner γ' differing from γ by connections in the encounters. (b) Other reconnections yield a pseudo-orbit decomposing into three periodic orbits (dashed, dotted, and dash-dotted).

In [19], we showed that the τ^3 contribution to the form factor originates from pairs of orbits which differ either in two encounters of the above kind, or in one encounter that involves *three* orbit stretches.

In the present paper we demonstrate how the whole series expansion of $K(\tau)$ is obtained from periodic orbits. Beyond furnishing details left out in our previous Letter [20] we here cover systems with more than 2 degrees of freedom and from all three Wigner-Dyson symmetry classes. For the symplectic case we employ ideas presented in [21,22]. For related work on quantum graphs, see [23] for the first three orders of $K(\tau)$ and [24] for a complete treatment.

B. Overview

We set out to identify the families of orbit pairs responsible for all orders of the τ expansion. The key point is that long orbits have a huge number of close self-encounters which may involve arbitrarily many orbit stretches. We speak of an l-encounter whenever l stretches of an orbit get "close" in phase space. "Closeness" will be quantified below such that we may speak of the beginning, the end, and the duration of an encounter. Figure 2(a) highlights two such encounters inside a periodic orbit, one 2-encounter and one 4-encounter. Here, as always, we sketch orbit pairs in configuration space, with arrows $\rightrightarrows$ indicating the direction of motion inside the encounter stretches. The relevant encoun-

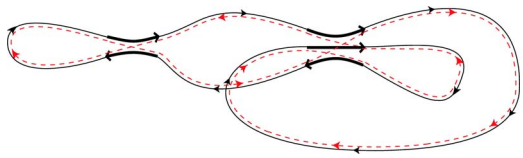

FIG. 3. (Color online) Periodic orbit γ with one 2- and one 3-encounter highlighted, and a partner γ' obtained by reconnection; the encounters depicted exist only in $\mathcal{T}$-invariant systems.

ters will turn out to have durations of the order of the Ehrenfest time $T_E \sim \ln(\text{const}/\hbar)$; even though logarithmically divergent in the semiclassical limit (and thus larger than all classical time scales), these encounter durations are vanishingly small compared to the orbit periods, which are of the order of the Heisenberg time, $T_\gamma \sim T_H \sim \hbar^{-f+1}$. In between different self-encounters an orbit goes through "loops," represented by thin full lines.

Self-encounters are of interest since they lead us from a periodic orbit γ to partners γ' which differ from γ noticeably only inside a set of encounters [see the dashed orbit in Fig. 2(a)]. In contrast, the orbit loops in between encounters are almost identical. The almost coinciding loops of γ and γ' are differently connected inside the encounters.

Not all reshufflings of connections inside an encounter yield a partner orbit. For example, reconnections as in Fig. 2(b) give rise to a "pseudo-orbit" decomposing into three separate periodic orbits. Pseudo-orbits are not admitted in the Gutzwiller trace formula.

For $\mathcal{T}$-invariant dynamics, we also must account for encounters whose stretches only get close *up to time reversal* as in $\rightleftarrows$ and $\rightleftarrows$; see Fig. 3. Correspondingly, loops inside mutual partner orbits may be related by time reversal.

We thus obtain a natural extension of Berry's diagonal approximation. Instead of considering only pairs of orbits which exactly coincide (or are mutually time reversed), we employ all pairs whose members are composed of similar (up to time reversal) loops.

We proceed to classify these orbit pairs. Partner orbits may differ in the *number* v_l of *l-encounters*; we shall assemble these numbers to a "vector" $\vec{v}=(v_2,v_3,\ldots)$. The total number of encounters is given by $V=\Sigma_{l\geqslant 2} v_l$. The number of orbit stretches involved in encounters, coinciding with the number of intervening loops, reads $L=\Sigma_{l\geqslant 2} l v_l$.

The orbit pairs (γ,γ') related to a fixed vector $\vec{v}$ may have various *structures*. Each structure corresponds to a different ordering (and, given $\mathcal{T}$ invariance, different sense of traversal) of the loops of γ inside the partner orbit γ'. When drawing orbit pairs as in Figs. 2 and 3, these structures differ by the order in which encounters are visited in the original orbit γ, and by the relative directions of the stretches within each encounter (i.e., $\rightrightarrows$ vs $\rightleftarrows$, or $\rightrightarrows$ vs $\rightleftarrows$ in time-reversal invariant systems). Moreover, different reconnections inside the same encounter may give rise to different partners, and hence different structures. We will see that structures have a one-to-one correspondence to permutations, which will be used in Sec. III to determine the number $N(\vec{v})$ of structures related to the same $\vec{v}$.

Orbit pairs sharing the same $\vec{v}$ and the same structure may still differ in the *phase-space separations* between the encounter stretches. We shall parametrize those separations by suitable variables s,u and determine their density $w_T(s,u)$ inside orbits of period T. The double sum (5) over orbits defining the spectral form factor will be written as a sum of contributions from families of orbit pairs, with the family weight proportional to $N(\vec{v})w_T(s,u)$.

This paper is organized as follows. To free the presentation of unnecessary details we mostly disregard complications due to $f>2$ and "nonhomogeneous" hyperbolicity (i.e., Lyapunov exponents different for different periodic orbits). In Sec. II, we will study the phase-space geometry of encounters and derive the density $w_T(s,u)$. The purely combinatorial task of determining the number of structures $N(\vec{v})$ is attacked in Sec. III with the help of the theory of permutations. We thus obtain series expansions of $K(\tau)$ for individual chaotic systems with and without $\mathcal{T}$ invariance; those series fully coincide with the RMT predictions for the Gaussian orthogonal ensemble (GOE) and the Gaussian unitary ensemble (GUE), respectively. Section IV generalizes these results to systems where spin dynamics accompanies translational motion; in particular, we find agreement with the Gaussian symplectic ensemble (GSE) given $\mathcal{T}$ invariance with $\mathcal{T}^2=-1$. In Sec. V, we show that our semiclassical procedure bears a close analogy to quantum field theory. In fact, our families of orbit pairs are equivalent to Feynman diagrams met within the theory of disordered systems and the perturbative implementation of the so-called nonlinear σ model. Finally, we present conclusions in Sec. VI. Further details, including a generalization to $f>2$ and nonhomogeneous hyperbolicity, and remarks on the action correlation function of [6], are given in the Appendices.

II. PHASE-SPACE GEOMETRY OF ENCOUNTERS

A. Fully chaotic dynamics

At issue are fully chaotic, i.e., hyperbolic and ergodic Hamiltonian flows without geometric symmetries with $f=2$ "classical" freedoms. In the orthogonal case, the Hamiltonian is assumed to be $\mathcal{T}$ invariant, $\mathcal{T}H\mathcal{T}^{-1}=H$, with an antiunitary time-reversal operator $\mathcal{T}$ squaring to unity. For convenience, we assume $\mathcal{T}$ to be the conventional time-reversal operator $\mathcal{T}(\mathbf{q},\mathbf{p})=(\mathbf{q},-\mathbf{p})$; that assumption does not restrict generality, since all Hamiltonians with nonconventional time-reversal invariance can be brought to conventionally time-reversal invariant form by a suitable canonical transformation [17].

For each phase-space point $\mathbf{x}=(\mathbf{q},\mathbf{p})$ it is possible to define a Poincaré surface of section $\mathcal{P}$ orthogonal to the trajectory passing through $\mathbf{x}$. Assuming a Cartesian configuration space (and thus a Cartesian momentum space), $\mathcal{P}$ consists of all points $\mathbf{x}+\delta\mathbf{x}=(\mathbf{q}+\delta\mathbf{q},\mathbf{p}+\delta\mathbf{p})$ in the same energy shell as $\mathbf{x}$ whose configuration-space displacement $\delta\mathbf{q}$ is orthogonal to $\mathbf{p}$. For $f=2$, $\mathcal{P}$ is a two-dimensional surface within the three-dimensional energy shell. Given hyperbolicity, $\mathcal{P}$ is spanned by one stable direction $\mathbf{e}^s(\mathbf{x})$ and one unstable direction $\mathbf{e}^u(\mathbf{x})$ [25]. We may thus decompose $\delta\mathbf{x}$ as

$$\delta\mathbf{x} = \hat{s}\mathbf{e}^s(\mathbf{x}) + \hat{u}\mathbf{e}^u(\mathbf{x}). \tag{6}$$

As long as two trajectories passing, respectively, through $\mathbf{x}$ and $\mathbf{x}+\delta\mathbf{x}$ remain sufficiently close, we may follow their separation by linearizing the equations of motion around one trajectory,

$$\hat{s}(t) = \Lambda(\mathbf{x},t)^{-1}\hat{s}(0),$$

$$\hat{u}(t) = \Lambda(\mathbf{x},t)\hat{u}(0). \tag{7}$$

Here, $\hat{s}(t)$ and $\hat{u}(t)$ denote stable and unstable components in a *comoving* Poincaré section at $\mathbf{x}(t)$, the image of $\mathbf{x}=\mathbf{x}(0)$ under time evolution over time t. In the long-time limit, the fate of the stretching factor $\Lambda(\mathbf{x},t)$ and thus of the stable and unstable components is governed by the (local) Lyapunov exponent $\lambda(\mathbf{x})>0$

$$\Lambda(\mathbf{x},t) \sim e^{\lambda(\mathbf{x})t}. \tag{8}$$

The $\mathbf{x}$ dependence of λ and Λ will be relevant only in Appendix B 1, when we treat nonhomogeneous hyperbolicity; until then, we may think of these quantities as constants. As in [15,16,18], the directions $\mathbf{e}^s(\mathbf{x})$ and $\mathbf{e}^u(\mathbf{x})$ are mutually normalized by fixing their symplectic product as

$$\mathbf{e}^u(\mathbf{x}) \wedge \mathbf{e}^s(\mathbf{x}) = \mathbf{e}^u(\mathbf{x})^T \begin{pmatrix} 0 & 1 \\ -1 & 0 \end{pmatrix} \mathbf{e}^s(\mathbf{x}) = 1. \tag{9}$$

In ergodic systems, almost all trajectories fill the corresponding energy shell uniformly. The time average of any observable along such a trajectory coincides with an energy-shell average.

Periodic orbits are exceptional in the sense that they cannot visit the whole energy shell. However, *long* periodic orbits still behave ergodically: According to the equidistribution theorem [26] (see also Appendix B 1), a time average over an orbit γ augmented by an average over all γ from a small time window, with the squared stability coefficient as a weight, equals the energy-shell average with the Liouville measure. A special case is the sum rule of Hannay and Ozorio de Almeida [27]

$$\left\langle \sum_{\gamma} |A_\gamma|^2 \delta(T - T_\gamma) \right\rangle_{\Delta T} = T. \tag{10}$$

Ergodicity makes, in the limit of long times, for a uniform return probability: A trajectory starting at $\mathbf{x}$ again pierces through $\mathcal{P}$ in a time interval $(t,t+dt)$ with stable and unstable components of $\mathbf{x}(t)-\mathbf{x}(0)$ [or $\mathcal{T}\mathbf{x}(t)-\mathbf{x}(0)$] lying in intervals $(\hat{s},\hat{s}+d\hat{s})$, $(\hat{u},\hat{u}+d\hat{u})$ with uniform probability $(1/\Omega)d\hat{s}\,d\hat{u}\,dt$.

B. Encounters

To parametrize an l-encounter, we introduce a Poincaré surface of section $\mathcal{P}$ transversal to the orbit at an arbitrary phase-space point $\mathbf{x}_1$ (passed at time t_1) inside one of the encounter stretches. The exact location of $\mathcal{P}$ inside the encounter is not important. The remaining stretches pierce through $\mathcal{P}$ at times t_j $(j=2,\ldots,l)$ in points $\mathbf{x}_j$. If the jth encounter stretch is close to the first one in phase space, we must have $\mathbf{x}_j \approx \mathbf{x}_1$; if it is almost time reversed with respect to the first one, we have $\mathcal{T}\mathbf{x}_j \approx \mathbf{x}_1$. In the following, we shall use the shorthand $\mathbf{y}_j \approx \mathbf{x}_1$ with $\mathbf{y}_j$ either $\mathbf{x}_j$ or $\mathcal{T}\mathbf{x}_j$.

The small difference $\mathbf{y}_j - \mathbf{x}_1$ can be decomposed in terms of the stable and unstable directions at $\mathbf{x}_1$,

$$\mathbf{y}_j - \mathbf{x}_1 = \hat{s}_j \mathbf{e}^s(\mathbf{x}_1) + \hat{u}_j \mathbf{e}^u(\mathbf{x}_1); \tag{11}$$

the stable and unstable components $\hat{s}_j, \hat{u}_j$ depend on the location $\mathbf{x}_1$ of the Poincaré section $\mathcal{P}$ chosen within the encounter. If we shift $\mathcal{P}$ through the encounter, the stable components will asymptotically decrease and the unstable components will asymptotically increase with growing t_1, according to Eqs. (7) and (8).

We can now give a more precise definition of an l-encounter. To guarantee that all l stretches are mutually close, we demand the stable and unstable differences $|\hat{s}_j|, |\hat{u}_j|$ of all stretches from the first one to be smaller than a constant c. The bound c must be chosen small enough for the motion around the l orbit stretches to allow for the mutually linearized treatment of Eq. (7); however, the exact value of c is irrelevant.

The stable and unstable coordinates determine the *duration* t_{enc} of an encounter. We have to sum the durations of the "head" of the encounter (i.e., the time t_u until the end of the encounter, when the first of the unstable components $|\hat{u}_j|$ reaches c) and its "tail" (i.e., the time t_s passed since the beginning of the encounter, when the last of the stable components $|\hat{s}_j|$ has fallen below c). Using the exponential divergence of the unstable phase-space separations (8), we see that the coordinates $|\hat{u}_j|$ approximately need the time $(1/\lambda)\ln(c/|\hat{u}_j|)$ to reach c; similarly, the stable coordinates need $(1/\lambda)\ln(c/|\hat{s}_j|)$. We thus obtain

$$t_u = \min_j \left\{ \frac{1}{\lambda} \ln \frac{c}{|\hat{u}_j|} \right\}, \quad t_s = \min_j \left\{ \frac{1}{\lambda} \ln \frac{c}{|\hat{s}_j|} \right\},$$

$$t_{\mathrm{enc}} = t_s + t_u = \frac{1}{\lambda} \ln \frac{c^2}{\max_i\{|\hat{s}_i|\} \max_j\{|\hat{u}_j|\}}; \tag{12}$$

in view of Eq. (7), the duration t_{enc} remains invariant if the Poincaré section $\mathcal{P}$ is shifted through the encounter.

An l-encounter involves l different orbit stretches whose initial and final phase-space points will be referred to as "entrance" and "exit" ports. If all encounter stretches are (almost) parallel, as in $\rightrightarrows$, all entrance ports are located on the same side of the encounter, and the exit ports are located on the opposite side. If the encounter involves mutually time-reversed orbit stretches like $\rightleftarrows$, this is no longer the case. Thus, it is useful to introduce the following convention: All ports on the side where the first stretch begins are called "left ports," while those on the opposite side are "right ports." For parallel encounters, entrance and "left" are synonymous, as well as exit and "right."

C. Partner orbits

The partner orbits (γ,γ') differ from one another only inside the encounters, by their connections between left and right ports. We shall number these ports in order of traversal by γ, such that the ith encounter stretch of γ connects left

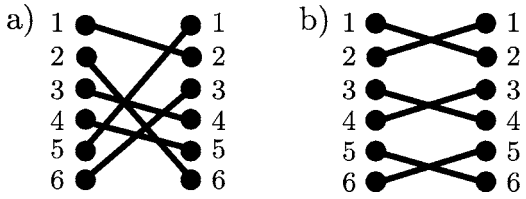

FIG. 4. Connections between left and right ports in partner orbit γ'. In (b), the encounter splits into three pieces, respectively, containing the two upper, middle, and lower stretches.

port i to right port i. Inside γ', the left port i is connected to a different right port j; see Fig. 4(a).

We must reshuffle connections between *all* stretches of a given encounter. In contrast, Fig. 4(b) shows reconnections only between stretches 1 and 2, stretches 3 and 4, and stretches 5 and 6 of a 6-encounter, which therefore decomposes into three 2-encounters.

1. Piercing points

The partner γ' also pierces through our Poincaré section $\mathcal{P}$. The corresponding piercing points are determined by those of γ. In particular, the unstable coordinates of a piercing point depend on the following right port. If two stretches of γ and γ' lead to the same right port, they have to approach each other for a long time—at least until the end of the encounter (which has a duration $\sim T_E$) and halfway through the subsequent loop. Hence, their difference must be close to the stable manifold, and the unstable coordinates almost coincide. Similarly, the stable coordinates are determined by the previous left port, since stretches with the same left port approach for large negative times. If a stretch of γ' connects left port i to right port j, it thus pierces through our Poincaré section with stable and unstable coordinates

$$\hat{s}_i' \approx \hat{s}_i, \quad \hat{u}_i' \approx \hat{u}_j. \tag{13}$$

For instance, if γ and γ' differ in a 2-encounter, γ' connects left port 1 to right port 2, and left port 2 to right port 1; see Fig. 5(a). Thus, the encounter stretches of γ' pierce through $\mathcal{P}$ in $\mathbf{y}_1'$ with $\hat{s}_1' \approx \hat{s}_1 = 0$, $\hat{u}_1' \approx \hat{u}_2$, and in $\mathbf{y}_2'$ with $\hat{s}_2' \approx \hat{s}_2$, $u_2' \approx \hat{u}_1 = 0$, which together with the piercings of γ span a parallelogram in phase space [17] [a rectangle in Fig. 5(b), by artist's license]. In Fig. 6, we visualize the locations of $\mathbf{y}_i'$ inside $\mathcal{P}$ for a 3-encounter.

2. Action difference

We can now determine the difference between the actions of the two partner orbits, first for γ, γ' only differing in one 2-encounter. Generalizing the results for configuration-space crossings in [7,14], we will show that the action difference is just the symplectic area of the rectangle in Fig. 5(b) [15,16]. Consider two segments of the encounter stretches in Fig. 5(a), leading from the first left port to the piercing point $\mathbf{x}_1$ of γ, and to the piercing point $\mathbf{y}_1'$ of γ', respectively. Since the action variation brought about by a shift $d\mathbf{q}$ of the final coordinate is $\mathbf{p} \cdot d\mathbf{q}$, the action difference between the two segments will be given by $\Delta S^{(1)} = \int_{\mathbf{y}_1'}^{\mathbf{x}_1} \mathbf{p} \cdot d\mathbf{q}$. The integration line

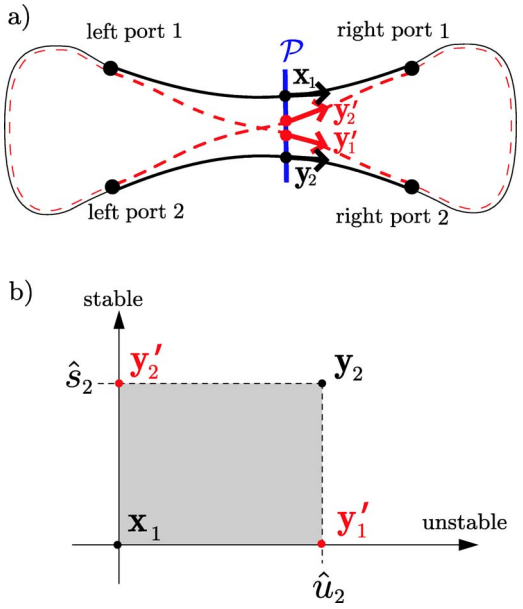

FIG. 5. (Color online) Piercings $\mathbf{x}_1, \mathbf{y}_2$ of γ (full line) and piercings $\mathbf{y}_1', \mathbf{y}_2'$ of γ' (dashed line) for a Sieber-Richter pair, depicted (a) in configuration space, with arrows indicating the momentum of the above phase-space points, and (b) in the Poincaré section $\mathcal{P}$ parametrized by stable and unstable coordinates. The symplectic area of the rectangle is the action difference ΔS.

may be chosen to lie in the Poincaré section; then it coincides with the unstable axis. Repeating the same reasoning for the remaining segments, we obtain the overall action difference $\Delta S \equiv S_\gamma - S_{\gamma'}$ as the line integral $\Delta S = \oint \mathbf{p} \cdot d\mathbf{q}$ along the contour of the parallelogram $\mathbf{y}_1' \to \mathbf{x}_1 \to \mathbf{y}_2' \to \mathbf{y}_2 \to \mathbf{y}_1'$, spanned by $\mathbf{y}_1' - \mathbf{x}_1 = \hat{u}_2 \mathbf{e}^u(\mathbf{x}_1)$ and $\mathbf{y}_2' - \mathbf{x}_1 = \hat{s}_2 \mathbf{e}^s(\mathbf{x}_1)$. This integral indeed gives the symplectic area

$$\Delta S = \hat{u}_2 \mathbf{e}^u(\mathbf{x}_1) \wedge \hat{s}_2 \mathbf{e}^s(\mathbf{x}_1) = \hat{s}_2 \hat{u}_2. \tag{14}$$

To generalize to arbitrary l-encounters, we imagine a partner orbit γ' constructed out of γ by $l-1$ successive steps, as illustrated for a special example in Fig. 7. Each step interchanges the right ports of two encounter stretches and con-

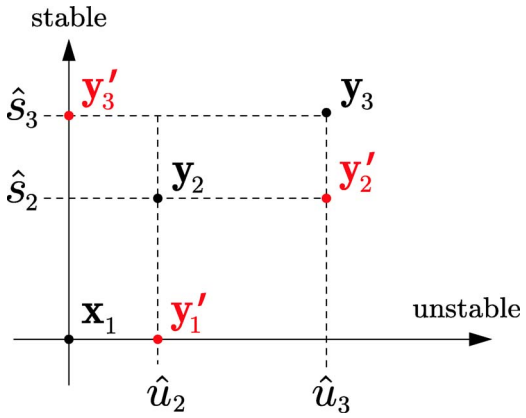

FIG. 6. (Color online) Piercing points of γ, γ' differing in a 3-encounter; inside γ', left ports 1,2,3 are connected to right ports 2,3,1, respectively.

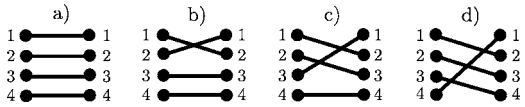

FIG. 7. Steps from connections in γ [depicted in (a)] to those in γ' [shown in (d)], in each step interchanging right ports of two encounter stretches.

tributes to the action difference an amount given by Eq. (14). At the same time, the two piercings points change their position as discussed in Sec. II C 1. This step-by-step process suggests a useful transformation of coordinates. Let s_j, u_j denote the stable and unstable differences between the two stretches affected by the jth step. Note that in contrast to $\hat{s}_j, \hat{u}_j$ the index j no longer represents encounter stretches 2,…, l but steps 1,…, $(l-1)$. Now, the change of action in each step is simply given by $s_j u_j$. Summing over all steps, we obtain a total action difference

$$\Delta S = \sum_{j=1}^{l-1} s_j u_j. \tag{15}$$

The transformation leading from $\hat{s}_j, \hat{u}_j$ to s_j, u_j is linear and volume preserving.[1] Due to the elegant form of Eq. (15), it will be convenient to use s_j, u_j rather than $\hat{s}_j, \hat{u}_j$ in defining the encounter regions, demanding all $|s_j|, |u_j|$ to be smaller than our bound c. Employing Eq. (7), one easily shows that ΔS remains invariant if the Poincaré section $\mathcal{P}$ is shifted through the encounter. Moreover, if the orbits γ and γ' differ in several encounters, the total action difference is additive in their contributions, and each is given by Eq. (15).

At this point, we can finally appreciate that the encounters relevant for spectral universality have a duration of the order of the Ehrenfest time. The form factor is determined by orbit pairs with an action difference ΔS of order $\hbar$. According to our expression (14) for ΔS, the relevant stable and unstable coordinates are of the order $\sqrt{\hbar}$. The encounter duration, logarithmic in s and u, must consequently be of the order of the Ehrenfest time.

D. Structures

We want to define more precisely the notion of "structures" of orbit pairs γ, γ'.

(i) First of all, these structures are characterized by *the order in which encounters are traversed in* γ. We enumerate the encounter stretches of γ in their order of traversal, starting from some arbitrarily chosen stretch, and assemble the labels 1,…, $L(\vec{v})$ in $V = V(\vec{v})$ groups according to the encounters they belong to. Such a division uniquely defines the order in which the encounters are visited. For example, in an orbit pair differing in two 2-encounters the four stretches can be distributed among the encounters as (1,2)(3,4) or (1,3)(2,4) or (1,4)(2,3); each of these three possibilities determines a different structure.

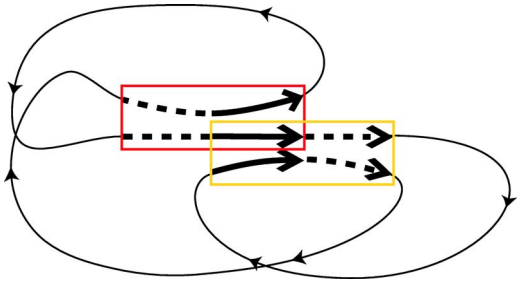

FIG. 8. (Color online) Two 2-encounters (marked by boxes) overlap in one stretch and thus merge to a 3-encounter (solid bold arrows)

Some structures refer to the same orbit pair. Indeed, a different choice of the initial stretch in the same γ would lead to a cyclic shift in the enumeration of stretches, and that shift may change the structure associated with γ. In the example of two 2-encounters, cyclic shifts may either leave the structure (1,2)(3,4) invariant or turn it into (1,4)(2,3), such that the structures (1,2)(3,4) and (1,4)(2,3) are physically equivalent.

Moreover, structures are characterized (ii) by the *relative directions* of the encounter stretches (i.e., $\rightrightarrows$ or $\rightleftarrows$ for 2-encounters, and $\rightrightarrows$ or $\rightleftarrows$ for 3-encounters in $\mathcal{T}$-invariant systems), and (iii) by the *reconnections* leading from γ to γ'; the latter distinction is important if there exist several such reconnections inside the same encounter set, each leading to a different connected partner.

E. Statistics of encounter sets

The statistics of close self-encounters inside periodic orbits can be established using the *ergodicity* of the classical motion. As a second ingredient, it is important to only consider sets of encounters whose stretches are *separated by nonvanishing loops, i.e., do not overlap*. For example, if two stretches of *different encounters* overlap, the two encounters effectively merge, leaving one larger encounter with more internal stretches; see Fig. 8. The partners are thus seen as differing in one larger encounter, rather than in two smaller ones. For the more involved case of stretches belonging to the same encounter; see Appendix D.

In the following, we will consider encounter sets within orbit pairs (γ, γ') with fixed $\vec{v}$ and fixed structure. Each of the V encounters of γ is parametrized with the help of a Poincaré section $\mathcal{P}_\alpha$ $(\alpha = 1, \ldots, V)$ crossing the orbit at an arbitrary phase-space point inside the encounter, traversed at time $t_{\alpha 1}$. The orbit again pierces through these sections at times $t_{\alpha j}$ with $j = 2, \ldots, l_\alpha$ numbering the remaining stretches of the αth encounter. The first piercing may occur anywhere

[1] First, consider reconnections as depicted in Fig. 7(d) for $l=4$. We proceed from Fig. 7(a) to Fig. 7(d) in $l-1=3$ steps. In the jth step, we change connections between left ports j and $j+1$, and right ports 1 and $j+1$. Recall that stable and unstable coordinates of piercing points are determined by the left and right ports, respectively. Thus, the separation between the stretches affected has a stable component $s_j = \hat{s}_{j+1} - \hat{s}_j$ and an unstable component $u_j = \hat{u}_{j+1} - \hat{u}_1$. The Jacobian of the transformation $\hat{s}, \hat{u} \to s, u$ is equal to 1. All other permissible reconnections can be brought to a form similar to Fig. 7(d) (albeit with different l), by appropriately changing the numbering of stretches; hence they allow for the same step-by-step procedure.

inside the orbit at a time $0<t_{11}<T$, T denoting the period. The remaining $t_{\alpha j}$ follow in an order fixed by the structure at times $t_{11}<t_{\alpha j}<T+t_{11}$. Each of the v_l l-encounters is characterized by $l-1$ *stable and unstable coordinates* $s_{\alpha j},u_{\alpha j}(j=1,\ldots,l-1)$, which in total make for $2\Sigma_{l\geqslant 2}(l-1)v_l=2(L-V)$ components. If $\mathcal{P}_\alpha$ is shifted through the encounter, the stable and unstable coordinates change while the contributions to the action difference $\Delta S_{\alpha j}=s_{\alpha j}u_{\alpha j}$ remain invariant.

We proceed to derive a density $w_T(s,u)$ of phase-space separations s,u. To understand the normalization of $w_T(s,u)$, assume that it is multiplied with $\Pi_{\alpha j}\delta(\Delta S_{\alpha j}-s_{\alpha j}u_{\alpha j})$ and integrated over all s,u. The result will be the average density of partners γ' per one orbit γ such that the pair (γ,γ') has the given structure and action difference components $\Delta S_{\alpha j}$. Averaging will be carried out over the ensemble of all periodic orbits γ with period T in a given time window, assuming that the contribution of each orbit is weighted with the square of its stability amplitude. According to the equidistribution theorem this ensemble is ergodic yielding the same averages as integrating over the energy shell with the Liouville measure.

We need to count the piercings through Poincaré sections parametrized by stable and unstable coordinates. Due to ergodicity, the expected number of such piercings through a given section in the time interval $(t,t+dt)$ with stable and unstable components in $(\hat{s},\hat{s}+d\hat{s})\times(\hat{u},\hat{u}+d\hat{u})$ is equal to $d\hat{s}\,d\hat{u}\,dt/\Omega$, i.e., corresponds to the uniform Liouville density $1/\Omega$.

In fact, we need the number of *sets* of $L-V$ piercings through our sections $\mathcal{P}_\alpha$ occurring in time intervals $(t_{\alpha j},t_{\alpha j}+dt_{\alpha j})$, $j=2,\ldots,l_\alpha$, with stable and unstable coordinates inside $(s_{\alpha j},s_{\alpha j}+ds_{\alpha j})$, $(u_{\alpha j},u_{\alpha j}+du_{\alpha j})$, $j=1,\ldots,l_\alpha-1$; that number will be denoted by $\rho_T(s,u)d^{L-V}s\,d^{L-V}u\,d^{L-V}t$. The uniform Liouville density carries over to the coordinates $s_{\alpha j},u_{\alpha j}$ since the transformation from $\hat{s},\hat{u}$ to s,u is volume preserving; so we may expect $\rho_T(s,u)$ equal to $1/\Omega^{L-V}$.

However, recall that we are only interested in encounters separated by nonvanishing loops. To implement that restriction, we employ a suitable characteristic function $\Theta_T(s,u,t)$ which vanishes if the piercings described by s, u, and t correspond to overlapping stretches, and otherwise equals 1. We thus obtain

$$\rho_T(s,u,t)=\Theta_T(s,u,t)\frac{1}{\Omega^{L-V}}. \tag{16}$$

(Actually the duration of the connecting loops must be not just positive but also larger than all classical relaxation times describing correlation decay, to guarantee the statistical independence of the piercings. However, that classical minimal loop length t_{cl} is not worth further mention since it is vanishingly small compared to the Ehrenfest time, the smallest time scale of semiclassical relevance.)

Proceeding toward $w_T(s,u)$ we integrate over the $L-V$ piercing times $t_{\alpha j}$, $j\geqslant 2$, still for fixed Poincaré sections $\mathcal{P}_\alpha$. The integral yields a density of the stable and unstable components s,u of $L-V$ piercings, reckoned from the V reference piercings. To finally get to w_T, we must keep track of all encounters along the orbits in question. To that end we have to consider all possible positions of Poincaré sections and thus integrate over the times $t_{\alpha 1}$ (of the reference piercings) as well. Doing so, we weigh each encounter with its duration t^α_{enc}, since we may move each Poincaré section to any position inside the duration of the encounter. In order to count each encounter set exactly once, we divide out the factors t^α_{enc}, and thus arrive at the desired density

$$w_T(s,u)=\frac{\int d^Lt\,\Theta_T(s,u,t)}{\prod_\alpha t^\alpha_{\mathrm{enc}}\Omega^{L-V}}. \tag{17}$$

It remains to evaluate the L-fold time integral in Eq. (17). The integration over t_{11} runs from 0 to T; it will be done as the last integral and then give a factor T. The $L-1$ other $t_{\alpha j}$ must lie inside the interval $(t_{11},t_{11}+T)$ and respect the ordering dictated by the encounter structure. Moreover, subsequent encounter stretches must not overlap. Thus, the time between the piercings of two subsequent stretches must be so large as to contain both the head of the first stretch and, after a nonvanishing loop, the tail of the second stretch. (Given $\mathcal{T}$ invariance, we rather need to include the tail of the first stretch, if it is time reversed with respect to the earliest stretch of its encounter; likewise the second stretch may also participate with its head.) These minimal distances sum up to the total duration of all encounter stretches $\Sigma_\alpha l_\alpha t^\alpha_{\mathrm{enc}}$, since each stretch appears in this sum once with head and tail.

The minimal distances effectively reduce the integration range, as we may proceed to a new set of times $\tilde{t}_{\alpha j}$ obtained by subtracting from $t_{\alpha j}$ both t_{11} and the sum of minimal distances between t_{11} and $t_{\alpha j}$. The $\tilde{t}_{\alpha j}$ just have to obey the ordering in question, and lie in an interval $(0,T-\Sigma_\alpha l_\alpha t^\alpha_{\mathrm{enc}})$, where the subtrahend is the total sum of minimal distances. We are thus left with a trivial integral over a constant. Perhaps surprisingly, the resulting density

$$w_T(s,u)=\frac{T\left(T-\sum_\alpha l_\alpha t^\alpha_{\mathrm{enc}}\right)^{L-1}}{(L-1)!\prod_\alpha t^\alpha_{\mathrm{enc}}\Omega^{L-V}} \tag{18}$$

depends only on $\vec{v}$ but not on the structure considered, and that fact strongly simplifies our treatment.

The number $P_{\vec{v}}(\Delta S)d\Delta S$ of orbit pairs with given $\vec{v}$ and action difference within $(\Delta S,\Delta S+d\Delta S)$ now reads

$$P_{\vec{v}}(\Delta S)d\Delta S=d\Delta S\frac{N(\vec{v})}{L}\times\int d^{L-V}s\,d^{L-V}u\,\delta\left(\Delta S-\sum_{\alpha j}s_{\alpha j}u_{\alpha j}\right)w_T(s,u) \tag{19}$$

where $N(\vec{v})$ is the number of structures existing for the given $\vec{v}$. [$P_{\vec{v}}(\Delta S)$ is closely related to the action correlation function of Ref. [6]; compare Appendix C.] Multiplication by $N(\vec{v})$ is equivalent to summation over all structures belonging to the same $\vec{v}$, since w_T is the same for all such structures. The denominator L prevents an overcounting. To understand

this, remember that one encounter stretch was arbitrarily singled out as "the first" and assigned the piercing time t_{11}. Each of the L possible such choices leads to a different parametrization by s,u of the same encounter set, and may also lead to a different structure. The integral over s,u in Eq. (19) includes the contributions of all equivalent parametrizations, and this is why the factor L must be divided out.

F. Contribution of each structure

To determine the spectral form factor, we have to evaluate the double sum over periodic orbits γ,γ' in Eq. (5). In doing so, we will account for all families of orbit pairs whose members are composed of loops similar up to time reversal, i.e., both "diagonal" pairs and orbit pairs differing in encounters. We assume that these are the only orbit pairs to give rise to a systematic contribution (an assumption that will be further discussed in the conclusions). For the pairs γ,γ' related to encounters not only the action difference $S_\gamma - S_{\gamma'}$ but also the difference of the stability amplitudes and the difference of the periods are very small.[2] Since only the action difference is discriminated by the small quantum unit we may simplify the double sum (5) as

$$K(\tau) = \frac{1}{T_H}\left\langle \sum_{\gamma,\gamma'} |A_\gamma|^2 e^{i(S_\gamma - S_{\gamma'})/\hbar}\delta(\tau T_H - T_\gamma)\right\rangle. \tag{20}$$

The summation over γ is evaluated using the rule of Hannay and Ozorio de Almeida (10). The diagonal pairs contribute $\kappa\tau$, with $\kappa=1$ in the unitary and 2 in the orthogonal case. The sum over partners γ' differing from γ in encounters can be performed with the help of the density $P_{\vec{v}}(\Delta S)$,

$$K(\tau) = \kappa\tau + \kappa\tau\sum_{\vec{v}} \int d\Delta S\, P_{\vec{v}}(\Delta S) e^{i\Delta S/\hbar}. \tag{21}$$

The factor κ in the second member is inserted since apart from the partner orbits considered so far, time-reversal invariance demands we also take into account their time-reversed versions; the factor τ comes from the sum rule, setting $\tau = T/T_H$. Substituting Eq. (19) for $P_{\vec{v}}(\Delta S)$ we get

$$K(\tau) = \kappa\tau + \kappa\tau\sum_{\vec{v}} N(\vec{v}) \int d^{L-V}s\, d^{L-V}u \frac{w_T(s,u)}{L} \times \exp\left(\frac{i}{\hbar}\sum_{\alpha j} s_{\alpha j}u_{\alpha j}\right). \tag{22}$$

Here, the orbit pairs with fixed $\vec{v}$, structures, and separations s,u appear with the weight $N(\vec{v})w_T(s,u)/L$.

The integral over s and u, multiplied by $\kappa\tau$, yields the contribution to the form factor from each structure associated with $\vec{v}$. The integral is surprisingly simple to do. Consider the multinomial expansion of $(T-\Sigma_\alpha l_\alpha t^\alpha_{\rm enc})^{L-1}$ in our expression (18) for the density $w_T(s,u)$. We shall show that only a single term of that expansion contributes, the one that involves a product of all $t^\alpha_{\rm enc}$ and therefore cancels with the denominator,

$$\frac{w_T^{\rm contr}}{L} = \frac{T}{L!\ \Omega^{L-V}} \frac{(L-1)!\, T^{L-V-1}\prod_\alpha (-l_\alpha)}{(L-V-1)!} = h(\vec{v})\left(\frac{T}{\Omega}\right)^{L-V}, \tag{23}$$

$$h(\vec{v}) \equiv \frac{(-1)^V \prod_l l^{v_l}}{L(L-V-1)!}.$$

Due to the cancellation of $t^\alpha_{\rm enc}$, $w_T^{\rm contr}$ does not depend on the stable and unstable coordinates and therefore the remaining integral over s and u is easily calculated,

$$\kappa\tau \int d^{L-V}s\, d^{L-V}u \frac{w_T^{\rm contr}}{L}\exp\left(\frac{i}{\hbar}\sum_{\alpha j} s_{\alpha j}u_{\alpha j}\right) = \kappa\tau h(\vec{v})\left(\frac{T}{\Omega}\right)^{L-V}\int_{-c}^{c} d^{L-V}s\, d^{L-V}u \exp\left(\frac{i}{\hbar}\sum_{\alpha j} s_{\alpha j}u_{\alpha j}\right) \to \kappa h(\vec{v})\tau^{L-V+1}; \tag{24}$$

we have just met with the $(L-V)$th power of the integral

$$\int_{-c}^{c} ds\, du\, e^{isu/\hbar} \to 2\pi\hbar \tag{25}$$

and used $2\pi\hbar T/\Omega = T/T_H = \tau$. In the semiclassical limit, the contributions of all other terms in the multinomial expansion vanish for one of two possible reasons.

First, consider terms in which at least one encounter duration $t^\alpha_{\rm enc}$ in the *denominator* is not compensated by a power of $t^\alpha_{\rm enc}$ in the numerator. The corresponding contribution to the form factor is proportional to

$$\int_{-c}^{c}\prod_j ds_{\alpha j}du_{\alpha j}\frac{1}{t^\alpha_{\rm enc}}\exp\left(\frac{i}{\hbar}\sum_j s_{\alpha j}u_{\alpha j}\right). \tag{26}$$

As shown in Appendix A, such integrals oscillate rapidly and effectively vanish in the semiclassical limit, as $\hbar\to 0$.

Second, there are terms with, say, p factors $t^\alpha_{\rm enc}$ in the *numerator* left uncanceled. To show that such terms do not contribute we employ a scaling argument. Obviously, the considered terms may only involve a smaller order of T than $w_T^{\rm contr}$; they are of order T^{L-V-p}. However, Ω still appears in the same order $1/\Omega^{L-V}$. To study the scaling with $\hbar$, we transform to variables $\tilde{s}_{\alpha j} = s_{\alpha j}/\sqrt{\hbar}$, $\tilde{u}_{\alpha j} = u_{\alpha j}/\sqrt{\hbar}$, eliminating the $\hbar$ dependence in the phase factor of Eq. (22). The resulting expression is proportional to $\hbar^{L-V}$ due to the Jacobian of the foregoing transformation, and proportional to $(\ln\hbar)^p$ due to the p remaining encounter durations $\sim\ln\hbar$. Together with the factor τ originating from the sum rule, the corresponding contribution to the form factor scales as

[2] As shown in [18], the quantities determining A_γ (the period, the Lyapunov exponent, and the Maslov index of γ) may be written as integrals of time-reversal invariant quantities along the orbit; see also [14,16,28] for the Maslov index. Since γ' locally almost coincides with γ up to time reversal, we have $A_\gamma \approx A_{\gamma'}$. For the case of the Hadamard-Gutzwiller model, a more careful treatment of these points is given in [29,30].

$$\tau T^{L-V-p}\left(\frac{\hbar}{\Omega}\right)^{L-V}(\ln\hbar)^p \propto \tau\frac{T^{L-V-p}}{T_H^{L-V}}(\ln\hbar)^p \propto \left(\frac{\ln\hbar}{T_H}\right)^p \tau^{L-V+1-p}, \tag{27}$$

and thus disappears as $\hbar\to 0$, $T_H\propto\hbar^{-1}\to\infty$.

Therefore, the contribution to the form factor arising from each structure with the same $\vec{v}$ is indeed determined by Eq. (24). Remarkably, this result is due to a subleading term in the multinomial expansion of $w_T(s,u)$, originating only from the small corrections due to the ban of encounter overlap.

The calculation of the form factor is now reduced to the purely combinatorial task of determining the numbers $N(\vec{v})$ of structures and evaluating the sum

$$K(\tau)=\kappa\tau+\kappa\sum_{\vec{v}} N(\vec{v})h(\vec{v})\tau^{L-V+1}. \tag{28}$$

The nth term in the series $K(\tau)=\kappa\tau+\Sigma_{n\geqslant 2}K_n\tau^n$ is exclusively determined by structures with $\nu(\vec{v})\equiv L(\vec{v})-V(\vec{v})+1=n$. It will be convenient to represent K_n as[3]

$$K_n=\frac{\kappa}{(n-2)!}\sum_{\vec{v}}^{\nu(\vec{v})=n}\tilde{N}(\vec{v}), \tag{29}$$

$$\tilde{N}(\vec{v})\equiv N(\vec{v})\frac{(-1)^V\prod_l l^{v_l}}{L(\vec{v})}. \tag{30}$$

The present reasoning can be generalized to nonhomogeneously hyperbolic systems with arbitrarily many degrees of freedom, again yielding Eqs. (29) and (30); the changes arising are listed in Appendix B.

III. COMBINATORICS

A. Unitary case

1. Structures and permutations

To determine the combinatorial numbers $N(\vec{v})$, first for systems without $\mathcal{T}$ invariance, we must relate structures of orbit pairs to permutations.

Most importantly, we require the notion of cycles [31]. We may denote a permutation of l objects (say the natural numbers 1,2,…,l) by $\{a\to P(a), a=1,\ldots,l\}$ or

$$P=\begin{pmatrix}1 & 2 & \ldots & l\\ P(1) & P(2) & \ldots & P(l)\end{pmatrix}.$$

An alternative bookkeeping starts with some object a_1 and notes the sequence of successors, $a_1\to a_2=P(a_1)\to a_3=P(a_2)\ldots$; if that sequence first returns to the starting object a_1 after precisely l steps one says that the permutation in question is a single cycle, denotable simply as $(a_1,a_2,\ldots,a_l)$. A cycle is defined up to cyclic permutations of its member objects. The number l of objects in a cycle is called the length of that cycle. Obviously, not every permutation is a cycle. A more general permutation can be decomposed into several cycles.

We now turn to applying the notion of cycles to self-encounters of a long periodic orbit γ and its partner orbit(s). We first focus on an orbit pair differing in a single l-encounter. This encounter involves l orbit stretches, whose entrance and exit ports will be labeled by 1,2,…, l. Inside γ the jth encounter stretch connects the jth entrance and the jth exit; the permutation defining which entrance port is connected to which exit port thus trivially reads

$$P_{\rm enc}^{\gamma}=\begin{pmatrix}1 & 2 & \ldots & l\\ 1 & 2 & \ldots & l\end{pmatrix}.$$

A partner orbit γ' differing from γ in the said encounter has the ports differently connected: The jth encounter stretch connects the jth entrance with a different exit $P_{\rm enc}(j)$. This reconnection can be expressed in terms of a different permutation

$$P_{\rm enc}=\begin{pmatrix}1 & 2 & \ldots & l\\ P_{\rm enc}(1) & P_{\rm enc}(2) & \ldots & P_{\rm enc}(l)\end{pmatrix};$$

e.g., reconnections as in Fig. 4(a) are described by the permutation

$$P_{\rm enc}=\begin{pmatrix}1 & 2 & 3 & 4 & 5 & 6\\ 2 & 6 & 4 & 5 & 1 & 3\end{pmatrix}.$$

Note that we refrain from indexing the latter permutation by a superscript γ'.

A permutation $P_{\rm enc}$ accounting for a single l-encounter is a single cycle of length l, e.g., (1,2,6,3,4,5) in the above example. If it were a multiple cycle, the encounter would effectively fall into several disjoint encounters. For example, Fig. 4(b) visualizes a permutation with three cycles (1, 2), (3, 4), and (5, 6). As already mentioned, reconnections take place only between stretches 1 and 2, stretches 3 and 4, and stretches 5 and 6, which thus have to be considered as three independent encounters.

If γ and γ' differ in several encounters, the connections between entrance and exit ports are reshuffled separately within these encounters. The corresponding permutation $P_{\rm enc}$ then has precisely one l-cycle corresponding to each of the v_l l-encounters, for all $l\geqslant 2$, the total number of permuted objects being $L=\Sigma_{l\geqslant 2}lv_l$.

We also have to account for the orbit loops. The ath loop connects the exit of the $(a-1)$st encounter stretch with the entrance of the ath one. These connections can be associated with the permutation

$$P_{\rm loop}=\begin{pmatrix}1 & 2 & \ldots & L\\ 2 & 3 & \ldots & 1\end{pmatrix}=(1,2,\ldots,L)$$

which obviously is single cycle. The order in which entrance ports (and thus loops) are traversed in γ is then given by the product $P^{\gamma}=P_{\rm loop}P_{\rm enc}^{\gamma}=P_{\rm loop}$. This product is single cycle—as it should be, because γ is a periodic orbit and hence returns to the first entrance port only after traversing all others.

Similarly, the sequence of entrance ports (or, equivalently, loops) traversed by γ' is represented by

$$P=P_{\rm loop}P_{\rm enc} \tag{31}$$

with the same $P_{\rm loop}$ as above. We must demand P to be single cycle for γ' not to decompose to a pseudo-orbit.

[3]We slightly depart from the notation in [20], where $\tilde{N}(\vec{v})$ was defined to include the denominator $(n-2)!$.

TABLE I. Permutations, and thus structures of orbit pairs, giving rise to orders τ^3 and τ^5 of the form factor, for systems without $\mathcal{T}$ invariance. We represent $\vec{v}$ by $(2)^{v_2}(3)^{v_3}\cdots$. The order of each contribution is given by $n=L-V+1$. We see that contributions add up to zero for odd n, whereas there are no permutations for even n.

Order	$\vec{v}$	L	V	$N(\vec{v})$	$\tilde{N}(\vec{v})$	Contribution
τ^3	$(2)^2$	4	2	1	1	$1\tau^3$
	$(3)^1$	3	1	1	−1	$-1\tau^3$
				Total	0	$0\tau^3$
τ^5	$(2)^4$	8	4	21	42	$7\tau^5$
	$(2)^2(3)^1$	7	3	49	−84	$-14\tau^5$
	$(2)^1(4)^1$	6	2	24	32	$16/3\,\tau^5$
	$(3)^2$	6	2	12	18	$3\tau^5$
	$(5)^1$	5	1	8	−8	$-4/3\,\tau^5$
				Total	0	$0\tau^5$

We shall denote by $\mathcal{M}(\vec{v})$ the set of permutations P_{enc} (representing intraencounter connections) which have v_l l-cycles, for each $l \geqslant 2$, and upon multiplication with P_{loop} yield single-cycle permutations as in Eq. (31). These permutations P_{enc} are in one-to-one correspondence to the structures of orbit pairs defined in Sec. II D, i.e., they determine how the encounter stretches are ordered, and how they are reconnected to form a partner orbit. The number of elements of $\mathcal{M}(\vec{v})$ is thus precisely the number $N(\vec{v})$ of structures related to $\vec{v}$.

2. Examples

The numbers $N(\vec{v})$ can be determined numerically, by generating all possible permutations P_{enc} with v_l l-cycles and counting only those for which $P=P_{\text{loop}}P_{\text{enc}}$ is single cycle. The P_{enc}'s contributing to the orders $n=3$ and 5 of the spectral form factor are shown in Table I.

Interestingly, no qualifying P_{enc}'s exist for even $L-V+1=n$. For example, the only candidate for $n=2$ would be $P_{\text{enc}}=\left(\begin{smallmatrix}1&2\\2&1\end{smallmatrix}\right)$, describing reconnections inside an encounter of two parallel orbit stretches $\rightrightarrows$. However, the corresponding partner decomposes into two separate periodic orbits [corresponding to the cycles 1 and 2 of $P=P_{\text{loop}}P_{\text{enc}}=\left(\begin{smallmatrix}1&2\\1&2\end{smallmatrix}\right)$]; see Fig. 9. The same happens for all other permutations with n even.[4]

For n odd, the individual numbers $N(\vec{v})$ and $\tilde{N}(\vec{v})$ do not vanish. However, we see in Table I that the $\tilde{N}(\vec{v})$ related to the same n sum up to zero. That remarkable cancellation, a nontrivial property of the permutation group to be discussed below, is the reason why all off-diagonal contributions to the spectral form factor vanish in the unitary case. For example, the τ^3 term is determined by $P_{\text{enc}}=\left(\begin{smallmatrix}1&2&3&4\\3&4&1&2\end{smallmatrix}\right)$ describing reconnections inside two 2-encounters of parallel stretches $\rightrightarrows$ (case *ppi* in [19]), and $P_{\text{enc}}=\left(\begin{smallmatrix}1&2&3\\2&3&1\end{smallmatrix}\right)$ describing reconnections inside a 3-encounter of parallel orbit stretches $\rightrightarrows$ (case *pc* in [19]). The respective contributions τ^3 and $-\tau^3$ mutually cancel; Fig. 10 displays the orbits.

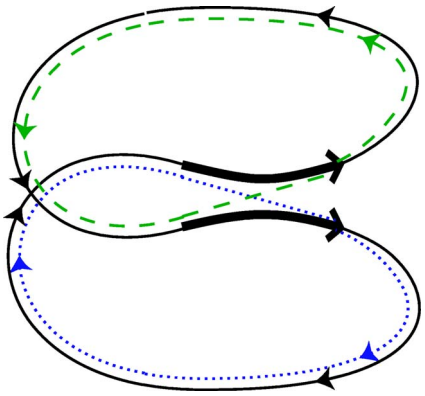

FIG. 9. (Color online) Reconnections inside a parallel 2-encounter yield a pseudo-orbit decomposing into two separate periodic orbits.

3. Recursion relation for $N(\vec{v})$

We now derive a recursion formula for $N(\vec{v})$, imagining one loop (e.g., the one with index L) of an orbit removed and studying the consequences on the encounters. We shall reason with permutations but the translation rule *cycle* $\rightarrow$ *encounter* yields an interpretation for orbits. Readers wanting to skip the reasoning may jump to the result in Eq. (44).

As a preparation, let us introduce a subset $\mathcal{M}(\vec{v},l)$ of $\mathcal{M}(\vec{v})$ such that the largest of the permuted numbers, i.e., $L(\vec{v})=\Sigma_k k v_k$, belongs to a cycle of length l (it is assumed that $v_l>0$). The full set can be obtained by applying to this subset all $L(\vec{v})$ possible cyclic permutations. In fact, we thus get the set $\mathcal{M}(\vec{v})$ in lv_l copies, since cyclic permutations shifting the element $L(\vec{v})$ inside an l-cycle or between different l-cycles with the same l leave the subset $\mathcal{M}(\vec{v},l)$ unchanged. Consequently, the sizes of $\mathcal{M}(\vec{v})$ and $\mathcal{M}(\vec{v},l)$ are related as

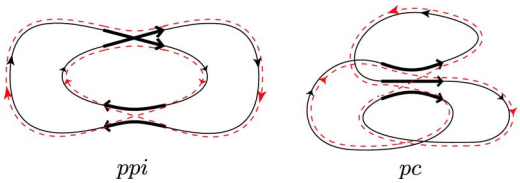

FIG. 10. (Color online) Two families of pairs of orbits differing in parallel encounters; both exist for systems with and without $\mathcal{T}$ invariance; each contributes to τ^3, but the contributions mutually cancel. For labels see text.

[4]The proof is based on the parities of the permutations involved. A permutation is said to have parity 1 if it can be written as a product of an even number of transpositions, and to be of parity −1 if it is a product of an odd number of transpositions. Parity is given by $(-1)^{L-V}$, where L is the number of permuted elements and V the number of cycles, and the parity of a product of permutations equals the product of parities of the factors. Since P and P_{loop} both consist of one single cycle, they are of the same parity. Therefore, $P=P_{\text{loop}}P_{\text{enc}}$ implies that all allowed P_{enc} need to have parity 1, i.e., $n=L-V+1$ must be odd.

$$N(\vec{v},l) = \frac{lv_l}{L(\vec{v})} N(\vec{v}). \tag{32}$$

We need a mapping that leads from a given permutation $P_{\rm enc}$ to a permutation $Q_{\rm enc}$ of smaller size, with a different cycle structure. Recall that any permutation $P_{\rm enc} \in \mathcal{M}(\vec{v},l)$ may be written as $P_{\rm enc} = P_{\rm loop}^{-1} P$, with $P_{\rm loop}$ the single-cycle permutation $(1,2,\ldots,L)$, and P single cycle as well. Now suppose that the element L (corresponding to the entrance port following the Lth orbit loop) is deleted from the cycle representations of both $P_{\rm loop}$ and P. We thus obtain two new single-cycle permutations $Q_{\rm loop}$ and Q, acting on the numbers $1,2,\ldots,L-1$. Here, $Q_{\rm loop}$ is simply given by $Q_{\rm loop} = (1,2,\ldots,L-1)$, and Q differs from P only by mapping the predecessor of L, i.e., $P^{-1}(L)$, to the successor of L, i.e., $P(L)$. Let us now define the new "encounter" permutation $Q_{\rm enc}$ in analogy to Eq. (31),

$$Q_{\rm enc} = Q_{\rm loop}^{-1} Q. \tag{33}$$

The $Q_{\rm enc}$ thus obtained acts on the elements $a = 1,2,\ldots, L-1$ as

$$Q_{\rm enc}(a) = \begin{cases} P_{\rm enc}(L) & \text{if } a = P_{\rm enc}^{-1}(L-1), \\ L-1 & \text{if } a = P_{\rm enc}^{-1}(L), \\ P_{\rm enc}(a) & \text{otherwise}. \end{cases} \tag{34}$$

To verify this, recall that $Q_{\rm loop}$ differs from $P_{\rm loop}$ only in the mapping of one number, as for Q and P. Thus $Q_{\rm enc}$ acts like $P_{\rm enc}$ on all but two numbers a. These exceptional cases, given in the first two lines of Eq. (34), are checked by carefully applying the above definitions of $Q_{\rm loop}$ and Q as follows:

$$\begin{aligned} Q_{\rm enc} P_{\rm enc}^{-1}(L-1) &= Q_{\rm loop}^{-1} Q P^{-1} P_{\rm loop}(L-1) \\ &= Q_{\rm loop}^{-1} Q P^{-1}(L) = Q_{\rm loop}^{-1} P(L) \\ &\overset{(*)}{=} P_{\rm loop}^{-1} P(L) = P_{\rm enc}(L), \end{aligned}$$

$$\begin{aligned} Q_{\rm enc} P_{\rm enc}^{-1}(L) &= Q_{\rm loop}^{-1} Q P^{-1} P_{\rm loop}(L) \\ &\overset{(**)}{=} Q_{\rm loop}^{-1} Q P^{-1}(1) = Q_{\rm loop}^{-1} P P^{-1}(1) \\ &= Q_{\rm loop}^{-1}(1) = L-1; \end{aligned} \tag{35}$$

here, we used $P(L) \neq 1$ for relation $(*)$, since otherwise $P_{\rm enc}$ would have a 1-cycle [i.e., $P_{\rm enc}(L) = P_{\rm loop}^{-1} P(L) = P_{\rm loop}^{-1}(1) = L$], and $P(L) \neq L$, since otherwise P would have a 1-cycle. To check relation $(**)$, we need $P^{-1}(1) \neq L$ [since $P(L) \neq 1$] and $P^{-1}(1) \neq P^{-1}(L)$.

We need to connect the cycle structures of $Q_{\rm enc}$ and $P_{\rm enc}$. Let us first consider the case that *the element $L-1$ of the permutation $P_{\rm enc}$ belongs to a different cycle than L*, say a k-cycle. Hence, $P_{\rm enc}$ has the form

$$P_{\rm enc} = [\cdots](L-1, a_2, a_3, \ldots, a_k)(L, b_2, b_3, \ldots, b_l) \tag{36}$$

where the two aforementioned cycles are written in parentheses, and $[\cdots]$ stands for all other cycles. Then $Q_{\rm enc}$ differs from $P_{\rm enc}$ by mapping $P_{\rm enc}^{-1}(L-1) = a_k$ to $P_{\rm enc}(L) = b_2$, and $P_{\rm enc}^{-1}(L) = b_l$ to $L-1$. It follows that the k- and l-cycles of $P_{\rm enc}$ merge to a $(k+l-1)$-cycle of

$$Q_{\rm enc} = [\cdots](L-1, a_2, a_3, \ldots, a_k, b_2, b_3, \ldots, b_l) \tag{37}$$

where $[\cdots]$ is the same as in Eq. (36). Compared to $P_{\rm enc}$, $Q_{\rm enc}$ has one k-cycle and one l-cycle less, but one additional $(k+l-1)$-cycle. The changed cycle structure with $v_k \to v_k - 1$, $v_l \to v_l - 1$, $v_{k+l-1} \to v_{k+l-1} + 1$ will be denoted as $\vec{v}^{[k,l \to k+l-1]}$. In general, $\vec{v}^{[\alpha_1,\ldots,\alpha_m \to \beta_1,\ldots,\beta_n]}$, $m \geq 0$, $n \geq 0$, denotes the vector obtained from $\vec{v}$ if we decrease all v_{α_i} by 1, increase all v_{β_i} by 1, and leave all other components unchanged; if no β_i appear on the right-hand side (RHS), no components of $\vec{v}$ are increased.

The permutation $Q_{\rm enc}$ thus belongs to the subset $\mathcal{M}(\vec{v}^{[k,l \to k+l-1]}, k+l-1)$ since the largest permuted number $L-1$ belongs to a cycle with the length $k+l-1$. Each $P_{\rm enc}$ with the structure (36) (k and l fixed) generates one member of this subset. Vice versa, for fixed k the $Q_{\rm enc}$ given in Eq. (37) uniquely determines one $P_{\rm enc}$ as given in Eq. (36). Hence, there are

$$N(\vec{v}^{[k,l \to k+l-1]}, k+l-1) \tag{38}$$

members of $\mathcal{M}(\vec{v},l)$ structured like Eq. (36). Physically, the present scenario corresponds to the merger of a k- and an l-encounter into a $(k+l-1)$-encounter, by shrinking away an intervening loop.

We now turn to the second scenario where *L and $L-1$ belong to the same l-cycle of $P_{\rm enc}$*. If L follows $L-1$ after m iterations [i.e., $L = P_{\rm enc}^m(L-1)$, $1 \leq m \leq l-2$],[5] the permutation $P_{\rm enc}$ is of the form

$$P_{\rm enc} = [\cdots](L-1, a_2, a_3, \ldots, a_m, L, a_{m+2}, \ldots, a_l). \tag{39}$$

According to Eq. (34), $Q_{\rm enc}$ differs from $P_{\rm enc}$ by mapping $P_{\rm enc}^{-1}(L-1) = a_l$ to $P_{\rm enc}(L) = a_{m+2}$ and mapping $P_{\rm enc}^{-1}(L) = a_m$ to $L-1$; $Q_{\rm enc}$ thus reads

$$Q_{\rm enc} = [\cdots](L-1, a_2, a_3, \ldots, a_m)(a_{m+2}, \ldots, a_l); \tag{40}$$

the l-cycle of $P_{\rm enc}$ is broken up into two cycles, with the lengths m and $l-m-1$. Since the largest number $L-1$ is included in an m-cycle, $Q_{\rm enc}$ belongs to $\mathcal{M}(\vec{v}^{[l \to m, l-m-1]}, m)$.

In contrast to the first scenario, there are typically several $P_{\rm enc}$ producing the same $Q_{\rm enc}$. Indeed Eq. (40) would result not only from Eq. (39), but also from all $l-m-1$ permutations $P_{\rm enc}$ obtained by cyclic permutation of the last elements $a_{m+2}, \ldots, a_l$ in Eq. (39). In addition, $[\cdots]$ in $P_{\rm enc}$ contains v_{l-m-1} cycles of length $l-m-1$. If we transpose the content of one of these cycles with the subsequence $a_{m+2}, \ldots, a_l$ in Eq. (39), the resulting $P_{\rm enc}$ will lead to the same $Q_{\rm enc}$. Thus, for each m, the subset of elements $P_{\rm enc} \in \mathcal{M}(\vec{v},l)$ structured like Eq. (39) is $(l-m-1)(v_{l-m-1}+1)$ times larger than $\mathcal{M}(\vec{v}^{[l \to m, l-m-1]}, m)$, i.e., it has the size

$$(l-m-1)(v_{l-m-1}+1) N(\vec{v}^{[l \to m, l-m-1]}, m). \tag{41}$$

[5] Note $m = l-1$ is excluded: otherwise P would have a 1-cycle because $L = P_{\rm enc}^{l-1}(L-1) = P_{\rm enc}^{-1}(L-1) = P^{-1} P_{\rm loop}(L-1) = P^{-1}(L)$.

We have now decomposed $\mathcal{M}(\vec{v},l)$ into several subsets of size $N(\vec{v}^{[k,l\to k+l-1]},k+l-1)$, $k\geqslant 2$, and further subsets of size $(l-m-1)(v_{l-m-1}+1)N(\vec{v}^{[l\to m,l-m-1]},m)$, $m=1,\ldots,l-2$. The size of $\mathcal{M}(\vec{v},l)$ thus reads

$$N(\vec{v},l)=\sum_{k\geqslant 2}N(\vec{v}^{[k,l\to k+l-1]},k+l-1)+\sum_{m=1}^{l-2}(l-m-1)(v_{l-m-1}+1)N(\vec{v}^{[l\to m,l-m-1]},m). \tag{42}$$

We may rewrite the latter equation using $N(\vec{v},l)=(lv_l/L(\vec{v}))N(\vec{v})$ and $\tilde{N}(\vec{v})=N(\vec{v})(-1)^V\Pi_l l^{v_l}/L(\vec{v})$, to get

$$v_l\tilde{N}(\vec{v})+\sum_{k\geqslant 2}(v_{k+l-1}+1)k\tilde{N}(\vec{v}^{[k,l\to k+l-1]})+\sum_{1\leqslant m\leqslant l-2}(v_{l-m-1}+1)v_m^{[l\to m,l-m-1]}\tilde{N}(\vec{v}^{[l\to m,l-m-1]})=0; \tag{43}$$

Eqs. (42) and (43) are the general recursion relations in search. (Note that $v_{k+l-1}+1=v_{k+l-1}^{[k,l\to k+l-1]}$. Of course, the kth summand vanishes if there are no k-cycles present, i.e., if $v_k=0$ and thus formally $v_k^{[k,l\to k+l-1]}=-1$.)

To determine the form factor for systems without time-reversal invariance, we need only the special case $l=2$. In this case, our recursion strongly simplifies,

$$v_2\tilde{N}(\vec{v})+\sum_{k\geqslant 2}v_{k+1}^{[k,2\to k+1]}k\tilde{N}(\vec{v}^{[k,2\to k+1]})=0, \tag{44}$$

since only the first of the two above scenarios is possible. That is, a 2-cycle may only merge with a k-cycle to form a $(k+1)$-cycle, but not split into two separate cycles. Recall that $\vec{v}^{[k,2\to k+1]}$ is obtained from $\vec{v}$ by decreasing both v_k and v_2 by 1, and increasing v_{k+1} by 1.

4. Spectral form factor

We had expressed the Taylor coefficients of the form factor as a sum over the combinatorial numbers $\tilde{N}(\vec{v})$,

$$K_n=\frac{1}{(n-2)!}\sum_{\vec{v}}^{\nu(\vec{v})=n}\tilde{N}(\vec{v}),\quad n\geqslant 2 \tag{45}$$

[see Eq. (29)], where the sum runs over all $\vec{v}$ with $v_1=0$ which satisfy $\nu(\vec{v})\equiv L(\vec{v})-V(\vec{v})+1=n$. Our recursion relation for $\tilde{N}(\vec{v})$ now translates into one for K_n, albeit a trivial one in the unitary case, implying that all K_n except K_1 vanish. (Alternatively, one may use a rather involved explicit formula for $N(\vec{v})$ [32].)

To show this, consider the recursion (44) for $\tilde{N}(\vec{v})$ and sum over $\vec{v}$ as above,

$$\sum_{\vec{v}}^{\nu(\vec{v})=n}\left(v_2\tilde{N}(\vec{v})+\sum_{k\geqslant 2}v_{k+1}^{[k,2\to k+1]}k\tilde{N}(\vec{v}^{[k,2\to k+1]})\right)=0. \tag{46}$$

Each of the sums $\Sigma_{\vec{v}}^{\nu(\vec{v})=n}v_{k+1}^{[k,2\to k+1]}\tilde{N}(\vec{v}^{[k,2\to k+1]})$ may be transformed into a sum over the argument of $\tilde{N}$, i.e., $\vec{v}'=\vec{v}^{[k,2\to k+1]}$. Due to $\nu(\vec{v})=n$, we also have $\nu(\vec{v}')=n$, since going from $\vec{v}$ to $\vec{v}'$ decreases both L and V by 1 and thus leaves ν invariant. Given that by construction we must have $v'_{k+1}\geqslant 1$, the sum over $\vec{v}'$ extends over all $\vec{v}'$ with $\nu(\vec{v}')=n$ and $v'_{k+1}\geqslant 1$. However, the latter restriction may be dropped because due to the prefactor v'_{k+1} terms with $v'_{k+1}=0$ do not contribute. Consequently, the sum may be simplified as

$$\sum_{\vec{v}}^{\nu(\vec{v})=n}v_{k+1}^{[k,2\to k+1]}\tilde{N}(\vec{v}^{[k,2\to k+1]})=\sum_{\vec{v}'}^{\nu(\vec{v}')=n}v'_{k+1}\tilde{N}(\vec{v}'). \tag{47}$$

Applying this rule to all terms in Eq. (46) and dropping the primes, we obtain

$$\sum_{\vec{v}}^{\nu(\vec{v})=n}\left(v_2+\sum_{k\geqslant 2}v_{k+1}k\right)\tilde{N}(\vec{v})=0. \tag{48}$$

Since the term in parentheses is just $\Sigma_{l\geqslant 2}v_l(l-1)=L-V=n-1$ we have

$$(n-1)\sum_{\vec{v}}^{\nu(\vec{v})=n}\tilde{N}(\vec{v})=(n-1)!\,K_n=0,\quad n\geqslant 2. \tag{49}$$

We see that all Taylor coefficients except K_1 vanish: orbit pairs differing in encounters yield no net contribution; the diagonal approximation exhausts the small-time form factor in full. GUE behavior is thus ascertained.

B. Orthogonal case

1. Structures and permutations

In $\mathcal{T}$-invariant systems the partners of an orbit γ may involve loops of both γ and its time-reversed $\bar{\gamma}$. To capture all partners γ' of γ in terms of permutations the permuted objects must refer to both γ and $\bar{\gamma}$ and thus be doubled in number compared to the unitary case. Each permutation will describe simultaneously both γ' and $\bar{\gamma}'$.

We number the entrance and exit ports of self-encounters of γ in their order of traversal, 1,2,…, L, such that the ath encounter stretch leads from the ath entrance to the ath exit port; see Fig. 11 for the example of a 2-encounter. The time-reversed orbit $\bar{\gamma}$ passes the same ports as γ, but with opposite sense and entrance and exit swapped. The ports of $\bar{\gamma}$ are labeled by $\bar{1},\bar{2},\ldots,\bar{L}$, such that the exit port $\bar{a}$ of $\bar{\gamma}$ is the time reversal of the entrance port a of γ, and the entrance port $\bar{a}$ of $\bar{\gamma}$ is the time reversal of the exit port a of γ; again compare Fig. 11. Consequently, inside $\bar{\gamma}$ the stretch $\bar{a}$ leads from entrance $\bar{a}$ to exit $\bar{a}$.

The intraencounter connections of γ and $\bar{\gamma}$ are represented by the trivial permutation

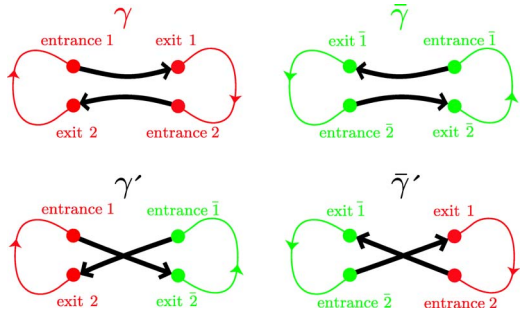

FIG. 11. (Color online) Entrance-to-exit connections for a Sieber-Richter pair, in an orbit γ, its time-reversed $\bar{\gamma}$, and the partners $\gamma', \bar{\gamma}'$.

$$P_{\text{enc}}^{\gamma} = \begin{pmatrix} 1\ 2 \ldots L\ \bar{1}\ \bar{2} \ldots \bar{L} \\ 1\ 2 \ldots L\ \bar{1}\ \bar{2} \ldots \bar{L} \end{pmatrix}$$

which maps each entrance (upper line) to the following exit (lower line). The loops are associated with

$$P_{\text{loop}} = \begin{pmatrix} 1\ 2 \ldots L\ \bar{2}\ \bar{3} \ldots \bar{1} \\ 2\ 3 \ldots 1\ \bar{1}\ \bar{2} \ldots \bar{L} \end{pmatrix},$$

since if one loop of γ leads from the exit of the $(a-1)$st stretch to the entrance of the ath one, its time reversal must go from exit $\bar{a}$ to entrance $\overline{a-1}$. Finally, $P^{\gamma} = P_{\text{loop}} P_{\text{enc}}^{\gamma} = P_{\text{loop}}$ specifies the ordering of entrance ports along γ and $\bar{\gamma}$. This P^{γ} has two cycles $(1,2,\ldots,L)$ and $(\bar{L}, \overline{L-1}, \ldots, \bar{1})$, one each for γ and $\bar{\gamma}$.

The reconnections leading to $\gamma', \bar{\gamma}'$ are described by a permutation P_{enc} determining the exit port connected to each entrance. In the example of a Sieber-Richter pair, Fig. 11, the partner γ' connects the entrance 1 of γ to the exit $\bar{2}$ of $\bar{\gamma}$, and the entrance $\bar{1}$ of $\bar{\gamma}$ to the exit 2 of γ. Including the connections in the time-reversed partner $\bar{\gamma}'$, we write

$$P_{\text{enc}} = \begin{pmatrix} 1\ 2\ \bar{1}\ \bar{2} \\ \bar{2}\ \bar{1}\ 2\ 1 \end{pmatrix}.$$

Note that the sequence of columns in P_{enc} may be ordered arbitrarily. We shall mostly order such that the first lines in P_{enc} and P_{enc}^{γ} coincide; columns describing γ' and $\bar{\gamma}'$ may thus become mutually interspersed.

$\mathcal{T}$ invariance imposes a restriction on P_{enc}: If a stretch connects entrance a to exit b, the time-reversed stretch must connect the entrance $\bar{b}$ of $\bar{\gamma}$ to the exit $\bar{a}$. Thus, if P_{enc} maps a to b, it has to map $\bar{b}$ to $\bar{a}$, with a, b standing for elements out of $1,\ldots, L, \bar{1}, \ldots, \bar{L}$ (we define $\bar{\bar{a}} = a$). This restriction on P_{enc} will be referred to as "$\mathcal{T}$ covariance."

It follows that if $(a_1, a_2, \ldots, a_{l-1}, a_l)$ is a cycle of P_{enc}, then so is its time-reversed partner $(\overline{a_l}, \overline{a_{l-1}}, \ldots, \overline{a_2}, \overline{a_1})$. These two cycles may not be identical. Indeed a cycle coinciding with its time reversal would have the form $(a_1, \ldots, a_k, \overline{a_k}, \ldots, \overline{a_1})$, $k = l/2$; such cycles are not allowed, since the entrance port a_k and the exit port $\overline{a_k}$ coincide in configuration space and thus may not be connected by an encounter stretch.

We see that given time reversal there must be a pair of twin l-cycles of P_{enc} associated with each l-encounter; an encounter associated with more than one pair of cycles would decompose into several independent ones. In general, each cycle in a pair describes stretches both of γ' and of $\bar{\gamma}'$; only in case of all stretches nearly parallel one cycle refers exclusively to γ' and the other to $\overline{\gamma'}$.

The final restriction on the permutations P_{enc} is analogous to the one encountered in the unitary case. To obtain two connected partner orbits γ' and $\overline{\gamma'}$, we now have to demand the permutation $P = P_{\text{loop}} P_{\text{enc}}$ to consist of only two L-cycles, listing the entrance ports in γ' and $\overline{\gamma'}$, respectively. [The second cycle can also be interpreted as the list of exit ports of γ', time reversed and written in reverse order. Since an entrance a_i is connected by a loop to the exit $b_i \equiv P_{\text{loop}}^{-1}(a_i)$, the two cycles of P read $(a_1, a_2, \ldots, a_L)$ and $(\overline{b_L}, \overline{b_{L-1}}, \ldots, \overline{b_1})$.]

To summarize, we consider the set $\mathcal{M}(\vec{v})$ of permutations P_{enc} acting on $1,2,\ldots,L,\bar{1},\bar{2},\ldots,\bar{L}$ which (i) are time-reversal covariants, (ii) have v_l pairs of l-cycles for all $l \geqslant 2$, and (iii) lead to a permutation $P = P_{\text{loop}} P_{\text{enc}}$ consisting of two cycles as above. Each element P_{enc} of the set $\mathcal{M}(\vec{v})$ thus stands for one of the "structures" introduced in Sec. II D. We need to calculate the number $N(\vec{v})$ of elements of $\mathcal{M}(\vec{v})$.

2. Examples

Again, the numbers $N(\vec{v})$ can be determined by numerically counting permutations. From the results shown in Table II, we see that indeed the form factor of the Gaussian orthogonal ensemble is reproduced semiclassically.

The τ^2 contribution comes from pairs of orbits differing in one antiparallel 2-encounter [7]. We have already shown that the corresponding "encounter permutation" reads

$$P_{\text{enc}} = \begin{pmatrix} 1\ 2\ \bar{1}\ \bar{2} \\ \bar{2}\ \bar{1}\ 2\ 1 \end{pmatrix}.$$

The τ^3 contribution originates from (compare Figs. 10 and 12 and Ref. [19]) four permutations related to 3-encounters and five permutations related to pairs of 2-encounters. The permutation

$$P_{\text{enc}} = \begin{pmatrix} 1\ 2\ 3\ \bar{1}\ \bar{2}\ \bar{3} \\ 2\ 3\ 1\ \bar{3}\ \bar{1}\ \bar{2} \end{pmatrix}$$

describes encounters of three parallel orbit stretches $\rightrightarrows$ (case pc). For triple encounters in which one of the stretches is time reversed with respect to the other two $\rightleftarrows$ (case ac), there are three related permutations,

$$P_{\text{enc}} = \begin{pmatrix} 1\ 2\ 3\ \bar{1}\ \bar{2}\ \bar{3} \\ \bar{3}\ 3\ \bar{1}\ 2\ 1\ \bar{2} \end{pmatrix}$$

and its two images under cyclic permutation of 1,2,3 as well as $\bar{1}, \bar{2}, \bar{3}$; physically, the three latter are equivalent since they

TABLE II. Permutations, and thus structures of orbit pairs, giving rise to orders τ^2–τ^5 of the form factor, for systems with $\mathcal{T}$ invariance; notation as in Table I. The results coincide with the predictions of RMT for the GOE.

Order	$\vec{v}$	L	V	$N(\vec{v})$	$\tilde{N}(\vec{v})$	Contribution
τ^2	$(2)^1$	2	1	1	-1	$-2\tau^2$
			Total:		-1	$-2\tau^2$
τ^3	$(2)^2$	4	2	5	5	$10\tau^3$
	$(3)^1$	3	1	4	-4	$-8\tau^3$
			Total:		1	$2\tau^3$
τ^4	$(2)^3$	3	6	41	$-\frac{164}{3}$	$-\frac{164}{3}\tau^4$
	$(2)^1(3)^1$	5	2	60	72	$72\tau^4$
	$(4)^1$	4	1	20	-20	$-20\tau^4$
			Total:		$-\frac{8}{3}$	$-\frac{8}{3}\tau^4$
τ^5	$(2)^4$	8	4	509	1018	$\frac{1018}{3}\tau^5$
	$(2)^2(3)^1$	7	3	1092	-1872	$-624\tau^5$
	$(2)^1(4)^1$	6	2	504	672	$224\tau^5$
	$(3)^2$	6	2	228	342	$114\tau^5$
	$(5)^1$	5	1	148	-148	$-\frac{148}{3}\tau^5$
			Total:		12	$4\tau^5$

differ only in which of the three stretches is considered the first. (In Ref. [19] such equivalences were taken into account by multiplicity factors $\mathcal{N}_{pc}$ and $\mathcal{N}_{ac}$.)

Pairs of 2-encounters may be composed of either (i) two parallel encounters (family *ppi*)

$$P_{\text{enc}} = \begin{pmatrix} 1\ 2\ 3\ 4\ \bar{1}\ \bar{2}\ \bar{3}\ \bar{4} \\ 3\ 4\ 1\ 2\ \bar{3}\ \bar{4}\ \bar{1}\ \bar{2} \end{pmatrix},$$

or (ii) one parallel and one antiparallel encounter (family *api*)

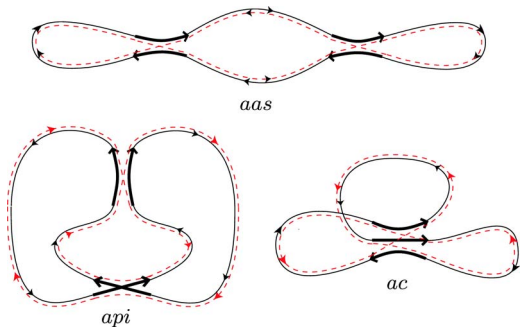

FIG. 12. (Color online) Pairs of orbits existing only for systems with $\mathcal{T}$-invariance and giving all of τ^3. For labels see text. Two further families do not require $\mathcal{T}$-invariance, see Fig. 10.

$$P_{\text{enc}} = \begin{pmatrix} 1\ 2\ 3\ 4\ \bar{1}\ \bar{2}\ \bar{3}\ \bar{4} \\ \bar{3}\ 4\ \bar{1}\ 2\ 3\ \bar{4}\ 1\ \bar{2} \end{pmatrix}$$

and

$$P_{\text{enc}} = \begin{pmatrix} 1\ 2\ 3\ 4\ \bar{1}\ \bar{2}\ \bar{3}\ \bar{4} \\ 3\ \bar{4}\ 1\ \bar{2}\ \bar{3}\ 4\ \bar{1}\ 2 \end{pmatrix},$$

or (iii) two antiparallel ones (family *aas*)

$$P_{\text{enc}} = \begin{pmatrix} 1\ 2\ 3\ 4\ \bar{1}\ \bar{2}\ \bar{3}\ \bar{4} \\ \bar{4}\ \bar{3}\ \bar{2}\ \bar{1}\ 4\ 3\ 2\ 1 \end{pmatrix}$$

and

$$P_{\text{enc}} = \begin{pmatrix} 1\ 2\ 3\ 4\ \bar{1}\ \bar{2}\ \bar{3}\ \bar{4} \\ \bar{2}\ \bar{1}\ \bar{4}\ \bar{3}\ 2\ 1\ 4\ 3 \end{pmatrix}.$$

Again, equivalent permutations differ by cyclic permutations (of now 1,2,3,4 as well as $\bar{1},\bar{2},\bar{3},\bar{4}$), i.e., in which of the stretches is assigned the number 1.

3. Recursion relation for $N(\vec{v})$

We are now fully equipped to establish a recursion relation for $N(\vec{v})$ in much the same way in the unitary case. Impatient readers may want to jump to the resulting recursion (68) for K_n.

First of all, we recover Eq. (32), $N(\vec{v},l)=(v_l l/L)N(\vec{v})$ using exactly the same arguments as in the unitary case. From each element $P_{\text{enc}} \in \mathcal{M}(\vec{v},l)$ we obtain L elements of $\mathcal{M}(\vec{v})$ by the L possible cyclic permutations. Applying these cyclic permutations to the set $\mathcal{M}(\vec{v},l)$ we obtain $v_l l$ copies of $\mathcal{M}(\vec{v})$, since the v_l pairs of twin l-cycles have altogether $v_l l$ members without overbar, and permutations shifting L among these members leave $\mathcal{M}(\vec{v},l)$ invariant.

Choosing a permutation $P_{\text{enc}}=P_{\text{loop}}^{-1}P \in \mathcal{M}(\vec{v},l)$ we set $Q_{\text{enc}}=Q_{\text{loop}}^{-1}Q$ with Q_{loop} and Q obtained from P_{loop} and P by omitting L and $\overline{L-1}$, and replacing $\bar{L}$ by $\overline{L-1}$. (This prescription can be interpreted as removing the loop leading from exit $L-1$ to entrance L, and its time-reversed partner leading from exit $\bar{L}$ to entrance $\overline{L-1}$; hence the corresponding entrance ports must be removed from P and $P_{\text{loop}}=P^{\gamma}$.) In particular Q_{loop} will have the form

$$Q_{\text{loop}} = (1,2,\ldots,L-1)(\overline{L-1},\overline{L-2},\ldots,\bar{1}).$$

The two cycles of Q satisfy the same relation as those of P and may thus indeed be interpreted as lists of entrance ports of two time reversed orbits. The resulting "encounter

permutation" $Q_{\rm enc}$ maps the remaining elements $a=1,2,\ldots,L-1,\bar{1},\bar{2},\ldots,\overline{L-1}$ as[6]

$$Q_{\rm enc}(a)=\begin{cases} P_{\rm enc}(L) & \text{if } a=P_{\rm enc}^{-1}(L-1),\\ P_{\rm enc}(\overline{L-1}) & \text{if } a=P_{\rm enc}^{-1}(\bar{L}),\\ L-1 & \text{if } a=P_{\rm enc}^{-1}(L),\\ P_{\rm enc}(\bar{L}) & \text{if } a=\overline{L-1},\\ P_{\rm enc}(a) & \text{otherwise.}\end{cases} \tag{50}$$

Here, the second and fourth lines extend Eq. (34) as required by $\mathcal{T}$ invariance; the present $Q_{\rm enc}$ is indeed $\mathcal{T}$ covariant.

When analyzing the cycle structure of $Q_{\rm enc}$, we now have to distinguish between *three* cases, the first two paralleling the treatment of Sec. III A 3. Note, however, a factor 2 appearing in the second case. For each $Q_{\rm enc}\in\mathcal{M}(\vec{v}^{[l\to m,l-m-1]},m)$, there are now twice as many, namely, $2(l-m-1)(v_{l-m-1}+1)$ related $P_{\rm enc}\in\mathcal{M}(\vec{v},l)$ structured like Eq. (39), since $Q_{\rm enc}$ also remains unaffected by time reversal of $a_{m+2},\ldots,a_l$ in Eq. (39). The second and fourth lines in Eq. (50) make sure that merging or splitting of cycles is mirrored by the corresponding twins.

A third possibility appears since *the cycles involving L and L−1 may be twins*, and hence belong to the same encounter. Since the twin cycles are mutually time reversed there is one cycle containing both L and $\overline{L-1}$, and another one containing $\bar{L}$ and $L-1$. Assume that inside the first cycle, the element $\overline{L-1}$ follows L after m iterations, i.e., $\overline{L-1}=P_{\rm enc}^{m}(L)$ (with $1\leqslant m\leqslant l-1$). Then $P_{\rm enc}$ can be written as

$$P_{\rm enc}=[\cdots](L,a_2,\ldots,a_m,\overline{L-1},a_{m+2},\ldots,a_l)\times(\overline{a_l},\ldots,\overline{a_{m+2}},L-1,\overline{a_m},\ldots,\overline{a_2},\bar{L}). \tag{51}$$

Due to Eq. (50), $Q_{\rm enc}$ differs from $P_{\rm enc}$ by mapping

$$Q_{\rm enc}(\overline{a_{m+2}})=a_2,\quad Q_{\rm enc}(\overline{a_2})=a_{m+2},$$

$$Q_{\rm enc}(a_l)=L-1,\quad Q_{\rm enc}(\overline{L-1})=\overline{a_l}. \tag{52}$$

The initial pair of twin cycles of $P_{\rm enc}$ is transformed to the following pair of twin $(l-1)$-cycles of

$$Q_{\rm enc}=[\cdots](a_2,\ldots,a_m,\overline{L-1},\overline{a_l},\ldots,\overline{a_{m+2}})\times(a_{m+2},\ldots,a_l,L-1,\overline{a_m},\ldots,\overline{a_2}). \tag{53}$$

Given that the largest number permuted by $Q_{\rm enc}$, i.e., $L-1$, is included in one of these cycles, we have $Q_{\rm enc}\in\mathcal{M}(\vec{v}^{[l\to l-1]},l-1)$. Conversely, for any such $Q_{\rm enc}$ and each $1\leqslant m\leqslant l-1$, there is exactly one related $P_{\rm enc}$, since we may read off $a_2,\ldots,a_l$ from $Q_{\rm enc}$ in Eq. (53) and recombine them to form a permutation $P_{\rm enc}$ as in Eq. (51). We thus see that each of the $l-1$ subsets of $\mathcal{M}(\vec{v},l)$ with $\overline{L-1}=P_{\rm enc}^{m}(L)$ is in one-to-one correspondence with $\mathcal{M}(\vec{v}^{[l\to l-1]},l-1)$ and thus has an equal number of elements.

We have seen that $\mathcal{M}(\vec{v},l)$ falls into subsets similar to the unitary case, time-reversal invariance making for the factor 2 explained above, and for $l-1$ additional subsets of size $N(\vec{v}^{[l\to l-1]},l-1)$. The various sizes combine to the orthogonal analogue of the recursion relation (42),

$$N(\vec{v},l)=\sum_{k\geqslant 2}N(\vec{v}^{[k,l\to k+l-1]},k+l-1)+\sum_{m=1}^{l-2}2(l-m-1)(v_{l-m-1}+1)N(\vec{v}^{[l\to m,l-m-1]},m)+(l-1)N(\vec{v}^{[l\to l-1]},l-1), \tag{54}$$

which using Eq. (32) and the shorthand

$$\widetilde{N}(\vec{v})=\frac{(-1)^V\Pi_l l^{v_l}}{L}N(\vec{v})$$

may be written as

$$v_l\widetilde{N}(\vec{v})+\sum_{k\geqslant 2}(v_{k+l-1}+1)k\widetilde{N}(\vec{v}^{[k,l\to k+l-1]})+\sum_{m=1}^{l-2}2(v_{l-m-1}+1)v_m^{[l\to m,l-m-1]}\widetilde{N}(\vec{v}^{[l\to m,l-m-1]})-(l-1)(v_{l-1}+1)\widetilde{N}(\vec{v}^{[l\to l-1]})=0; \tag{55}$$

recall that $v_{k+l-1}+1=v_{k+l-1}^{[k,l\to k+l-1]}$.

4. Spectral form factor

Similarly as in Sec. III A 4 we now turn the recursion relation for $\widetilde{N}(\vec{v})$ into one for the Taylor coefficients K_n. As a preparation we generalize our rule (47). For all similar sums over $\vec{v}$ with fixed $\nu(\vec{v})=n$ and $v_1=0$ we find

$$\sum_{\vec{v}}^{\nu(\vec{v})=n}f(\vec{v}^{[\alpha_1,\alpha_2,\ldots\to\beta]})\widetilde{N}(\vec{v}^{[\alpha_1,\alpha_2,\ldots\to\beta]})=\sum_{\vec{v}'}^{\nu(\vec{v}')=n'}f(\vec{v}')\widetilde{N}(\vec{v}'), \tag{56}$$

with integers $\alpha_i\geqslant 2$, $\beta\geqslant 2$, $n'=\nu(\vec{v}')=\nu(\vec{v}^{[\alpha_1,\alpha_2,\ldots\to\beta]})=n-\Sigma_i(\alpha_i-1)+(\beta-1)$, and f any function of $\vec{v}'$ vanishing for $v'_\beta=0$. Equation (56) follows in the same way as Eq. (47), i.e., by switching to $\vec{v}'=\vec{v}^{[\alpha_1,\alpha_2,\ldots\to\beta]}$ as the new summation variable and dropping the restriction $v'_\beta\geqslant 1$ ($\vec{v}'$ with $v'_\beta=0$ do not contribute due to the vanishing of f). One similarly shows that the foregoing rule holds even without any conditions on f if β is removed, i.e., if no new cycles are created. It is convenient to abbreviate the RHS of Eq. (56) with the help of

$$S_{n'}[f]\equiv\sum_{\vec{v}'}^{\nu(\vec{v}')=n'}f(\vec{v}')\widetilde{N}(\vec{v}') \tag{57}$$

for arbitrary f; we note that $K_n=[2/(n-2)!]S_n[1]$. Thus equipped we turn to the three special cases $l=1,2,3$ of our recursion relations (54) and (55) which we shall need below.

[6] In the special case $P_{\rm enc}(\overline{L-1})=L$, Eq. (50) has to be modified to $Q_{\rm enc}(\overline{L-1})=P_{\rm enc}(L)$, $Q_{\rm enc}P_{\rm enc}^{-1}(\bar{L})=L-1$, and $Q_{\rm enc}(a)=P_{\rm enc}(a)$ for the remaining elements. The result (53) remains in force even in that special case, with $m=l-1$; the sequences $a_{m+2},\ldots,a_l$, and $\overline{a_l},\ldots,\overline{a_{m+2}}$, are then absent.

First, the case $l=1$ involves permutations with 1-cycles, appearing only in intermediate steps of our calculation. If the element L forms a 1-cycle, it may simply be removed from a permutation without affecting the other cycles, which corresponds to a transition $\vec{v}\to\vec{v}^{[1\to]}$. We thus have $N(\vec{v},1)=N(\vec{v}^{[1\to]})$ and equivalently

$$v_1\tilde{N}(\vec{v})+L(\vec{v}^{[1\to]})\tilde{N}(\vec{v}^{[1\to]})=0. \tag{58}$$

Second, for $l=2$ (and $v_1=0$) the recursion (55) boils down to

$$v_2\tilde{N}(\vec{v})+\sum_{k\geqslant 2}\left(v_{k+1}^{[k,2\to k+1]}\right)k\tilde{N}(\vec{v}^{[k,2\to k+1]})-\tilde{N}(\vec{v}^{[2\to 1]})=0, \tag{59}$$

where only the last term is new compared to the unitary case. We bring it to a form free from 1-cycles by invoking Eq. (58) and thus $\tilde{N}(\vec{v}^{[2\to 1]})=-L(\vec{v}^{[2\to]})\tilde{N}(\vec{v}^{[2\to]})$, to get

$$v_2\tilde{N}(\vec{v})+\sum_{k\geqslant 2}\left(v_{k+1}^{[k,2\to k+1]}\right)k\tilde{N}(\vec{v}^{[k,2\to k+1]})+L(\vec{v}^{[2\to]})\tilde{N}(\vec{v}^{[2\to]})=0. \tag{60}$$

As in the unitary case, we sum over all $\vec{v}$ with $v_1=0$ and $\nu(\vec{v})=n$. The rule Eq. (56) and the shorthand Eq. (57) give

$$\begin{aligned}S_n\left[v_2+\sum_{k\geqslant 2}v_{k+1}k\right]+S_{n-1}[L(\vec{v})]&=(n-1)S_n[1]+S_{n-1}[L(\vec{v})]\\&=0.\end{aligned} \tag{61}$$

A further relation is obtained by multiplying Eq. (60) with $L(\vec{v})-1=L(\vec{v}^{[k,2\to k+1]})=L(\vec{v}^{[2\to]})+1$ and again summing over $\vec{v}$ with the help of Eq. (56). The resulting equation

$$(n-1)S_n[L(\vec{v})]-S_n[v_2]+S_{n-1}[L(\vec{v})(L(\vec{v})+1)]=0 \tag{62}$$

can be simplified by Eq. (61) and replacing $n\to n-2$,

$$-(n-2)(n-3)S_{n-1}[1]=S_{n-2}[v_2]-S_{n-3}[L(\vec{v})(L(\vec{v})+1)]. \tag{63}$$

Finally, we consider $l=3$ (and $v_1=0$)

$$v_3\tilde{N}(\vec{v})+\sum_{k\geqslant 2}\left(v_{k+2}^{[k,3\to k+2]}k\tilde{N}(\vec{v}^{[k,3\to k+2]})\right)+4\tilde{N}(\vec{v}^{[3\to 1,1]})-2v_2^{[3\to 2]}\tilde{N}(\vec{v}^{[3\to 2]})=0. \tag{64}$$

The 1-cycles in the third term are eliminated using the identity $\tilde{N}(\vec{v}^{[3\to 1,1]})=\frac{1}{2}L(\vec{v}^{[3\to]})(L(\vec{v}^{[3\to]})+1)\tilde{N}(\vec{v}^{[3\to]})$, which follows by twice applying Eq. (58) to $\vec{v}^{[3\to 1,1]}$. Summing over $\vec{v}$ in Eq. (64) we find

$$S_n\left[v_3+\sum_{k\geqslant 2}v_{k+2}k\right]+2S_{n-2}[L(\vec{v})(L(\vec{v})+1)]-2S_{n-1}[v_2]=0. \tag{65}$$

This expression can be simplified using $v_3+\Sigma_{k\geqslant 2}v_{k+2}k=\Sigma_{k\geqslant 2}v_k(k-2)=L(\vec{v})-2V(\vec{v})=2(\nu(\vec{v})-1)-L(\vec{v})$, i.e.,

$$2(n-1)S_n[1]-S_n[L(\vec{v})]+2S_{n-2}[L(\vec{v})(L(\vec{v})+1)]-2S_{n-1}[v_2]=0. \tag{66}$$

Finally applying Eq. (61), substituting $n\to n-1$, and dividing by 2, we proceed to

$$\frac{n-1}{2}S_n[1]+(n-2)S_{n-1}[1]=S_{n-2}[v_2]-S_{n-3}[L(\vec{v})(L(\vec{v})+1)]. \tag{67}$$

Upon comparing the recursion relations (63) and (67), obtained for the cases $l=2$ and 3, we find the coefficients $S_n[1]=[(n-2)!/2]K_n$ and $S_{n-1}[1]=[(n-3)!/2]K_{n-1}$ related as $[(n-1)/2]S_n[1]=-(n-2)^2S_{n-1}[1]$ or

$$(n-1)K_n=-2(n-2)K_{n-1}. \tag{68}$$

An initial condition is provided by the Sieber-Richter result for orbits differing in one 2-encounter, $K_2=-2$. Thus started, our recursion yields the Taylor coefficients

$$K_n=\frac{(-2)^{n-1}}{n-1} \tag{69}$$

coinciding with the random-matrix result. Universal behavior is thus ascertained for the small-time form factor of fully chaotic dynamics from the orthogonal symmetry class; the resulting series converges for $\tau<\frac{1}{2}$.

IV. SPINNING PARTICLES AND THE SYMPLECTIC SYMMETRY CLASS

We now allow for a spin with arbitrary but fixed spin quantum number S. Assuming time-reversal invariance we know that for integer S the time-reversal operator $\mathcal{T}$ squares to unity, $\mathcal{T}^2=1$, whereas for half-integer spin, $\mathcal{T}^2=-1$; we face the orthogonal and symplectic symmetry class, respectively. The semiclassical theory of spinning particles is discussed in [33]; off-diagonal terms of the form factor were considered in a preliminary version in [21], and for quantum graphs in [22].

The Pauli Hamiltonian reads $H=H_0+\hat{\mathbf{B}}\cdot\hat{\mathbf{S}}$ where $\hat{\mathbf{S}}$ is the spin operator, with $\hat{\mathbf{S}}^2=\hbar^2S(S+1)$. The vector operator $\hat{\mathbf{B}}(\hat{\mathbf{q}},\hat{\mathbf{p}})$ describes the influence of the translational motion and external fields on the spin. The spin-orbit interaction formally behaves like $\mathcal{O}(\hbar)$ and tends to zero in the semiclassical limit; it is not a small quantum perturbation though, since its matrix elements are infinitely larger than the energy spacing $\Delta\sim\mathcal{O}(\hbar^f)$, $f>1$.

The state of the system is given by a spinor with $2S+1$ components and the propagator by a $(2S+1)\times(2S+1)$ matrix. In the leading order of the semiclassical approximation the propagator consists of the scalar translational part which is the van Vleck propagator of the spinless system, multiplied by the spin evolution matrix d [belonging to the spin S representation $D^{(S)}$ of SU(2)]; the latter matrix has to be evaluated on the classical orbit (of the translational motion) connecting the initial and final points. Along such an orbit γ the d matrix is a function of the initial and final times, d

$=d_\gamma(t,t_0)$. It satisfies the equation $i\partial_t d_\gamma(t,t_0) = \mathbf{B}_\gamma(t)\cdot(\hat{\mathbf{S}}/\hbar)d_\gamma(t,t_0)$ where the classical time-dependent vector $\mathbf{B}_\gamma(t)$ is obtained by substituting the classical coordinates and momenta along γ for the operator valued arguments of $\hat{\mathbf{B}}(\hat{\mathbf{q}},\hat{\mathbf{p}})$; the initial condition is $d_\gamma(t_0,t_0)=\mathbf{1}_{2S+1}$. Such semiclassical treatment keeps the translational motion unaffected by the quantum spin. The spin, however, is driven by the translational motion. No semiclassical approximation for the spin itself (which would require the assumption of large S) is invoked.

The full quantum nature of the spin (finite S) notwithstanding, a seemingly classical manner of speaking about the spin is possible, due to the following fact: any matrix from $D^{(S)}$ can be parametrized by three Euler angles [e.g., $d(\theta,\phi,\psi)=e^{i\psi\hat{S}_z/\hbar}e^{i\theta\hat{S}_x/\hbar}e^{i\phi\hat{S}_z/\hbar}$), which are time dependent for $d=d(t)$. The angles $\psi(t)$, $\theta(t)$, $\phi(t)$ may also be imagined to specify the orientation of a fictitious rigid body in classical rotation; as in [21,22,33] we shall speak of that motion as "spin rotation."

We assume the translational motion chaotic as before and require ergodicity of the combined spin rotation and translational motion. The spin rotation itself is then also ergodic. This means that time averages of the spin-dependent properties over intervals longer than a certain relaxation time $t_{\rm cl}$ can be replaced by averages over all $d\in D^{(S)}$; the measure to be used reads $d\mu=d\phi\sin\theta\, d\theta\, d\psi/8\pi^2$.

A. Integer spin

The trace formula for a particle with spin [33] gives the level density as a sum over periodic orbits γ

$$\rho_{\rm osc}(E)\sim\frac{1}{\pi\hbar}{\rm Re}\sum_\gamma({\rm tr}\, d_\gamma)A_\gamma e^{iS_\gamma/\hbar}; \tag{70}$$

in addition to the stability amplitude (including period and Maslov phase) and the classical action of the γth orbit, the factor ${\rm tr}\, d_\gamma\equiv{\rm tr}\, d_\gamma(t_0+T_\gamma,t_0)$ appears and reflects the spin evolution over a period of the translational motion. That ${\rm tr}\, d_\gamma$ is independent of the initial moment t_0: its shift leads only to a similarity transformation of d_γ.

The form factor becomes the double sum

$$K(\tau)=\frac{1}{T_H}\left\langle\sum_{\gamma,\gamma'}({\rm tr}\, d_\gamma)({\rm tr}\, d_{\gamma'})A_\gamma A^*_{\gamma'}e^{i(S_\gamma-S_{\gamma'})/\hbar}\times\delta\left(\tau T_H-\frac{T_\gamma+T_{\gamma'}}{2}\right)\right\rangle. \tag{71}$$

Due to the spin, the average level density and thus the Heisenberg time T_H are increased by the factor $2S+1$.

The diagonal approximation yields the sum

$$K_{\rm diag}(\tau)=\frac{2}{T_H}\left\langle\sum_\gamma({\rm tr}\, d_\gamma)^2|A_\gamma|^2\delta(\tau T_H-T_\gamma)\right\rangle. \tag{72}$$

Since the spin dynamics is ergodic and since we are averaging over an ensemble of orbits, the equidistribution theorem [26] allows us to treat d_γ as random and to integrate over all matrices of the spin-S representation $D^{(S)}$ of SU(2); the sum over γ gives the usual factor T. The spin integral gives unity for any S, and so we have [33]

$$K_{\rm diag}(\tau)=2\tau\int d\mu(\mathcal{A})({\rm tr}\,\mathcal{A})^2=2\tau. \tag{73}$$

As to off-diagonal contributions from orbit pairs γ,γ', spin makes for two modifications compared to the previous sections. First, T_H contains a factor $2S+1$, such that the $L-V$ factors $2\pi\hbar T/\Omega$ in Eq. (24) give $(2S+1)T/T_H=(2S+1)\tau$ rather than τ. Second, the contribution of each orbit pair comes with the factor $({\rm tr}\, d_\gamma)({\rm tr}\, d_{\gamma'})$.

To evaluate the factor $({\rm tr}\, d_\gamma)({\rm tr}\, d_{\gamma'})$, we decompose the orbit γ into L pieces by cutting it once in each encounter, and represent d_γ as a product of L matrices $\mathcal{A}_i$ describing the spin evolution over one orbit piece. In the orbit pairs contributing to the form factor the duration of each piece (the orbit loop + segments of the preceding and following encounter stretches) exceeds the Ehrenfest time T_E, and thus also the classical relaxation time $t_{\rm cl}$. Therefore, keeping in mind that we are summing over an ensemble of orbits, we may invoke ergodicity and replace the partial spin evolution matrices by matrices randomly chosen out of $D^{(S)}$. Numbering the orbit pieces and the corresponding random matrices in the order of their traversal in γ we may replace d_γ by a product $\mathcal{A}_L\mathcal{A}_{L-1}\cdots\mathcal{A}_1$, the earliest propagator matrix written rightmost. The orbit partner γ' consists of practically the same pieces passed in a different order, some of them in the opposite direction. Hence $d_{\gamma'}$ can be expressed in terms of the same L matrices $\mathcal{A}_i$, but with the order suitably rearranged and with $\mathcal{A}_i\to\mathcal{A}_i^{-1}$ for the time-reversed pieces. The expectation value of the trace product can now be evaluated as an integral over $\mathcal{A}_i$, $i=1,\ldots,L$. Using the results of [22], one obtains

$$\begin{aligned}({\rm tr}\, d_\gamma)({\rm tr}\, d_{\gamma'})&\to\int({\rm tr}\mathcal{A}_L\mathcal{A}_{L-1}\cdots\mathcal{A}_1)\\&\quad\times({\rm tr}\mathcal{A}_{k_L}^{\eta_L}\mathcal{A}_{k_{L-1}}^{\eta_{L-1}}\cdots\mathcal{A}_{k_1}^{\eta_1})\prod_{i=1}^{L}d\mu(\mathcal{A}_i)\\&=\left(\frac{(-1)^{2S}}{2S+1}\right)^{L-V};\end{aligned} \tag{74}$$

most remarkably, for an orbit pair with a given $\vec{v}$ the L-fold integral depends only on the difference $L(\vec{v})-V(\vec{v})=n-1$; in particular, it is independent of the special ordering of loops in the partner orbit γ' (expressed by the subscripts $k_1,k_2,\ldots,k_L$), as well as of the senses of traversal (expressed by the exponents $\eta_a=\pm1$).[7]

[7] If desired, these indices can be determined from the permutation $P=P_{\rm loop}P_{\rm enc}$ describing the partner γ'; see Sec. III. The permutation P consists of two L-cycles relating to γ' and $\bar{\gamma}'$; the sequence of loops $k_1,\ldots,k_L$ in γ' is given by the appropriate cycle in which the elements with an overbar (indicating time reversal of the loop) are modified as $\bar{k}\to(k+1){\rm mod}L$ and simultaneously the associated exponents η are set to -1.

Now the two occurrences of $(2S+1)^{L-V}$ mutually cancel and the form factor reads

$$K(\tau) = 2\tau + 2\sum_{\vec{v}} N(\vec{v})h(\vec{v})(-1)^{2S(L-V)}\tau^{L-V+1}. \qquad (75)$$

For integer spin, $(-1)^{2S}=1$ whereupon we recover the expansion (28) of $K(\tau)$ for the orthogonal class.

B. Half-integer spin

For half-integer spin, the minus sign in Eq. (75) becomes relevant. Moreover, all levels become doubly degenerate in the Kramers sense [3]. With the density of levels reduced to half the density of states we are led to the rescaling $K(\tau) \to \frac{1}{2}K(\tau/2)$ [33]. In this case, the form factor reads

$$K(\tau) = \frac{\tau}{2} - \sum_{\vec{v}} N(\vec{v})h(\vec{v})\left(-\frac{\tau}{2}\right)^{L-V+1} = \frac{\tau}{2} - \frac{\tau}{4}\ln(1-\tau). \qquad (76)$$

To understand the final step, we compare the sums over $\vec{v}$ in Eqs. (28) and (76), the latter pertinent to the orthogonal class, and find $K(\tau)=-\frac{1}{2}K_{\mathrm{GOE}}(-\tau/2)$. We have thus verified the random-matrix result Eq. (3) for the Gaussian symplectic ensemble. As predicted in [21] the sign change of the argument τ, which entails the logarithmic singularity of the symplectic form factor at $\tau=1$, comes from the contributions of the spin integrals (74).

V. RELATION TO THE σ MODEL

A. Introduction

The so-called σ model [34,35] is a convenient framework for calculating averaged products of Green functions of random Hamiltonians. Its zero-dimensional variant affords, in particular, the two-point correlator of the level density (and its Fourier transform, the spectral form factor) for the Gaussian ensembles of RMT; see Appendix E for a brief introduction. Perturbative implementations exist for the three Wigner-Dyson symmetry classes and yield the corresponding spectral form factors $K(\tau)$ as power series in the time τ, i.e., precisely the series extracted from Gutzwiller's semiclassical periodic-orbit theory in the preceding sections.

The σ model for random-matrix theory proved of great heuristic value for our semiclassical endeavor: We were led to the correct combinatorics of families of orbit pairs by an analysis of the perturbation series of the sigma model. The analogy of periodic-orbit expansions to perturbation series might prove fruitful for future applications of periodic-orbit theory, and that possibility motivates the following exposition.

Before entering technicalities it is appropriate to point to some qualitative analogies and differences between the two approaches. Very roughly, different Feynman diagrams of the σ model (for both the Wigner-Dyson ensembles and disorder) correspond to different families of (pairs of) periodic orbits, vertices to close self-encounters, and propagator lines to orbit loops. An important difference lies in the point character of vertices and the nonzero duration, of the order of the Ehrenfest time $T_E \propto \ln \hbar$, of the relevant self-encounters. Of course, the relevant encounter durations are vanishingly small compared to the typical loop lengths ($\sim T_H \propto \hbar^{-f+1}$); nevertheless, we may say that self-encounters give internal structure to vertices.

B. Expansions of two-point correlator and form factor

The connected two-point correlator of the density of levels $\bar{R}=(\overline{\rho\rho}-\bar{\rho}^2)/\bar{\rho}^2$ can be obtained from the ensemble averaged product of the retarded and advanced Green functions $G_{\pm}(E)=(E\pm i\delta-H)^{-1}$ as [3]

$$R(s) = \frac{\mathrm{Re}\,\overline{\delta\,\mathrm{tr}\,G_+(E+s/2\pi\bar{\rho})\,\delta\,\mathrm{tr}\,G_-(E-s/2\pi\bar{\rho})}}{2\pi^2\bar{\rho}^2},$$

$$\delta\,\mathrm{tr}\,G_{\pm} = \mathrm{tr}\,G_{\pm} - \overline{\mathrm{tr}\,G_{\pm}}. \qquad (77)$$

Here, the overbar denotes an average over a Gaussian ensemble of random matrices. The argument E (the average energy) is suppressed. The energy difference is expressed in terms of the dimensionless offset s. The Fourier transform of R with respect to the offset s gives the central object of the present paper, the spectral form factor,

$$K(\tau) = \frac{1}{\pi}\int_{-\infty}^{\infty} ds\, e^{2is\tau}R(s). \qquad (78)$$

As briefly shown in Appendix E, a bosonic replica variant of the σ model yields the $(1/s)$ expansion of the Fourier transform of the small-time form factor as an integral over matrices B,

$$R(s) \sim -\frac{1}{2}\mathrm{Re}\lim_{r\to 0}\frac{1}{r^2}\partial_s^2 s^{-\kappa r^2} \times \int dB\,\exp\left((2\mathrm{i}/\kappa)\sum_{l=1}^{\infty} s^{1-l}\mathrm{tr}(BB^{\dagger})^l\right), \qquad (79)$$

where on the RHS the offset s must be read as $s+i\delta$ with $\delta\downarrow 0$; the matrices $B, B^{\dagger}$ are $r\times r$ for the GUE and $2r\times 2r$ for the GOE; as before, the factor κ takes the respective values 1 and 2 for the two classes. The essence of the replica "trick" is to find the foregoing integral as a power series in r and to isolate the coefficient of r^2.

In the limit $s\to\infty$ the principal contribution to $R(s)$ comes from the Gaussian factor $\exp[(2i/\kappa)\mathrm{tr}\,M]$ in the integrand of Eq. (79), where $M=BB^{\dagger}$. The remaining factor can be expanded as

$$\exp\left(\frac{2i}{\kappa}\sum_{l\geq 2} s^{1-l}\mathrm{tr}\,M^l\right) = \sum_{V=0}^{\infty}\frac{1}{V!}\left(\frac{2i}{\kappa}\right)^V\left(\sum_{l\geq 2} s^{1-l}\mathrm{tr}\,M^l\right)^V = \sum_{\vec{v}}\frac{1}{\prod_{l\geq 2} v_l!}\left(\frac{2i}{\kappa}\right)^V s^{V-L}\prod_{l\geq 2}(\mathrm{tr}\,M^l)^{v_l}. \qquad (80)$$

Here, the summation extends over integers $v_2, v_3, \ldots, v_l, \ldots$

each of which runs from zero to infinity, and we write $\vec{v}=(v_2,v_3,\ldots)$ just as in our semiclassical treatment. The total number of traces in the summand $\vec{v}$ is $V(\vec{v})=\Sigma_{l\geqslant 2}v_l$, and again we define $L(\vec{v})=\Sigma_{l\geqslant 2}lv_l$. The integral over B and $B^\dagger$ in Eq. (79) may now be seen as a sum of averages like

$$\langle f(B,B^\dagger)\rangle \equiv \int dB\, f(B,B^\dagger)e^{(2i/\kappa)\mathrm{tr}(BB^\dagger)}. \tag{81}$$

We may thus write

$$R(s)\sim -\frac{1}{2}\mathrm{Re}\left\{\lim_{r\to 0}\frac{1}{r^2}\partial_s^2 s^{-\kappa r^2}\sum_{\vec{v}}\frac{1}{\prod_{l\geqslant 2}v_l!}\left(\frac{2i}{\kappa}\right)^V \times s^{V-L}\left\langle\prod_{l\geqslant 2}(\mathrm{tr}\,M^l)^{v_l}\right\rangle\right\}. \tag{82}$$

The leading term $\vec{v}=0$ corresponds to $\langle 1\rangle=(\mathrm{const})^{\kappa r^2}\overset{r\to 0}{\to}1$. The corresponding contribution to the two-point correlator is $-\frac{1}{2}\mathrm{Re}\lim_{r\to 0}(1/r^2)\partial_s^2(s+i\delta)^{-\kappa r^2}=-\mathrm{Re}[\kappa/2(s+i\delta)^2]$, and thus $\kappa|\tau|$ for the spectral form factor, reproducing the diagonal part in both the unitary and orthogonal cases.

For all other terms, the operations of taking the second derivative by s and going to the limit $r\to 0$ commute, meaning that the factor $s^{-\kappa r^2}$ can be disregarded. We shall show below that the averages of the trace products with nonzero $\vec{v}$ have the property

$$\lim_{r\to 0}\frac{1}{r^2}\left\langle\prod_l(\mathrm{tr}\,M^l)^{v_l}\right\rangle=\frac{\kappa^2}{(-2i)^{L(\vec{v})}}N_c(\vec{v}) \tag{83}$$

in which $N_c(\vec{v})$ take positive integer values; we shall in fact come to interpreting $N_c(\vec{v})$ as the "number of contractions"; the traces of M^l will be called l-traces, to stress the analogy with the l-encounters of periodic orbits. The form factor $K(\tau)$ is now obtained by Fourier transforming. Using $\int_{-\infty}^{\infty}(ds/\pi)e^{2is\tau}\mathrm{Re}[i^{-n+1}(s+i\delta)^{-n-1}]=(-2)^n|\tau|^n/n!$ one easily shows that the Taylor coefficients of $K(\tau)=\kappa|\tau|+\Sigma_{n\geqslant 2}K_n|\tau|^n$ are given by

$$K_n=\frac{\kappa}{(n-2)!}\sum_{\vec{v}}^{L(\vec{v})-V(\vec{v})+1=n}\frac{(-1)^V}{\kappa^{V-1}\prod_{l\geqslant 2}v_l!}N_c(\vec{v}). \tag{84}$$

C. Contraction rules

In the following, we will derive a recursion for $N_c(\vec{v})$ similar to the recursion in our semiclassical analysis. To that end, we calculate the averages of the products of traces in Eq. (83) by Wick's theorem. Each average becomes, for the GUE, a sum of contractions of a fixed matrix B in one of the traces and all matrices $B^\dagger$; for the GOE, contractions with other matrices B arise as well. In all formulas below, X and Y must provide the traces on the LHS with an alternating sequence of B's and $B^\dagger$'s; then the same will hold for all traces on the RHS. Moreover, the term $[\cdots]$ will stand for inert traces unchanged by the contraction. The GUE involves two contraction rules,

$$\langle\mathrm{tr}\,\overbrace{BX\,\mathrm{tr}B^\dagger}Y[\ldots]\rangle=-\frac{1}{2\mathrm{i}}\langle\mathrm{tr}(X\,Y)[\ldots]\rangle \tag{85a}$$

$$\langle\mathrm{tr}\,\overbrace{BX}\,\overbrace{B^\dagger}Y[\ldots]\rangle=-\frac{1}{2\mathrm{i}}\langle\mathrm{tr}\,X\,\mathrm{tr}\,Y[\ldots]\rangle. \tag{85b}$$

For the GOE, two more rules arise from contractions of B with B (and similarly $B^\dagger$ with $B^\dagger$):

$$\langle\mathrm{tr}\,\overbrace{BX\,\mathrm{tr}B}Y[\ldots]\rangle=-\frac{1}{2\mathrm{i}}\langle\mathrm{tr}(XY^\dagger)[\ldots]\rangle \tag{85c}$$

$$\langle\mathrm{tr}\,\overbrace{BX}\,\overbrace{B}Y[\ldots]\rangle=-\frac{1}{2\mathrm{i}}\langle\mathrm{tr}(X\,Y^\dagger)[\ldots]\rangle. \tag{85d}$$

The only possible ordering of $B,B^\dagger$ after contraction is alternation $BB^\dagger BB^\dagger$ …. We may thus express all quantities in terms of $M=BB^\dagger$. Each contraction reduces the number of M's by 1.

The sequences X,Y in Eq. (85b) may be absent; then they must be replaced by the unit matrix $\mathbf{1}$. In particular, if we repeatedly invoke Eqs. (85a)–(85d) in order to reduce the number of M's, the final step will always be

$$\langle\mathrm{tr}\,\overbrace{B\,\overbrace{B^\dagger}}\rangle=-\frac{1}{2\mathrm{i}}\langle(\mathrm{tr}\,\mathbf{1})^2\rangle=-\frac{1}{2\mathrm{i}}\kappa^2r^2\langle 1\rangle. \tag{86}$$

Thus, in the limit $r\to 0$ all averages of trace products vanish like r^2 or faster. Since only terms $\sim r^2$ count, the contractions between the neighboring B and $B^\dagger$ in the same trace may be disregarded, unless we are dealing with the case of Eq. (86). [Taking in Eq. (85b) $X=\mathbf{1}$, Y or $[\cdots]$ not equal to unity, the RHS would be r times another averaged trace product and thus vanish like r^3 or faster.]

D. Recursion formula for the number of contractions

To translate Eqs. (85a)–(85d) into a recursion relation for the numbers of contractions $N_c(\vec{v})$, let us select a trace inside the product in Eq. (83), say $\mathrm{tr}\,M^l$ (assuming $v_l>0$), and a matrix B inside. We must contract that B with all other suitable matrices in the product of traces. Three possibilities arise, paralleling the recursion relation for the combinatorial numbers in Sec. III.

(i) First, we take up the contractions between our selected B in $\mathrm{tr}\,M^l$ and all suitable matrices in some *other* trace $\mathrm{tr}\,M^k$. In the unitary case rule Eq. (85a) implies that one k-trace and one l-trace disappear while a $(k+l-1)$-trace is created:

$$\langle\mathrm{tr}\overbrace{M^l\,\mathrm{tr}M^k}[\ldots]\rangle=-\frac{1}{2\mathrm{i}}\langle\mathrm{tr}\,M^{k+l-1}[\ldots]\rangle. \tag{87}$$

The contractions with all matrices $B^\dagger$ in k-traces $\mathrm{tr}\,M^k$ give the same result. We thus get $k(v_k-\delta_{kl})$ contributions like Eq. (87), where δ_{kl} is subtracted to exclude contractions between matrices inside the same trace. In the orthogonal case we must also invoke rule Eq. (85c) for contractions with $k(v_k-\delta_{kl})$ matrices B in traces $\mathrm{tr}\,M^k$ which again all contribute identically.

Each time, one k-trace and one l-trace disappear and one $(k+l-1)$-trace is added to the trace product. The vector $\vec{v}$ thus changes according to $v_k \to v_k - 1$, $v_l \to v_l - 1$, $v_{k+l-1} \to v_{k+l-1} + 1$; using the same notation as in our semiclassical analysis we write $\vec{v}^{[k,l\to k+l-1]}$. The overall number of matrices M is decreased by 1 such that $L \to L-1$. Each of the above contractions provides a contribution $N_c(\vec{v}^{[k,l\to k+l-1]})$; here, the denominator $(-2i)$ in the contraction rules is compensated by the factor $(-2i)^{L(\vec{v})}$ in the definition of the contraction numbers. Thus, the overall contribution to $N_c(\vec{v})$ reads $\kappa k(v_k - \delta_{kl})N_c(\vec{v}^{[k,l\to k+l-1]})$.

(ii) Next, we turn to "internal" contractions between the selected B and all matrices $B^\dagger$ in the same trace $\mathrm{tr}\, M^l$, apart from those immediately preceding or following the selected B. As explained above, the latter contractions would increase the order in r and lead to a result that vanishes as $r \to 0$. We apply rule Eq. (85b) and replace $\mathrm{tr}\, M^l$ by the product of two traces which together contain $l-1$ factors M. Thus, one l-trace disappears and two traces, of M^m and M^{l-m-1}, are added, with m running 1,2,..., $l-2$; the vector $\vec{v}$ then changes to $\vec{v}^{[l\to m,l-m-1]}$. From each of these contractions, $N_c(\vec{v})$ receives a contribution $N_c(\vec{v}^{[l\to m,l-m-1]})$.

(iii) For the orthogonal case rule Eq. (85d) yields further internal contractions: Pairing the selected B with all other $l-1$ matrices B, we obtain $l-1$ times $\mathrm{tr}\, M^{l-1}$. Each time $\vec{v}$ is thus replaced by $\vec{v}^{[l\to l-1]}$. Altogether, we gain the contribution $(l-1)N_c(\vec{v}^{[l\to l-1]})$.

Summing up all contributions, we arrive at the recurrence for N_c, for any l with $v_l > 0$,

$$N_c(\vec{v}) = \kappa \sum_k k(v_k - \delta_{kl}) N_c(\vec{v}^{[k,l\to k+l-1]}) + \sum_{m=1}^{l-2} N_c(\vec{v}^{[l\to m,l-m-1]}) + (\kappa - 1)(l-1) N_c(\vec{v}^{[l\to l-1]}). \tag{88}$$

The recurrence relation Eq. (88) reflects a single contraction step according to the rules Eqs. (85a)–(85d) and gives a sum of terms each containing one matrix M less than the original trace. Repeated such contraction steps give a sum of an ever increasing number of terms. After $L(\vec{v})-1$ steps every summand will be reduced to $N_c(\vec{v}')$ with $v_1' = 1$, $v_l' = 0$ for $l \geqslant 2$, which due to Eqs. (83) and (86) just equals unity. Consequently, $N_c(\vec{v})$ gives the number of terms in the sum at the final stage, and is thus appropriately called "the number of contractions."

Remarkably, the numbers of contractions $N_c(\vec{v})$ and the numbers of structures $N(\vec{v})$ are related by

$$N_c(\vec{v}) = N(\vec{v}) \frac{\kappa^{V-1} \prod_l l^{v_l} v_l!}{L(\vec{v})}. \tag{89}$$

With this identification, the recursion relations for both quantities, Eqs. (30), (43), and (55) for $N(\vec{v})$ and Eq. (88) for $N_c(\vec{v})$, coincide. When comparing, note that we may substitute $v_k - \delta_{kl} = v_k^{[k,l\to k+l-1]} + 1$. A constant proportionality factor in Eq. (89) was chosen to satisfy the initial condition $N(\vec{v}') = N_c(\vec{v}') = 1$. In view of Eq. (89), the series for $K(\tau)$ obtained from periodic-orbit theory, Eq. (29), and the σ model, Eq. (84), agree term by term.

VI. CONCLUSIONS AND OUTLOOK

Within the semiclassical frame of periodic-orbit theory, we have studied the spectral statistics of individual fully chaotic (i.e., hyperbolic and ergodic) dynamics. Central to our work are pairs of orbits that differ only inside close self-encounters. These orbit pairs yield series expansions of the spectral form factor $K(\tau)$, and our series agree with the predictions of random-matrix theory to all orders in τ, for all three Wigner-Dyson symmetry classes. Note that we do not require any averaging over ensembles of systems. Moreover, we find a close analogy between semiclassical periodic-orbit expansions and perturbative treatments of the nonlinear sigma model.

Important questions about universal spectral fluctuations remain open. The perhaps most urgent challenge is to go beyond the range of small τ, and treat $\tau > 1$.

The precise conditions for a system to be faithful to random-matrix theory remain to be established. We certainly have to demand that the contributions of all orbit pairs unrelated to close self-encounters mutually cancel. While one may expect such cancellation for generic systems, there are important exceptions. For dynamics exhibiting arithmetic chaos, strong degeneracies in the periodic-orbit spectrum give rise to system-specific contributions to the form factor; hence the systems in question deviate from random-matrix theory [36]. On the other hand, for the Sinai billiard and the Hadamard-Gutzwiller model, system-specific families of orbit pairs found in [10,29], respectively, do not prevent universality. In order to formulate the precise conditions for the BGS conjecture, one has to clarify when nonuniversal contributions may occur.

Moreover, a better justification is needed for neglecting the difference between stability amplitudes and periods of the partner orbits. So far, such a justification is available only for Sieber-Richter pairs in the Hadamard-Gutzwiller model [29,30].

The study of "correlated" orbit pairs opens a rich variety of applications in mesoscopic physics. Recent results concern matrix-element fluctuations [18] and transport properties such as conductance, shot noise, or delay times [37]. In the latter cases, the relevant trajectories are no longer periodic, and even, e.g., quadruples of trajectories have interesting interpretations. While previous work was restricted to the lowest orders in series expansions of the quantities in question, our machinery of encounters and permutations, together with intuition drawn from field theory, should allow us to attack the full expansion.

Finally, one might wish to go beyond Wigner's and Dyson's "threefold way" and extend the present results to the new symmetry classes [38], of experimental relevance for normal-metal/superconductor heterostructures; the first steps are taken in [39]. Further possible applications concern localization, a clarification of open problems in the nonlinear σ model [40], and the crossover between universality classes [16,41].

ACKNOWLEDGMENTS

Financial support of the Sonderforschungsbereich SFB/TR12 of the Deutsche Forschungsgemeinschaft is gratefully acknowledged. We have enjoyed fruitful discussions with Gerhard Knieper, Jürgen Müller, Dmitry Savin, Martin Sieber, Hans-Jürgen Sommers, Dominique Spehner, and Martin Zirnbauer.

APPENDIX A: INTEGRALS INVOLVING $1/t_{\mathrm{enc}}$

We want to evaluate the integral

$$\int_{-c}^{c} d^{l-1}s\, d^{l-1}u \frac{1}{t_{\mathrm{enc}}(s,u)} e^{i\Delta S/\hbar} \tag{A1}$$

for an l-encounter. The integration goes over the $2(l-1)$ stable and unstable coordinates s_j, u_j. These variables determine both the duration $t_{\mathrm{enc}}(s,u)$ of the encounter in question and its contribution to the action difference $\Delta S = \Sigma_j s_j u_j$. We shall show that the integral may be neglected in the semiclassical limit.

The key is the following change of picture. So far, all Poincaré sections $\mathcal{P}$ inside a given encounter were integrated over; we thus had to divide out the duration t_{enc}. Instead, we may single out a section $\mathcal{P}^e$, fixed at the end of the encounter, and only consider the stable and unstable separations s_j^e, u_j^e therein. For homogeneously hyperbolic dynamics, i.e., $\Lambda(\mathbf{x},t) = e^{\lambda t}$ for all $\mathbf{x}$ and t, the separations inside $\mathcal{P}^e$ are given by $s_j^e = s_j e^{-\lambda t_u}$, $u_j^e = u_j e^{\lambda t_u}$ with t_u denoting the time difference between $\mathcal{P}$ and $\mathcal{P}^e$.

We recall that the encounter ends when the first of the unstable components, say the Jth one, reaches $\pm c$ such that $u_J^e = u_J e^{\lambda t_u} = \pm c$. All $l-1$ possibilities $J = 1,2,\ldots,l-1$ and the two possibilities for the sign $u_J^e/c = \pm 1$ give additive contributions $I_J^{\pm}$ to the integral Eq. (A1). Each of them is easily evaluated after transforming the integration variables from s_j, u_j to s_j^e, u_j^e (with $j \neq J$), s_J^e, and $t_u = (1/\lambda)\ln(c/|u_J|)$. The Jacobian of that transformation equals λc. The new coordinates are restricted to the ranges $\{-c < s_j^e < c,\ -c < u_j^e < c$ for $j \neq J\}$, $-c < s_J^e < c$, $0 < t_u < t_{\mathrm{enc}}$, and determine the action difference as $\Delta S = \Sigma_j s_j^e u_j^e = \Sigma_{j\neq J} s_j^e u_j^e \pm s_J^e c$. We thus obtain

$$\begin{aligned} I_J^{\pm} &= \lambda c \int_{-c}^{c} ds_J^e e^{\pm i s_J^e c/\hbar} \left(\prod_{j\neq J} \int_{-c}^{c} ds_j^e du_j^e e^{i s_j^e u_j^e/\hbar} \right) \\ &\quad \times \frac{1}{t_{\mathrm{enc}}(s^e,u^e)} \int_0^{t_{\mathrm{enc}}(s^e,u^e)} dt_u \\ &\sim \lambda (2\pi\hbar)^{l-2} 2\hbar \sin\frac{c^2}{\hbar}; \end{aligned} \tag{A2}$$

note that the divisor t_{enc} was canceled by the t_u-integral; moreover, the $2(l-2)$ integrals over s_j^e, u_j^e, of the form already encountered in Eq. (25) gave the factor $(2\pi\hbar)^{l-2}$. Most importantly, the factor $\sin(c^2/\hbar)$, provided by the integral over s_J^e, is a rapidly oscillating function of c and $\hbar$, annulled by averaging over these quantities; such rapidly oscillating terms are essentially spurious and would not appear if smooth encounter cutoffs were used (instead of our $|s| < c$, $|u| < c$). At any rate, the integral (A1), just the $2(l-1)$-fold of Eq. (A2), vanishes as $\hbar \to 0$.

APPENDIX B: EXTENSION TO GENERAL HYPERBOLICITY AND $f > 2$

So far, we mostly restricted ourselves to two-dimensional homogeneously hyperbolic systems. To generalize, we reason similarly to Ref. [18], where only Sieber-Richter pairs were considered.

1. General hyperbolicity

First, we shed the restriction to "homogeneously hyperbolic" dynamics, for which all phase-space points $\mathbf{x}$ have the same Lyapunov exponent λ and stretching factor $\Lambda(t) = e^{\lambda t}$. We shall now lift our reasoning to general hyperbolicity, where the stretching factors $\Lambda(\mathbf{x},t)$ do depend on $\mathbf{x}$. In such systems the Lyapunov exponents of almost all points still coincide with the $\mathbf{x}$ independent "Lyapunov exponent of the system," whereas each periodic orbit may come with its own Lyapunov exponent [25]. Most importantly, the divergence of the stretches involved in an encounter depends on the local stretching factor of that encounter, rather than the Lyapunov exponent of the system. Our formula (12) for the encounter duration can only be read as an approximation, and that approximation is now to be avoided. We will thus allow $t_{\mathrm{enc}}^{\alpha}(\mathbf{x}_{\alpha 1}, s_\alpha, u_\alpha)$ to depend not only on the stable and unstable separations $s_{\alpha j}$, $u_{\alpha j}$, but also on the phase-space location of the piercing $\mathbf{x}_{\alpha 1}$ chosen as the origin of the respective Poincaré section. The changes arising will be important only for showing that the contribution arising from the $1/t_{\mathrm{enc}}$ integrals of Appendix A vanishes; recall that for the contributing terms all occurrences of t_{enc} mutually cancel.

When generalizing the statistics of encounters of Sec. II E, we now have to discriminate between piercing points $\mathbf{x} = \{\mathbf{x}_{11}, \mathbf{x}_{21}, \ldots, \mathbf{x}_{V1}\}$ as well. Given that encounter stretches are separated by nonvanishing loops, these piercing points are uncorrelated. The analog of w_T will thus be a density with respect to $\mathbf{x}$, s, and u, differing from Eq. (18) only by t_{enc} being a function of $\mathbf{x}$, and by a normalization factor $1/\Omega^V$.

Preparing for a careful average over periodic orbits we first introduce the density $\rho^{\gamma}(\mathbf{x},s,u,t)$ of piercing points, separations, and piercing times *of one fixed orbit* γ,

$$\begin{aligned} \rho^{\gamma}(\mathbf{x},s,u,t) = \prod_{\alpha=1}^{V} \delta(\Phi_{t_{\alpha 1}}(\mathbf{z}_0) - \mathbf{x}_{\alpha 1}) \prod_{j=2}^{l_\alpha} \delta(\Phi_{t_{\alpha j}}(\mathbf{z}_0) \\ - \mathbf{x}_{\alpha 1} - \hat{s}_{\alpha j}\mathbf{e}^s(\mathbf{x}_{\alpha 1}) - \hat{u}_{\alpha j}\mathbf{e}^u(\mathbf{x}_{\alpha 1})). \end{aligned}$$

Here, $\mathbf{z}_0$ denotes an arbitrary point of reference on γ and $\Phi_t(\mathbf{z}_0)$ is the image of $\mathbf{z}_0$ under evolution over the time t; if the jth stretch of the αth encounter is almost time reversed with respect to the first one, we have to replace $\Phi_t(\mathbf{z}_0) \to \mathcal{T}\Phi_t(\mathbf{z}_0)$. In analogy to Sec. II E, we integrate over the piercing times and divide out the encounter durations, obtaining a density of piercings and stable and unstable separations only, i.e.,

$$w^\gamma(\mathbf{x},s,u)=\frac{\int d^L t\,\rho^\gamma(\mathbf{x},s,u,t)}{\prod_\alpha t^\alpha_{\rm enc}(\mathbf{x}_{\alpha 1},s_\alpha,u_\alpha)}.$$

The time integrals can be split into one over $0<t_{11}<T$, and integrals over the differences $t'_{\alpha j}=t_{\alpha j}-t_{11}$ of all other piercing times from the first one, the latter with the same minimal distances as in Sec. II E. Using the group property $\Phi_{t_{\alpha j}}(\mathbf{z}_0)=\Phi_{t_{11}}(\Phi_{t'_{\alpha j}}(\mathbf{z}_0))$, we may thus represent w^γ as the average of an observable $f(\mathbf{z})$ along γ,

$$w^\gamma(\mathbf{x},s,u)=\frac{1}{T}\int_0^T dt_{11} f(\Phi_{t_{11}}(\mathbf{z}_0))\equiv[f]_\gamma$$

with

$$f(\mathbf{z})=\frac{T}{\prod_\alpha t^\alpha_{\rm enc}(\mathbf{x}_{\alpha 1},s_\alpha,u_\alpha)}\int d^{L-1}t'\prod_{\alpha=1}^{V}\delta(\Phi_{t'_{\alpha 1}}(\mathbf{z})-\mathbf{x}_{\alpha 1})\times\prod_{j=2}^{l_\alpha}\delta(\Phi_{t'_{\alpha j}}(\mathbf{z})-\mathbf{x}_{\alpha 1}-\hat{s}_{\alpha j}\mathbf{e}^s(\mathbf{x}_{\alpha 1})-\hat{u}_{\alpha j}\mathbf{e}^u(\mathbf{x}_{\alpha 1})).\tag{B1}$$

The periodic-orbit sum for the form factor may now be written as [compare Eq. (22)]

$$K(\tau)=\kappa\tau+\frac{\kappa}{T_H}\left\langle\sum_{\vec{v}}\frac{N(\vec{v})}{L}\int d^V\mu(\mathbf{x})\int d^{L-V}s\,d^{L-V}u\,e^{i\Delta S/\hbar}\times\left\{\sum_\gamma|A_\gamma|^2\delta(T-T_\gamma)[f]_\gamma\right\}\right\rangle,$$

where the $\mathbf{x}$ integral is over V points $\mathbf{x}_{\alpha 1}$ in the energy shell, i.e., $d^V\mu(\mathbf{x})=\prod_{\alpha=1}^V d^4x_{\alpha 1}\delta(H(\mathbf{x}_{\alpha 1})-E)$.

We have not used the sum rule of Hannay and Ozorio de Almeida, except for the diagonal part. Instead, we invoke the equidistribution theorem [26] (recall Sec. II A), which says that *ensembles* of periodic orbits, weighted with their stability, behave ergodically. More precisely, if we average an observable $f(\mathbf{z})$ (i) along a periodic orbit γ and subsequently (ii) over the ensemble of all such γ (inside a small time window and weighted with $|A_\gamma|^2$), we obtain an energy-shell average,

$$\frac{1}{T}\left\langle\sum_\gamma|A_\gamma|^2\delta(T-T_\gamma)[f]_\gamma\right\rangle_{\Delta T}=\int\frac{d\mu(\mathbf{z})}{\Omega}f(\mathbf{z})\equiv\overline{f(\mathbf{z})}.\tag{B2}$$

For the observable given in Eq. (B1), the energy-shell average can be evaluated provided the dynamics is mixing [25], i.e., if for two observables $g(\mathbf{z}),h(\mathbf{z})$ we have

$$\lim_{t\to\infty}\overline{g(\mathbf{z})h(\Phi_t(\mathbf{z}))}=\bar{g}\bar{h}.\tag{B3}$$

Physically, Eq. (B3) implies that for sufficiently large times t, we may neglect any classical correlations between $\mathbf{z}$ and its time evolved $\Phi_t(\mathbf{z})$, and hence replace $\Phi_t(\mathbf{z})$ by a phase-space point $\mathbf{z}'$ and average over all $\mathbf{z}'$. We can then disregard correlations between subsequent piercing points with time differences at least of the order of the Ehrenfest time. Using Eq. (B2), repeatedly invoking Eq. (B3) for the product of δ functions in Eq. (B1), and subsequently integrating over $t'_{\alpha j}$ as in Sec. II F, we obtain

$$\frac{1}{T}\left\langle\sum_\gamma|A_\gamma|^2\delta(T-T_\gamma)[f]_\gamma\right\rangle_{\Delta T}=\frac{T\left(T-\sum_\alpha l_\alpha t^\alpha_{\rm enc}\right)^{L-1}}{(L-1)!\prod_\alpha t^\alpha_{\rm enc}\Omega^L}\tag{B4}$$

which as expected coincides with $w_T(s,u)$ of Eq. (17), up to division by Ω^V and the $\mathbf{x}$ dependence of $t^\alpha_{\rm enc}(\mathbf{x},s,u)$.

The $t_{\rm enc}$ independent terms in the multinomial expansion of Eq. (B4) yield the same contribution to the form factor as before, since the divisor Ω^V is canceled by integration over $\mathbf{x}$. All other contributions can be neglected in the semiclassical limit: they are either of a too low order in T or proportional to integrals of the form

$$\int\frac{d\mu(\mathbf{x})}{\Omega}\int_{-c}^{c}d^{l-1}s\,d^{l-1}u\frac{1}{t_{\rm enc}(\mathbf{x},s,u)}e^{i\Delta S/\hbar},$$

which we reveal as negligible similarly as Eq. (A1). For each contribution $I^\pm_J$, we transform from $\mathbf{x},s,u$ to phase-space points $\mathbf{x}^e$ and separations s^e_j,u^e_j ($u^e_J=\pm c$ fixed) inside a Poincaré section $\mathcal{P}^e$ in the encounter end, and the separation t_u between $\mathcal{P}$ and $\mathcal{P}^e$. For general hyperbolic dynamics, the stable and unstable coordinates are related by $s^e_j=\Lambda(\mathbf{x},t_u)^{-1}s_j$ and $u^e_j=\Lambda(\mathbf{x},t_u)u_j$; see Eq. (7). The Jacobian[8] now reads $\chi(\mathbf{x}^e)c$ with the local stretching rate defined as $\chi(\Phi_t(\mathbf{x}))=d\ln|\Lambda(\mathbf{x},t)|/dt$ [25]. We thus obtain

$$I^\pm_J=\int\frac{d\mu(\mathbf{x}^e)}{\Omega}\chi(\mathbf{x}^e)c\int_{-c}^{c}ds^e_J e^{\pm is^e_J c/\hbar}\times\prod_{j\neq J}\left(\int_{-c}^{c}ds^e_j du^e_j e^{is^e_j u^e_j/\hbar}\right)\times\frac{1}{t_{\rm enc}(\mathbf{x}^e,s^e,u^e)}\int_0^{t_{\rm enc}(\mathbf{x}^e,s^e,u^e)}dt_u,\tag{B5}$$

coinciding with Eq. (A2) since the energy-shell average of the local stretching rate yields the Lyapunov exponent of the system λ [25].

The Jacobian $\chi(\mathbf{x}^e)c$ has an interesting physical interpretation [18]. If we shift our Poincaré section along the orbit, the piercing points travel, changing their unstable coordinates with the velocity $du_j/dt=\chi(\mathbf{x}(t))u_j$; see Fig. 13. The Jacobian $\chi(\mathbf{x}^e)c$ thus gives the velocity in the end of the encounter region. Restricting ourselves to $\mathcal{P}^e$ and multiplying with the above velocity, we simply measure the flux of piercings through the line $u_J=\pm c$. Since each point has to traverse that line, our transformation indeed provides an alternative counting of piercings. Note that the unstable coordinates

[8] In particular, we have $du_J/dt_u=-\Lambda(\mathbf{x},t_u)^{-1}[d\ln|\Lambda(\mathbf{x},t_u)|/dt_u]u^e_J=-\Lambda(\mathbf{x},t_u)^{-1}\chi(\mathbf{x}^e)u^e_J$ with $u^e_J=\pm c$, where we used that $\Phi_{t_u}(\mathbf{x})=\mathbf{x}^e$. The factor $\Lambda(\mathbf{x},t_u)^{-1}$ is compensated by the remaining transformations $u_j\to u^e_j$ ($j\neq J$) and $s_j\to s^e_j$.

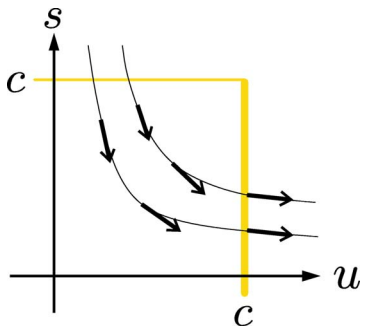

FIG. 13. (Color online) Motion of piercing points through Poincaré section $\mathcal{P}$ of a 2-encounter. As $\mathcal{P}$ is shifted, unstable components grow and stable ones shrink, traveling on a hyperbola $\Delta S = su$; arrows denote the direction of motion. At the end of the encounter, piercing points traverse the line $u=c$. Negative s, u are not shown.

temporarily shrink rather than grow if the local stretching rate is negative, and thus may traverse the line $u_j = \pm c$ several times. Due to the asymptotic growth of $|u_J|$, there is one more traversal with growing $|u_J|$ [and positive contribution to Eq. (B5)] than with shrinking $|u_J|$ (and negative contribution); hence only one contribution remains effective.

2. More than two freedoms

For dynamics with any number $f \geqslant 2$ of degrees of freedom, the Poincaré section $\mathcal{P}$ at point $\mathbf{x}$ is spanned by $f-1$ pairs of stable and unstable directions $\mathbf{e}_k^s(\mathbf{x}), \mathbf{e}_k^u(\mathbf{x})$ $(k = 1,2,\ldots,f-1)$. A displacement $\delta\mathbf{x}$ inside $\mathcal{P}$ may thus be decomposed as

$$\delta\mathbf{x} = \sum_{k=1}^{f-1} [\hat{s}_k \mathbf{e}_k^s(\mathbf{x}) + \hat{u}_k \mathbf{e}_k^u(\mathbf{x})]$$

[compare Eq. (6)]. Each pair of directions comes with separate stretching factors $\Lambda_k(\mathbf{x},t)$ and Lyapunov exponent λ_k. The directions are mutually normalized as [18]

$$\mathbf{e}_k^u(\mathbf{x}) \wedge \mathbf{e}_l^s(\mathbf{x}) = \delta_{kl},$$

$$\mathbf{e}_k^u(\mathbf{x}) \wedge \mathbf{e}_l^u(\mathbf{x}) = \mathbf{e}_k^s(\mathbf{x}) \wedge \mathbf{e}_l^s(\mathbf{x}) = 0,$$

where $\mathbf{e}_k^u(\mathbf{x}) \wedge \mathbf{e}_k^s(\mathbf{x}) = 1$ is a useful convention, whereas all other relations follow from hyperbolicity.

Writing out the additional index k, the uniform piercing probability (see Sec. II A) reads $(dt/\Omega)\Pi_{k=1}^{f-1} d\hat{s}_k d\hat{u}_k$. The encounters (defined by $|\hat{s}_{jk}|, |\hat{u}_{jk}| < c$, for all j,k) have heads and tails with durations

$$t_u = \min_{j,k}\left\{\frac{1}{\lambda_k}\ln\frac{c}{|\hat{u}_{jk}|}\right\}, \quad t_s = \min_{j,k}\left\{\frac{1}{\lambda_k}\ln\frac{c}{|\hat{s}_{jk}|}\right\}$$

[compare Eq. (12)], and contribute to the action difference an amount given by $\Delta S = \Sigma_{jk} s_{jk} u_{jk}$, with s_{jk}, u_{jk} defined similarly to Sec. II C 2. The integral over $s_{\alpha jk}, u_{\alpha jk}$ in the second line of Eq. (24) yields $(2\pi\hbar)^{(L-V)(f-1)}$, which is just what we need since Heisenberg time now reads $T_H = \Omega/(2\pi\hbar)^{f-1}$. Given that the encounter ends as soon as one unstable component u_{JK} reaches $\pm c$, the $1/t_{\text{enc}}$ integral of Appendixes A and B 1 is split into components $I_{JK}^{\pm}$, with λ replaced by λ_K, and $\chi(\mathbf{x})$ by $\chi_K(\mathbf{x})$.

APPENDIX C: ACTION CORRELATIONS

The semiclassical form factor Eq. (5) can be written in terms of an "action correlation function" [6],

$$P(y) = \left\langle \frac{1}{T}\sum_{\gamma,\gamma'} A_\gamma A_{\gamma'}^* \delta\left(T - \frac{T_\gamma + T_{\gamma'}}{2}\right) \times \delta\left(y - \frac{2\pi T(S_\gamma - S_{\gamma'})}{\Omega}\right)\right\rangle,$$

$$K(\tau) = \tau\int_{-\infty}^{\infty} P(y) e^{iy/\tau} dy, \quad \tau > 0. \tag{C1}$$

Using the density of action differences $P_{\vec{v}}(\Delta S)$, Eq. (19), we have evaluated the contributions to $P(y)$ which arise from diagonal pairs and orbits (γ,γ') differing by reconnections in close self-encounters. Collecting the terms relevant for the form factor we obtain

$$P(y) = \begin{cases} \delta(y) & \text{unitary}, \\ 2\delta(y) - \dfrac{\sin^2 y}{|y|} + \dfrac{1}{\pi}\dfrac{\sin 2y}{y}\ln|y|, & \text{orthogonal}. \end{cases} \tag{C2}$$

Random-matrix theory predicts, through the inverse Fourier transform of the above Eq. (C1),

$$P_{\text{GUE}}(y) = \delta(y) - \frac{2}{\pi}\left(\frac{\sin(y/2)}{y}\right)^2,$$

$$P_{\text{GOE}}(y) = 2\delta(y) - \frac{4}{\pi}\left(\frac{\sin(y/2)}{y}\right)^2 + \frac{2}{\pi y}\{\cos^2 y \,\text{si}\, y - \cos 2y \,\text{si}\, 2y + \cos y \sin y[2\,\text{Ci}(2y) - \text{Ci}\, y]\}$$

with si y and Ci y the integral sine and cosine [42]. There appears to be, on first glance, a contradiction between periodic-orbit theory and RMT. However, for both symmetry classes the corresponding results differ by smooth functions of the real variable y, smooth implying continuous derivatives of all orders. According to the Riemann-Lebesgue theorem, the respective Fourier transforms Eq. (C1) have identical τ expansions of $K(\tau)$. The even and odd parts of that expansion are respectively caused by the logarithmic and modulus terms in Eq. (C2).

APPENDIX D: ENCOUNTER OVERLAP

So far, we have confined ourselves to encounters whose stretches are separated by intervening loops, i.e., do not overlap. To justify this, we shall show that encounters without

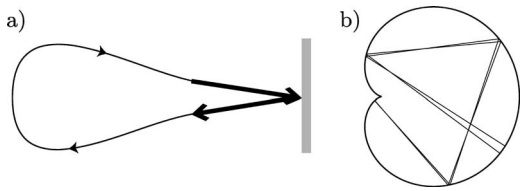

FIG. 14. Encounters with almost self-retracing reflections: (a) orbit scheme in configuration space; (b) example for cardioid billiard.

intervening loops do not contribute to the form factor. The overlap of stretches involved in different encounters has already been treated in Sec. II E. We will show that overlap of antiparallel stretches (if not prohibited for dynamical reasons, as in the Hadamard-Gutzwiller model) can be regarded as the reflection of a single stretch at a hard wall, e.g., in billiards.

We shall see that if parallel stretches overlap (or come very close), they have to follow multiple revolutions of a shorter orbit $\tilde{\gamma}$. In this case, several different encounters may lead to the same partner orbit. We will show how to select one of these encounters. The resulting condition leads to the same value for the form factor as leaving out encounters with overlapping stretches.

1. Antiparallel encounter stretches

First, let us consider two almost mutually time-reversed encounter stretches not separated by an intervening loop. Such a scenario is only possible if the orbit undergoes a nearly self-retracing reflection from a hard wall. After the reflection, the particle will for some time travel close to the precollision trajectory, such that technically an antiparallel 2-encounter is formed (Fig. 14), however with just one loop and two "ports" attached. As shown in [14], no partner can be connected to such an encounter; formally attempting to construct a "partner" one obtains either the original orbit or its time-reversed.

The proof becomes surprisingly simple if we use symbolic dynamics. Here, periodic orbits are fixed uniquely by sequences of symbols, e.g., denoting in certain billiards the pieces of the boundary where the orbit is reflected (see, e.g., [43]); symbol sequences of periodic orbits are defined modulo cyclic permutations. Even loops or encounter stretches can be assigned a sequence of symbols, which remains unchanged if the loop or stretch is slightly deflected. Given a Sieber-Richter pair, the orbit γ must have a sequence $\gamma=\mathcal{L}_1\mathcal{E}\mathcal{L}_2\bar{\mathcal{E}}$, $\mathcal{L}_1$ and $\mathcal{L}_2$ denoting the two loops and $\mathcal{E}$ and $\bar{\mathcal{E}}$ two almost time-reversed encounter stretches [14,44]. The symbol sequence $\bar{\mathcal{E}}$ is obtained from $\mathcal{E}$ by "time reversal"; in the above example we simply have to revert the order of symbols. The partner has one loop inverted in time, and is thus described by the symbol sequence $\gamma'=\mathcal{L}_1\mathcal{E}\bar{\mathcal{L}}_2\bar{\mathcal{E}}$.

As announced, both the symbol sequences of the two partner orbits turn out equal if the loop with symbol sequence $\mathcal{L}_2$ is absent. A generalization to systems without symbolic dynamics is given in [14–16,18].

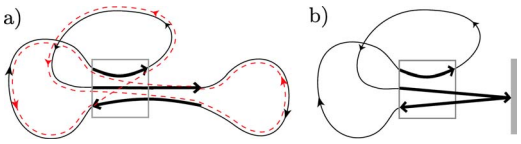

FIG. 15. (Color online) 3-encounter (in the box) with a "fringe" where only two antiparallel stretches remain close. Stretches are separated by a loop in (a) but not in (b); an almost self-retracing reflection arises in the latter case. A partner orbit which reconnects all three ports (dashed line) is obtained only in case (a).

We thus see that almost self-retracing orbit pieces as in Fig. 14 each have to be regarded as one single stretch, folded back into itself. Clearly this carries over if they form part of a larger l-encounter.

2. Antiparallel fringes

Recall that we define an l-encounter as a region inside a periodic orbit in which l orbit stretches come close up to time reversal. Attached to the sides of the encounter are "fringes" in which only some of the l stretches remain close while others have already gone astray, as shown in Fig. 15(a). We shall now show that these fringes do not affect the spectral form factor.

As a first example, let us assume that two *antiparallel* stretches remain close after the end of the encounter, as in Fig. 15(a). If there is no intervening loop [see Fig. 15(b)], the orbit has to undergo an almost self-retracing reflection, just like the one studied in Appendix D 1. Since no connections can be switched between the two stretches involved we have to disregard such encounters.

On the other hand, if the fringe stretches are separated by an external loop, a partner orbit is obtained as usual, by reshuffling connections inside the encounter; see Fig. 15(a). To make sure that there is an intervening loop, we impose minimal separations between piercing points, similar to those used for excluding overlap between encounters in Sec. II E. After two antiparallel stretches (labeled by j and $j+1$) have pierced through a Poincaré section $\mathcal{P}$ with unstable coordinates $\hat{u}_{\alpha j}$ and $\hat{u}_{\alpha,j+1}$, they will remain close for a time $(1/\lambda)\ln(c/|\hat{u}_{\alpha j}-\hat{u}_{\alpha,j+1}|)$. This duration contains both the time t_u (12) till the end of the αth encounter, and an additional time span *after* the end of the encounter, which gives the duration of the fringe. Using the unstable coordinates $\hat{u}^e_{\alpha j}$ of piercing through a section in the end of the encounter (depending on $\hat{u}_{\alpha j}$ via $\hat{u}^e_{\alpha j}=\hat{u}_{\alpha j}e^{\lambda t_u}$), this additional time may be written as $(1/\lambda)\ln(c/|\hat{u}^e_{\alpha j}-\hat{u}^e_{\alpha,j+1}|)$.

Hence, the minimal time difference $2t_u$ between piercings demanded in Sec. II E has to be incremented by a time $t_{\text{fringe}}=(2/\lambda)\ln(c/|\hat{u}^e_{\alpha j}-\hat{u}^e_{\alpha,j+1}|)$, depending on $\hat{u}$ (or, equivalently, the coordinates u defined in Sec. II C 2) only via $\hat{u}^e$ (or, equivalently, u^e). Similarly, the minimal separations related to stable coordinates have to be incremented by an amount purely depending on the stable coordinates s^b in the beginning of the encounter. The contribution of each encounter to the total sum of minimal separations t_{excl} can therefore be written in the form

$$t^{\alpha}_{\mathrm{excl}} = l_{\alpha} t^{\alpha}_{\mathrm{enc}} + \Delta t^{\alpha}_{s}(s^{b}) + \Delta t^{\alpha}_{u}(u^{e}) \tag{D1}$$

with Δt_s and Δt_u corresponding functions of s^b and u^e only (whose explicit forms will not be needed in the following). The numerator in the density of phase-space separations $w_T(s,u)$ Eq. (18) has to be modified accordingly.

By reasoning as in Sec. II F, we see that only those terms of the multinomial expansion of the numerator in $w_T(s,u)$ contribute which involve a product of all $t^{\alpha}_{\mathrm{excl}}$. They now have to be written as [compare Eq. (23)]

$$\frac{w_T^{\mathrm{contr}}(s,u)}{L} = h(\vec{v})\left(\frac{T}{\Omega}\right)^{L-V} \prod_{\alpha} \frac{t^{\alpha}_{\mathrm{excl}}}{l_{\alpha} t^{\alpha}_{\mathrm{enc}}}$$

$$= h(\vec{v})\left(\frac{T}{\Omega}\right)^{L-V} \prod_{\alpha} \left[1 + \frac{\Delta t^{\alpha}_{s} + \Delta t^{\alpha}_{u}}{l_{\alpha} t^{\alpha}_{\mathrm{enc}}}\right],$$

and contribute to the form factor as [compare Eq. (24)]

$$\kappa\tau h(\vec{v})\left(\frac{T}{\Omega}\right)^{L-V} \prod_{\alpha} \left[\int d^{L-V}s\, d^{L-V}u \times \left(1 + \frac{\Delta t^{\alpha}_{s}(s^{b}) + \Delta t^{\alpha}_{u}(u^{e})}{l_{\alpha} t^{\alpha}_{\mathrm{enc}}}\right) \exp\left(\frac{i}{\hbar}\sum_{j} s_{\alpha j} u_{\alpha j}\right)\right]. \tag{D2}$$

The integral in Eq. (D2) coincides with the one in Eq. (24) up to the fringe corrections proportional to $\Delta t^{\alpha}_{s}/t^{\alpha}_{\mathrm{enc}}$ and to $\Delta t^{\alpha}_{u}/t^{\alpha}_{\mathrm{enc}}$, respectively. By reasoning similarly to Appendix A, one easily shows that the resulting integrals vanish in the semiclassical limit. For the integrand $\Delta t^{\alpha}_{u}/t^{\alpha}_{\mathrm{enc}}$, the rapidly oscillating integral over s^e_j inside Eq. (A2) is not modified; for $\Delta t^{\alpha}_{s}/t^{\alpha}_{\mathrm{enc}}$ we have to consider a surface of section in the beginning rather than in the end of the encounter. For antiparallel orbit stretches, fringe corrections to the form factor are hence revealed as negligible semiclassically.

The present treatment immediately generalizes to $f>2$, by writing out the additional index k, and to nonhomogeneously hyperbolic systems by keeping the dependence on $\mathbf{x}$. In particular, Δt_s will depend on both s^b and the phase-space points $\mathbf{x}^b$ in the beginning of the encounter, and Δt_u on u^e and $\mathbf{x}^e$ in the end of the encounter.

3. Parallel encounter stretches

We now turn to parallel encounter stretches. We shall see that if two subsequent parallel stretches of an encounter overlap or follow each other after a relatively short loop, the encounter will have a very peculiar structure.

Whenever two points of a periodic orbit γ are close in phase space, the piece of trajectory between these points must be almost periodic—and hence in the vicinity of a shorter periodic orbit $\tilde{\gamma}$. The two phase-space points belong to mutually close encounter stretches, which thus are near to $\tilde{\gamma}$ as well. Typically, these stretches are short compared to the intervening loop(s). Hence γ follows only slightly more than one revolution of $\tilde{\gamma}$ [Fig. 16(a)].

In contrast, if the stretches are only separated by a short loop [see Fig. 16(b)], the orbit γ will remain close to $\tilde{\gamma}$ for almost two periods: Two phase-space points in the center of these stretches enclose one revolution of $\tilde{\gamma}$, consisting of the head of the first stretch, the short loop mentioned above, and the tail of the second stretch. The tail of the second stretch and the head of the first one make for slightly less than one additional revolution.

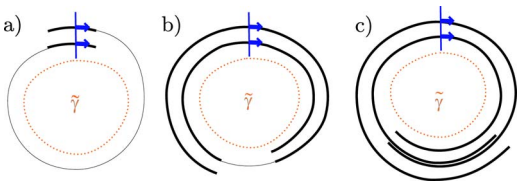

FIG. 16. (Color online) Two parallel encounter stretches (thick lines) (a) separated by a comparatively long loop (thin line), (b) separated by a short loop, and (c) overlapping in a region depicted by two very close thick lines. The long orbit respectively follows (a) slightly more than one, (b) slightly less than two, and (c) more than two periods of the shorter orbit $\tilde{\gamma}$ (dotted line). Also depicted are Poincaré sections approximately in the center of the encounters, each with two piercing points.

Finally, if the stretches overlap, γ will contain two or more repetitions of $\tilde{\gamma}$; see Fig. 16(c) for an example of γ following slightly more than two periods of $\tilde{\gamma}$.

All further stretches of the encounters considered also have to come close to $\tilde{\gamma}$. The orbit γ will thus approach $\tilde{\gamma}$ several times, at least one approach lasting significantly longer than one revolution of $\tilde{\gamma}$.

The crucial point is now the following. Recall that we describe orbit pairs in terms of their piercings through Poincaré sections. In the present scenario, it will turn out that we have large freedom in selecting such piercings. Some of the possible choices formally correspond to different encounters, even though they yield the same partner orbit. Therefore blindly considering all encounters and associating with each of them a partner orbit we would count certain orbit pairs several times. We will demonstrate that within each such family of encounters related to the same partner orbit, only for one member the stretches are separated by loops exceeding certain minimal durations. When evaluating the form factor, we shall only include this representative encounter and disregard all other members of the family, to avoid overcounting of orbit pairs. The resulting contribution will turn out the same as if we only demand the intervening loops to be positive; this is why the latter condition was used in the main part.

To start, we consider a parallel 3-encounter inside an orbit γ, piercing through a Poincaré section $\mathcal{P}$ in phase-space points $\mathbf{x}_1$, $\mathbf{x}_2$, and $\mathbf{x}_3$. We shall derive a restriction on the time difference t_{12} between $\mathbf{x}_1$ and $\mathbf{x}_2$. Since $\mathbf{x}_1$ and $\mathbf{x}_2$ are close in phase space, the part of γ between these points approximately follows a periodic orbit $\tilde{\gamma}$ with period close to t_{12}. The orbit γ will also stay close to $\tilde{\gamma}$ for some time before $\mathbf{x}_1$ and after $\mathbf{x}_2$. The whole region close to $\tilde{\gamma}$ is drawn as a thick full line in Fig. 17(a). In the vicinity of $\mathbf{x}_3$, the orbit γ has to approach $\tilde{\gamma}$ for a second time; compare the dash-dotted line in Fig. 17(a).

The piercings $\mathbf{x}_1$, $\mathbf{x}_2$, and $\mathbf{x}_3$ cut γ into three parts. When switching connections to form a partner orbit, we change the ordering of these parts. This reordering may be interpreted as cutting out the orbit part leading from $\mathbf{x}_1$ to $\mathbf{x}_2$ (close to $\tilde{\gamma}$)

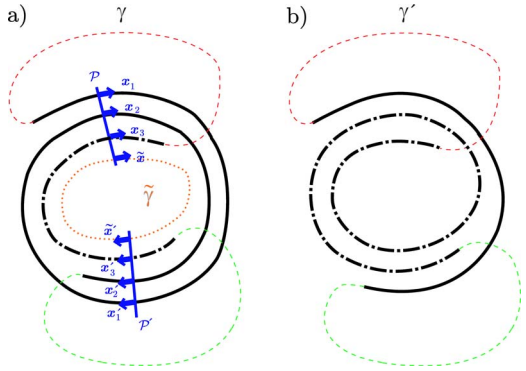

FIG. 17. (Color online) (a) An orbit γ approaches a shorter orbit $\tilde{\gamma}$ (dotted line) in two regions (marked by thick full and dash-dotted lines). It pierces three times through each of the Poincaré sections $\mathcal{P}$ and $\mathcal{P}'$; the two sets of piercings belong to two different encounters. (b) Reconnections in either encounter lead to the same partner γ', with one revolution of $\tilde{\gamma}$ transposed between the full and dash-dotted regions.

and reinserting it between the two other parts, i.e., when γ traverses $\mathbf{x}_3$. In other words, one revolution of $\tilde{\gamma}$ is transposed between the two regions approaching $\tilde{\gamma}$. The resulting partner is shown in Fig. 17(b), with one revolution of $\tilde{\gamma}$ taken out from the region depicted by the thick full line and reinserted inside the dash-dotted region. (Of course a simple transposition of orbit parts does not yield a continuous partner orbit, but the resulting trajectory can be turned into a periodic orbit by a small deformation.)

Most importantly, other piercing points through a (possibly) different Poincaré section $\mathcal{P}'$ may yield the same partner. The piercings $\mathbf{x}_1'$, $\mathbf{x}_2'$, and $\mathbf{x}_3'$ through $\mathcal{P}'$ will be shifted with respect to to $\mathbf{x}_1$, $\mathbf{x}_2$, and $\mathbf{x}_3$. However, they are required to be close to $\tilde{\gamma}$, with $\mathbf{x}_1'$ and $\mathbf{x}_2'$ inside the same region of approach to $\tilde{\gamma}$ as $\mathbf{x}_1$ and $\mathbf{x}_2$, and $\mathbf{x}_3'$ in the same region as $\mathbf{x}_3$; compare Fig. 17(a). The first two piercings both need to be shifted by the same amount of time t_A, to guarantee that they remain separated by one period of $\tilde{\gamma}$. The third one may be shifted by a different time t_B. Then, upon reconnection again one revolution of $\tilde{\gamma}$ (the piece leading from $\mathbf{x}_1'$ to $\mathbf{x}_2'$) is cut out from the first region approaching $\tilde{\gamma}$ and reinserted inside the second region of approach (at position $\mathbf{x}_3'$). Hence we obtain the same partner as for the "old" piercings.

If $t_A=t_B$ the piercings $\mathbf{x}_1'$, $\mathbf{x}_2'$, and $\mathbf{x}_3'$ form part of the same encounter as $\mathbf{x}_1$, $\mathbf{x}_2$, and $\mathbf{x}_3$, crossed by a different Poincaré section. However, if $t_A \neq t_B$ our "new" piercings belong to a different encounter than the old ones, with both encounters yielding the same partner orbit. In the example of Fig. 17(a), the piercings $\mathbf{x}_1'$ and $\mathbf{x}_2'$ are shifted to the future ($t_A>0$) compared to their counterparts $\mathbf{x}_1$ and $\mathbf{x}_2$, whereas $\mathbf{x}_3'$ is located to the past of $\mathbf{x}_3$ ($t_B<0$). Nevertheless, both sets of piercings lead to the same partner orbit [depicted in Fig. 17(b)] with one revolution of $\tilde{\gamma}$ transposed between the two regions approaching $\tilde{\gamma}$.

How far may the piercings be shifted without leaving the vicinity of $\tilde{\gamma}$? To give a quantitative answer (for the case $t_A>0$, $t_B<0$), we first determine the stable and unstable coordinates of the phase-space point $\tilde{\mathbf{x}}$ in which the orbit $\tilde{\gamma}$ intersects the section $\mathcal{P}$. The trajectories passing through $\tilde{\mathbf{x}}$ and $\mathbf{x}_1$ remain close at least for one period of $\tilde{\gamma}$ after which they are carried to $\tilde{\mathbf{x}}$ and $\mathbf{x}_2$, respectively. Thus by reasoning similar to that of Sec. II C 1 we see that both $\tilde{\mathbf{x}}$ and $\mathbf{x}_1$ have the same unstable component $\hat{\tilde{u}} \approx \hat{u}_1$. Likewise the trajectories passing through $\tilde{\mathbf{x}}$ and $\mathbf{x}_2$ remain close for large negative times, such that the stable component of $\tilde{\mathbf{x}}$ may be approximated by $\hat{\tilde{s}} \approx \hat{s}_2$.

The first two piercings may be shifted to the future as long as both remain close to $\tilde{\gamma}$. The second piercing will be the first to deviate significantly from $\tilde{\gamma}$; it will go astray when its unstable separation from the shorter orbit, i.e., $\hat{u}_2 - \hat{\tilde{u}} \approx \hat{u}_2 - \hat{u}_1$, grows beyond our bound c. Since this will happen after a time $(1/\lambda)\ln(c/|\hat{u}_2 - \hat{u}_1|)$, we will stay in the vicinity of $\tilde{\gamma}$ while

$$t_A < \frac{1}{\lambda} \ln \frac{c}{|\hat{u}_2 - \hat{u}_1|}. \tag{D3}$$

The third piercing may be shifted to the past as long as the stable component of its separation from $\tilde{\gamma}$, i.e., $\hat{s}_3 - \hat{\tilde{s}} \approx \hat{s}_3 - \hat{s}_2$ remains below c; this leads to the restriction

$$-t_B < \frac{1}{\lambda} \ln \frac{c}{|\hat{s}_3 - \hat{s}_2|}. \tag{D4}$$

We only consider piercing points located inside the same Poincaré section. This restriction is trivially satisfied if all piercings are shifted by the same amount ($t_A - t_B = 0$) from one section $\mathcal{P}$ to a different section $\mathcal{P}'$. If an encounter stretch follows multiple revolutions of $\tilde{\gamma}$, it will pierce through $\mathcal{P}'$ several times. We may thus subsequently switch to different piercings without leaving $\mathcal{P}'$. Doing so, $t_A - t_B$ is only changed by an integer number of periods of $\tilde{\gamma}$. For instance, if we, respectively, replace the first two piercings by the ones following after one revolution of $\tilde{\gamma}$, we will increase t_A and thus $t_A - t_B$ by one period of $\tilde{\gamma}$, i.e., by t_{12}. Altogether, the restriction of having $\mathbf{x}_1'$, $\mathbf{x}_2'$, and $\mathbf{x}_3'$ located inside the same Poincaré section can be formulated as

$$t_A - t_B = n\, t_{12}, \quad n = 0, 1, 2, \ldots \tag{D5}$$

Combining Eqs. (D3)–(D5), we are led to

$$n\, t_{12} < \frac{1}{\lambda} \ln \frac{c}{|\hat{u}_2 - \hat{u}_1|} + \frac{1}{\lambda} \ln \frac{c}{|\hat{s}_3 - \hat{s}_2|}. \tag{D6}$$

If the separation t_{12} is sufficiently large, i.e., if

$$t_{12} > \frac{1}{\lambda} \ln \frac{c}{|\hat{u}_2 - \hat{u}_1|} + \frac{1}{\lambda} \ln \frac{c}{|\hat{s}_3 - \hat{s}_2|}, \tag{D7}$$

Eq. (D6) will only possess the trivial solution $n=0$ and thus $t_A=t_B$, incompatible with our assumption $t_A>0$, $t_B<0$. In this case, no alternative encounter can be obtained by shifting the first two piercings to the future and the third to the past; otherwise such encounters can be found, one for each possible $n \geqslant 1$.

We are now prepared to single out one representative encounter for each orbit pair. Inside each family of equivalent encounters we take the member for which the time between piercings $\mathbf{x}_2$ and $\mathbf{x}_3$ is smallest. This time difference is de-

creased by all shifts with $t_A>0$, $t_B<0$, and increased if $t_A<0$, $t_B>0$. (t_A and t_B with equal sign need not be considered since we may shift $\mathcal{P}'$ until the signs are opposite.) Hence from the chosen encounter no alternative one may be accessible through a shift with $t_A>0$, $t_B<0$. Consequently our representative encounter has to satisfy Eq. (D7). Using the stable coordinates $\hat{s}_j^b=\hat{s}_j e^{\lambda t_s}$ in the beginning of the encounter and the unstable coordinates $\hat{u}_j^e=\hat{u}_j e^{\lambda t_u}$ in the end, and recalling that $t_{\mathrm{enc}}=t_s+t_u$, we may rewrite this condition as

$$t_{12} > t_{\mathrm{enc}} + \frac{1}{\lambda}\ln\frac{c}{|\hat{u}_2^e-\hat{u}_1^e|} + \frac{1}{\lambda}\ln\frac{c}{|\hat{s}_3^b-\hat{s}_2^b|}. \tag{D8}$$

Minimal separations between, say, the second and third piercing, are obtained from Eq. (D8) by cyclic permutation.

Demanding $t_{12}>t_{\mathrm{enc}}$ implies that we consider only encounters whose stretches do not overlap, as postulated in the main part. The additional increment in Eq. (D8) can be interpreted as a minimal loop duration. If the loop in between the encounter stretches is very large, γ will follow $\tilde{\gamma}$ only for slightly more than one period and there will be no alternative encounter. If the loop slightly exceeds our threshold, there typically are alternative encounters, but the one considered is the encounter representative for our orbit pair. The boundary between both scenarios is irrelevant for our considerations.

The minimal loop length depends purely on $\hat{s}^b$ and $\hat{u}^e$. In the language of Appendix D 2, the second summand gives the duration of the fringe where the first two stretches remain close after the end of the encounter; likewise the third summand represents the duration of the fringe where the second and third stretch come close before the beginning of the encounter. Due to the exclusive dependence on $\hat{s}^b$ and $\hat{u}^e$, respectively, both terms have a negligible impact on the form factor; again the sum of minimal time differences will be of the form Eq. (D1) met in case of antiparallel fringes.

The previous line of reasoning may be extended to all other relevant cases. For $\mathcal{T}$-invariant systems, the third piercing needs to be shifted by an amount $-t_B$ rather than t_B if it is approximately time reversed with respect to $\mathbf{x}_1$ and $\mathbf{x}_2$. See [30] for a generalization to l-encounters with arbitrary l, and [29,30] for more details on overlap in 3-encounters. Finally, our reasoning carries over to $f>2$ and nonhomogeneous hyperbolicity as outlined in the antiparallel case.

APPENDIX E: THE NONLINEAR σ MODEL

1. Replica trick and perturbation expansion

We here sketch the derivation of the integral representation Eq. (79) for the Wigner-Dyson ensembles. For simplicity, we concentrate on the GUE. For the GOE see Sec. E 2 below. We start from the "replica representation" of the Green function $G(z)\equiv(z-H)^{-1}$,

$$\mathrm{tr}\, G(z) = \partial_z \mathrm{tr}\ln[G(z)^{-1}]$$

$$= \partial_z \ln[\det G(z)^{-1}] = -\lim_{r\to 0}\frac{1}{r}\partial_z \det G(z)^r. \tag{E1}$$

We take the Hamiltonian H as an N-dimensional Hermitian random matrix whose Gaussian statistics is defined by the two moments

$$\overline{H_{\mu\nu}}=0,$$

$$\overline{H_{\mu\nu}H_{\nu'\mu'}} = \frac{\lambda^2}{N}\delta_{\mu\mu'}\delta_{\nu\nu'}; \tag{E2}$$

these imply Wigner's semicircle for the mean level density as $\bar{\rho}(E)=(N/\pi\lambda^2)\sqrt{\lambda^2-(E/2)^2}\Theta(\lambda^2-(E/2)^2)$ and thus the mean spacing $\pi\lambda/N$ at $E=0$.

The rth power of the determinant in Eq. (E1) can be written as the Gaussian integral (summation convention)

$$\det[G(z)]^r = \int d\psi \exp[\pm i\psi^{a\dagger}(z-H)\psi^a]; \tag{E3}$$

here $\psi^a=\{\psi_\mu^a\}$, $a=1,\ldots,r$ are N-dimensional complex vectors of integration variables; the measure $d\psi \propto \Pi_{\mu=1}^N\Pi_{a=1}^r d\,\mathrm{Re}\,\psi_\mu^a d\,\mathrm{Im}\,\psi_\mu^a$ comprises a normalization constant of the form $(\mathrm{const})^r\sim 1$; here and in the remainder of this appendix we let the symbol $\sim$ mean equality in the limit $r\to 0$; the positive or negative sign in the exponent applies to the case $\mathrm{Im}\,z>0$ or $\mathrm{Im}\,z<0$.

We proceed to the retarded and advanced Green functions $\mathrm{tr}\,G_\pm(E)=\mathrm{tr}\,G(E\pm i\delta)$ with real E and $\delta\downarrow 0$. Their ensemble averaged product

$$C(\epsilon) = \overline{[\mathrm{tr}\,G_+(E+\epsilon/2)][\mathrm{tr}\,G_-(E-\epsilon/2)]} \tag{E4}$$

leads to the spectral correlator and the form factor according to Eq. (77). Applying the replica trick Eq. (E1) and the integral representation Eq. (E3) twice, i.e., for both G_+ and G_-, we get to a *bosonic replica variant of the σ model*: the correlation function $C(\epsilon)$ appears as a twofold derivative of a generating function,

$$C(\epsilon) = \lim_{r\to 0}\frac{1}{r^2}\left[\frac{\partial^2 Z(\hat{\epsilon})}{\partial\epsilon_+\,\partial\,\epsilon_-}\right]_{\epsilon_{\pm}=\pm\epsilon/2}, \tag{E5}$$

$$\mathcal{Z}(\hat{\epsilon}) = \int d\psi\, \overline{\exp[i\psi^\dagger\Lambda(\hat{\epsilon}+E-H)\psi]},$$

$$\hat{\epsilon} = \mathrm{diag}(\epsilon_+ + i\delta, \epsilon_- - i\delta), \quad \delta\downarrow 0,$$

$$\Lambda = \mathrm{diag}(1,-1). \tag{E6}$$

Compared to Eq. (E3) the number of integrations is doubled in the generating function $\mathcal{Z}$: a doublet $\psi\equiv(\psi^1,\psi^2)$ comprises rN-dimensional vectors ψ^1 and ψ^2 needed to represent the retarded and the advanced Green functions by Gaussian integrals. The diagonal matrices $\hat{\epsilon},\Lambda$ act in the newly introduced advanced and retarded spaces like

$$\Lambda\begin{pmatrix}\psi^1\\ \psi^2\end{pmatrix} = \begin{pmatrix}\psi^1\\ -\psi^2\end{pmatrix},$$

and like unity in the replica space. Note that Λ and the imaginary part of $\hat{\epsilon}$ together secure convergence of the Gaussian integrals in $\mathcal{Z}$ as did the plus or minus sign in Eq. (E3). The replica index a is suppressed in the compact notation for $\mathcal{Z}$.

The GUE average is now easily done in Eq. (E6) since the random Hamiltonian appears linearly in the exponent,

$$\mathcal{Z}(\hat{\epsilon}) = \int d\psi \exp\left(i\psi^\dagger \Lambda(\hat{\epsilon} + E)\psi - \frac{\lambda^2}{2N} \mathrm{tr}\, A^2 \right)$$

with the $2r \times 2r$ matrix $A = \{A^{\alpha\beta} = \Sigma_{\mu=1}^{N} \psi_\mu^\alpha \psi_\mu^{\beta *} \Lambda^{\beta\beta}\}$; the index $\alpha = (p, a)$ comprises the replica index $a = 1, \ldots, r$ and an index $p = 1, 2$ discriminating between "advanced" and "retarded." We next decouple the term proportional to $\mathrm{tr}\, A^2$ quartic in the integration variables ψ by a Hubbard-Stratonovich transformation. To this end, we multiply $\mathcal{Z}$ by the unit-normalized Gaussian integral $1 = \mathcal{N} \int dQ \exp[(N/2)\mathrm{tr}\, Q^2]$, where $Q = \{Q^{\alpha\beta}\}$ is a $2r$-dimensional anti-Hermitian matrix and $\int dQ$ denotes integration over all its independent matrix elements; the latter comprise $(2r)^2$ independent real and imaginary parts such that the normalization constant is of the form $\mathcal{N} = (\mathrm{const})^{r^2} \sim 1$. The shift $Q \to Q - \lambda A/N$ leads to

$$\mathcal{Z}(\hat{\epsilon}) \sim \int d\psi \int dQ \exp\left(\frac{N}{2} \mathrm{tr}\, Q^2 + i\psi^\dagger \Lambda(\hat{\epsilon} + E + i\lambda Q)\psi \right)$$
$$\sim \int dQ \exp\left(\frac{N}{2} \mathrm{tr}\, Q^2 - N \mathrm{tr} \ln[\hat{\epsilon} + E + i\lambda Q] \right)$$

where in the second step we have performed the Gaussian integration over ψ. The large parameter N in the foregoing exponential allows for a stationary-phase approximation of the Q integral. Variation of the exponent, the so-called action, with respect to the independent matrix elements of Q yields the saddle-point equation

$$Q = \frac{i\lambda}{\hat{\epsilon} + E + i\lambda Q}. \tag{E7}$$

In order to shorten the saddle-point analysis we confine ourselves to $E = 0$; the final result is valid throughout Wigner's semicircle. The saddle-point equation then invites solution to zeroth order in $\hat{\epsilon}$ since the scale for the energy offset variables is the mean level spacing $\epsilon_\pm = \mathcal{O}(N^{-1})$; we can even dispatch the infinitesimal imaginary part $\mathrm{Im}(\hat{\epsilon}) = i\Lambda\delta$ which is only needed to ensure absolute convergence of all integrals. A simple matrix-diagonal saddle point thus arises, $Q \simeq \Lambda$. [Strictly speaking, there are 2^{2r} diagonal solutions with diagonal entries ± 1. However, the solutions different from $\Lambda = \mathrm{diag}(1, -1)$, have to be discarded since they cannot be reached without crossing the cuts of the logarithm in the action [45]].

A continuous manifold of more general (nondiagonal yet compatible with the cut structure of the logarithm) solutions of the saddle-point equation can now be obtained by the conjugation $\Lambda \to T\Lambda T^{-1} \equiv Q_s$, where $T \in \mathrm{U}(r, r)$ is a $(2r)$-dimensional pseudounitary matrix. (The pseudounitarity condition $T\Lambda T^\dagger = \Lambda$ is required to make the subsequent integration over all configurations Q convergent [46].) This observation identifies the noncompact symmetric space $\mathrm{U}(r, r)/\mathrm{U}(r) \times \mathrm{U}(r)$ as the saddle-point manifold. (Transformations $T \in \mathrm{U}(r) \times \mathrm{U}(r)$ commute with Λ and, therefore, do not affect the diagonal saddle.) It may be a noteworthy property of the saddle-point manifold in question that the matrices Q thereon are no longer anti-Hermitian [46].

We next substitute the saddle configurations $Q_s = T\Lambda T^{-1}$ into the action and expand to order $\hat{\epsilon}$,

$$\mathcal{Z}(\hat{\epsilon}) \sim \int dQ_s \exp\{-N \mathrm{tr}[\hat{\epsilon}(E + i\lambda Q_s)^{-1}]\}$$
$$\overset{(E7)}{\sim} \int dQ_s \exp\left(\frac{iN}{\lambda} \mathrm{tr}[\hat{\epsilon} Q_s] \right)$$
$$\sim \int dQ_s \exp\left(\frac{i(\epsilon_+ - \epsilon_- + i2\delta)\pi\bar{\rho}}{2} \mathrm{tr}[\Lambda Q_s] \right)$$
$$\sim \int dQ_s \exp\left(\frac{is^+}{2} \mathrm{tr}\, \Lambda Q_s \right), \tag{E8}$$

where now $\int dQ_s$ demands integration over the saddle-point manifold [45]; in the foregoing calculation we used that $\mathrm{tr}(Q_s^2) = \mathrm{tr}(\Lambda^2) = r \sim 0$ and that $\mathrm{tr}(Q_s \hat{\epsilon}) = (\epsilon_+ + \epsilon_-)\mathrm{tr}(Q_s)/2 + (\epsilon_+ - \epsilon_- + 2i\delta)\mathrm{tr}(Q_s\Lambda)/2 = (\epsilon_+ - \epsilon_- + 2i\delta)\mathrm{tr}(Q_s\Lambda)/2$; finally, in the last step we introduced the scaled offset $s^+ = (\epsilon_+ - \epsilon_- + 2i\delta)\pi\bar{\rho}$. In order to evaluate the matrix integral above we need an explicit parametrization of the Q matrices on the saddle-point manifold. Tailor made for perturbative calculations is the so-called rational parametrization[9]

$$Q_s = (1 - W)\Lambda(1 - W)^{-1}, \quad W = \frac{1}{\sqrt{s^+}} \begin{pmatrix} 0 & B \\ B^\dagger & 0 \end{pmatrix} \tag{E9}$$

where the scaling factor $1/\sqrt{s^+}$ makes for notational convenience. The main merit of that representation is that the invariant measure dQ_s is effectively (i.e., in view of the eventual limit $r \to 0$) the flat measure

$$(s^+)^{-r^2} \prod_{i,j}^{1,\ldots,r} d\,\mathrm{Re}\, B_{ij}\, d\,\mathrm{Im}\, B_{ij} \equiv (s^+)^{-r^2} dB$$

for $r \times r$ matrices B. Inserting the parametrization Eq. (E9) in the generating function Eq. (E8) we expand as $(1 - W)^{-1} = \Sigma_{n=0}^{\infty} W^n$ to get

$$\mathcal{Z}(\hat{\epsilon}) \sim (s^+)^{-r^2} e^{is^+ r} \int dB \exp\left((2i/\kappa) \sum_{l=1}^{\infty} (s^+)^{1-l} \mathrm{tr}(BB^\dagger)^l \right), \tag{E10}$$

where the factor $\kappa = 1$ has been sneaked in for later use.

We had shown in Sec. V B that the foregoing B integral yields $\{(\mathrm{const})^{r^2} + r^2 f_2(s^+) + r^3 f_3(s^+) + \mathcal{O}(r^4)\}$ with $f_i(s^+)$ polynomials in $1/s^+$. Therefore, nonzero contributions to the correlator $C(\epsilon)$ according to Eq. (E5) arise only when both derivatives $\partial^2/\partial\epsilon_+\partial\epsilon_-$ act together on each of the three factors on the RHS of Eq. (E10). It is easy to see that the contribution from $\partial^2 e^{is^+ r}/\partial\epsilon_+\partial\epsilon_-$ yields the disconnected part $\bar{\rho}^2$ such that upon simply setting $e^{is^+ r} \to 1$ and invoking Eq. (E5) we get (the nonoscillatory contributions to) the connected part $C_{\mathrm{conn}}(\epsilon)$ instead of $C(\epsilon)$. The connected correlation function defined in Eq. (77) is thus obtained as R

[9] Other parametrizations allow one to conveniently do the Q_s integral exactly, to get the nonoscillatory part of $R(s)$ in closed form instead of the asymptotic $1/s^+$ series we are after.

$=(1/2\pi^2\bar{\rho}^2)\mathrm{Re}\, C_{\mathrm{conn}}=-\frac{1}{2}\mathrm{Re}(\partial^2/\partial s^{+2})(Z|_{e^{is^+r}\to 1})$ which leads us to Eq. (79) for the unitary class, with $\kappa=1$.

2. Generalization to the orthogonal class

For the GOE, Eq. (E2) generalizes to

$$\langle H_{\mu\nu}\rangle = 0,$$

$$\langle H_{\mu\nu}H_{\nu'\mu'}\rangle = \frac{\lambda^2}{N}(\delta_{\mu\mu'}\delta_{\nu\nu'} + \delta_{\mu\nu'}\delta_{\nu\mu'}).$$

As a consequence, the averaged action will contain the sum of two contributions quartic in the integration variables $\psi_\mu^\dagger\Lambda\psi_\nu(\psi_\nu^\dagger\Lambda\psi_\mu+\psi_\mu^\dagger\Lambda\psi_\nu)=2\bar{\Psi}_\mu\Lambda\Psi_\nu\bar{\Psi}_\nu\Lambda\Psi_\mu$, where we have defined

$$\bar{\Psi} \equiv \frac{1}{\sqrt{2}}(\psi^\dagger,\psi^T), \quad \Psi = \frac{1}{\sqrt{2}}\begin{pmatrix}\psi\\ \psi^*\end{pmatrix}. \tag{E11}$$

Notice that the $4r$-component vectors Ψ and $\bar{\Psi}$ are connected by the symmetry relation

$$\bar{\Psi} = \Psi^T\sigma_1, \tag{E12}$$

where the Pauli matrix σ_1 acts in the two-component space of Eq. (E11). To decouple the quartic Ψ term in the action, we introduce a Q matrix subject to the constraint $Q=\sigma_1 Q^T\sigma_1$. Noting that $\psi^\dagger(\hat{\epsilon}+E)\psi=\bar{\Psi}(\hat{\epsilon}+E)\Psi$ and proceeding as in the unitary case we get

$$\mathcal{Z}(\hat{\epsilon}) = \int d\Psi \int dQ \exp\left(\frac{N}{4}\mathrm{tr}(Q^2) + i\bar{\Psi}\Lambda(\hat{\epsilon}+E+i\lambda Q)\Psi\right)$$
$$= \int dQ \exp\left(\frac{N^2}{4}\mathrm{tr}(Q^2) - \frac{N}{2}\mathrm{tr}\ln(\hat{\epsilon}+E+i\lambda Q)\right),$$

where we made use of the symmetry of Q. A stationary-phase approach yields the diagonal saddle $Q=\Lambda$ and its nondiagonal generalization $Q_s=T\Lambda T^{-1}$, where $T\in \mathrm{O}(2r,2r)$. [Compatibility with the symmetries of Q requires $T^T=\sigma_1 T^{-1}\sigma_1$; hence the restriction to the (pseudo)orthogonal group.] This identifies $\mathrm{O}(2r,2r)/\mathrm{O}(2r)\times\mathrm{O}(2r)$ as the saddle-point manifold.

As in the unitary case, we represent the Q_s matrices in the rational parametrization Eq. (E9). Presently, time-reversal invariance implies $T^T=\sigma_1 T^{-1}\sigma_1$ and the symmetry of the integration variables B,

$$B^\dagger = -\sigma_1 B^T\sigma_1. \tag{E13}$$

Simplifying the action to leading order in $\hat{\epsilon}$ and expanding in W, we recover Eq. (79), now with $\kappa=2$.

3. Contraction rules

To compute the matrix integral perturbatively in an expansion in $1/s^+$, one expands the exponentiated action in powers of traces $\mathrm{tr}[(BB^\dagger)^l]$, $l\geqslant 2$. This leads to a series of terms of the structure $\langle\{\mathrm{tr}[(BB^\dagger)^2]\}^{\upsilon_2}\{\mathrm{tr}[(BB^\dagger)^3]\}^{\upsilon_3}\ldots\rangle$, where υ_l are integers and the averaging over the quadratic action $\langle\cdots\rangle$ is defined by Eq. (81). Each term contributing to the series is then computed by Wick's theorem, i.e., as a sum over all nonvanishing pair contractions Eqs. (85a)–(85d) of B matrices. We now briefly outline the derivation of the basic contraction rules. In an index notation, the quadratic action reads $S^{(2)}[B,B^\dagger]=(i/\kappa)\Sigma_{\alpha\alpha'}|B_{\alpha\alpha'}|^2$. This implies the prototypical contraction rule

$$\langle B_{\alpha\alpha'}B^\dagger_{\beta'\beta}\rangle = -\frac{1}{2i}\delta_{\alpha\beta}\delta_{\alpha'\beta'},$$

the κ independence of which follows from the fact that in the orthogonal case, $\kappa=2$, only one-half of the matrix elements $B_{\alpha\alpha'}$ are independent integration variables—a consequence of the time-reversal relation Eq. (E13). When expressed as a sum over independent integration variables only, the coefficient of the action effectively doubles, i.e., in either case $\kappa=1$, 2 the integration over matrix components obtains a factor $i/2$. Using this relation we obtain

$$\langle \mathrm{tr}\,\overbrace{BX\,\mathrm{tr}B^\dagger Y}\rangle = \langle\overbrace{B_{\alpha\beta}X_{\beta\alpha}B^\dagger_{\gamma\delta}}Y_{\delta\gamma}\rangle$$
$$= -\frac{1}{2i}\langle X_{\beta\alpha}Y_{\alpha\beta}\rangle$$
$$= -\frac{1}{2i}\langle\mathrm{tr}(XY)\rangle,$$

which is the contraction rule Eq. (85a). Rule (85b) is proven in the same manner. Rule (85d) for the GOE results from

$$\langle \mathrm{tr}\,\overbrace{BX\,BY}\rangle = \langle\mathrm{tr}((\sigma_1X)\overbrace{B(Y\sigma_1)(\sigma_1B}\sigma_1))\rangle$$
$$= \langle(\sigma_1X)_{\alpha\beta}\overbrace{B_{\beta\gamma}(Y\sigma_1)_{\gamma\delta}(\sigma_1B\sigma_1)_{\alpha\delta}}\rangle$$
$$\overset{(E13)}{=} -\langle(\sigma_1X)_{\alpha\beta}\overbrace{B_{\beta\gamma}(Y\sigma_1)_{\gamma\delta}}B^\dagger_{\alpha\delta}\rangle$$
$$= +\frac{1}{2i}\langle(\sigma_1X)_{\alpha\beta}(\sigma_1Y^T)_{\beta\alpha}\rangle$$
$$= +\frac{1}{2i}\langle\mathrm{tr}(X(\sigma_1Y^T\sigma_1))\rangle$$
$$= -\frac{1}{2i}\langle\mathrm{tr}(XY^\dagger)\rangle,$$

where in the last step we used that Y contains an odd number of matrices B and $B^\dagger$ [i.e., that the time-reversal relation Eq. (E13) implies $\sigma_1Y^T\sigma_1=-Y^\dagger$]. The proof of rule Eq. (85c) proceeds along the same lines.

[1] O. Bohigas, M. J. Giannoni, and C. Schmit, Phys. Rev. Lett. **52**, 1 (1984); G. Casati, F. Valz-Gris, and I. Guarneri, Lett. Nuovo Cimento Soc. Ital. Fis. **28**, 279 (1980); M. V. Berry, Ann. Phys. (N.Y.) **131**, 163 (1981).
[2] H.-J. Stöckmann, *Quantum Chaos: An Introduction* (Cambridge University Press, Cambridge, U.K., 1999).
[3] F. Haake, *Quantum Signatures of Chaos*, 2nd ed. (Springer, Berlin, 2001).
[4] M. L. Mehta, *Random Matrices and the Statistical Theory of Spectra*, 2nd ed. (Academic, New York, 1991).
[5] M. V. Berry, Proc. R. Soc. London, Ser. A **400**, 229 (1985).
[6] N. Argaman, F.-M. Dittes, E. Doron, J. P. Keating, A. Yu. Kitaev, M. Sieber, and U. Smilansky, Phys. Rev. Lett. **71**, 4326 (1993).
[7] M. Sieber and K. Richter, Phys. Scr., T **90**, 128 (2001); M. Sieber, J. Phys. A **35**, L613 (2002).
[8] M. Gutzwiller, *Chaos in Classical and Quantum Mechanics* (Springer, New York, 1990).
[9] D. Cohen, H. Primack, and U. Smilansky, Ann. Phys. (N.Y.) **264**, 108 (1998).
[10] H. Primack and U. Smilansky, Phys. Rep. **327**, 1 (2000).
[11] U. Smilansky and B. Verdene, J. Phys. A **36**, 3525 (2003).
[12] I. L. Aleiner and A. I. Larkin, Phys. Rev. B **54**, 14423 (1996).
[13] R. A. Smith, I. V. Lerner, and B. L. Altshuler, Phys. Rev. B **58**, 10343 (1998); R. S. Whitney, I. V. Lerner, and R. A. Smith, Waves Random Media **9**, 179 (1999).
[14] S. Müller, Eur. Phys. J. B **34**, 305 (2003); Diplomarbeit, Universität Essen, 2001 (unpublished).
[15] D. Spehner, J. Phys. A **36**, 7269 (2003).
[16] M. Turek and K. Richter, J. Phys. A **36**, L455 (2003).
[17] P. A. Braun, F. Haake, and S. Heusler, J. Phys. A **35**, 1381 (2002).
[18] M. Turek, D. Spehner, S. Müller, and K. Richter, Phys. Rev. E **71**, 016210 (2005).
[19] S. Heusler, S. Müller, P. Braun, and F. Haake, J. Phys. A **37**, L31 (2004).
[20] S. Müller, S. Heusler, P. Braun, F. Haake, and A. Altland, Phys. Rev. Lett. **93**, 014103 (2004).
[21] S. Heusler, J. Phys. A **34**, L483 (2001).
[22] J. Bolte and J. Harrison, J. Phys. A **36**, 2747 (2003); **36**, L433 (2003).
[23] G. Berkolaiko, H. Schanz, and R. S. Whitney, Phys. Rev. Lett. **88**, 104101 (2002); J. Phys. A **36**, 8373 (2003); G. Berkolaiko, Waves Random Media **14**, S7 (2004).
[24] S. Gnutzmann and A. Altland, Phys. Rev. Lett. **93**, 194101 (2004).
[25] P. Gaspard, *Chaos, Scattering, and Statistical Mechanics* (Cambridge University Press, Cambridge, U.K., 1998).
[26] W. Parry and M. Pollicott, Asterisque **187**, 1 (1990).
[27] J. H. Hannay and A. M. Ozorio de Almeida, J. Phys. A **17**, 3429 (1984).
[28] J. A. Foxman and J. M. Robbins, J. Phys. A **30**, 8187 (1997).
[29] S. Heusler, Ph.D. thesis, Universität Duisburg-Essen, 2004 (unpublished).
[30] S. Müller, Ph.D. thesis, Universität Duisburg-Essen, 2005 (unpublished).
[31] E. P. Wigner, *Group Theory and Its Application to the Quantum Mechanics of Atomic Spectra* (Academic, New York, 1971).
[32] Jürgen Müller (private communication).
[33] J. Bolte and S. Keppeler, J. Phys. A **32**, 8863 (1999); S. Keppeler, *Spinning Particles—Semiclassics and Spectral Statistics* (Springer, Berlin, 2003).
[34] F. Wegner, Z. Phys. B **35**, 207 (1979).
[35] K. Efetov, *Supersymmetry in Disorder and Chaos* (Cambridge University Press, Cambridge, U.K., 1997).
[36] E. Bogomolny and C. Schmit, J. Phys. A **37**, 4501 (2004), and references therein.
[37] K. Richter and M. Sieber, Phys. Rev. Lett. **89**, 206801 (2002); H. Schanz, M. Puhlmann, and T. Geisel, *ibid.* **91**, 134101 (2003); M. Puhlmann, H. Schanz, T. Kottos, and T. Geisel, Europhys. Lett. **69**, 313 (2005); O. Zaitsev, D. Frustaglia, and K. Richter, Phys. Rev. Lett. **94**, 026809 (2005); R. S. Whitney and P. Jacquod, *ibid.* **94**, 116801 (2005).
[38] M. R. Zirnbauer, J. Math. Phys. **37**, 4986 (1996); J. J. M. Verbaarschot and I. Zahed, Phys. Rev. Lett. **70**, 3852 (1993); A. Altland and M. R. Zirnbauer, Phys. Rev. B **55**, 1142 (1997).
[39] S. Gnutzmann, B. Seif, F. v. Oppen, and M. R. Zirnbauer, Phys. Rev. E **67**, 046225 (2003); S. Gnutzmann and B. Seif, *ibid.* **69**, 056219 (2004); **69**, 056220 (2004).
[40] J. Müller and A. Altland, J. Phys. A **38**, 3097 (2005).
[41] T. Nagao and K. Saito, Phys. Lett. A **311**, 353 (2003).
[42] *Handbook of Mathematical Functions*, edited by M. Abramowitz and I. A. Stegun (Dover, New York, 1970).
[43] A. Bäcker and N. Chernov, Nonlinearity **11**, 79 (1998).
[44] P. A. Braun, S. Heusler, S. Müller, and F. Haake, Eur. Phys. J. B **30**, 189 (2002).
[45] J. J. M. Verbaarschot, H. A. Weidenmüller, and M. R. Zirnbauer, Phys. Rep. **129**, 367 (1985).
[46] M. R. Zirnbauer, J. Math. Phys. **38**, 2007 (1997).